Medizinische Fakultät Charité – Universitätsmedizin Berlin
Campus Benjamin Franklin

Aus dem Max-Delbrück-Centrum für Molekulare Medizin, Berlin-Buch

Direktor

GENETICALLY ALTERED ANIMAL MODELS TO STUDY TISSUE ACTIONS OF ANGIOTENSIN PEPTIDES

Inaugural-Dissertation

zur Erlangung des Grades Doctor rerum medicarum

Charite-Universitätsmedizin Berlin

Campus Benjamin Franklin

Vorgelegt von Frau Ping Xu,

aus Harbin, Hei Long Jiang province, VR China

Referent: Prof. Dr. Michael Bader

Koreferent: Prof. Dr. Thomas Unger

Gedruckt mit Genehmigung der Charité - Universitätsmedizin Berlin
Campus Benjamin Franklin

Promoviert am: 24 June 2008

Contents

Contents

Contents

Contents

Contents

Contents

1. Introduction

Hypertension, a disease with a high incidence in the population, affects all parts of the cardiovascular system. Blood pressure is physiologically determined as the product of cardiac output and total peripheral resistance to flow. The cardiac output and peripheral resistance are controlled by many factors, which include the autonomic nervous system, vasopressor/vasodepressor hormones and peptides such as the renin-angiotensin system (RAS), structure of the vessel, body fluid volume, renal function, and many others. Although many of the physiological systems involved in the regulation of blood pressure have been extensively studied, because of the complex interaction among these different physiologic pathways, it has not been determined which system is of major importance in hypertension patients (WHO, 1999). However, since vessels primarily determine the control of peripheral resistance, their homostasis is of importance for blood pressure control. Therefore, studying the alteration of vasomotor responses of vessels in hypertensive animals helps us to better understand the underlying cellular signalling pathway. On the other hand, endocrine RAS plays a key role to regulate blood pressure and most effective therapies for hypertension are derived from intensive research on RAS. In the following chapters, I will give a short overview of two important aspects affecting development and course of hypertension: endothelial function and RAS.

1.1. Endothelial function

The arterial vessel is composed of three distinct layers: tunica intima - a single layer of endothelium, tunica media - which comprises the vascular smooth muscle cell (VSMC), and tunica adventitia - an elastic lamina with terminal nerve fibers and surrounding connective tissue. The endothelium has a central role in the early functional adaptations. Hypertension is associated with abnormal endothelial function in the peripheral circulation.

Endothelium is composed of a single layer of endothelial cells, which are located at the interface between blood and tissue. It can sense changes in hemodynamic forces, ambient O_2 tension, and local blood-borne signals and respond with appropriate changes in function to maintain homeostasis. These responses include the paracrine release of diffusible vasodilatory mediators such as nitric oxide (NO), prostacyclin (PGI_2) and endothelium-derived hyperpolarizing factor (EDHF). Vasoconstrictor substances produced by the endothelium include endothelin, and prostanoids such as thromboxane A_2 and prostaglandin H_2 (PGH_2) and endothelin-1 (ET-1). Angiotensin converting enzyme (ACE) derived of endothelium, regulates local levels of bioactive

angiotensin II (Ang II) and bradykinin (BK). Thus, the endothelium can directly, through modulation of its vasoconstrictor and vasodilatory substances, alter vascular tone and blood pressure. The complex interplay of these mechanisms results in a perturbation of the physiological properties of NO in the maintenance of endothelial homeostasis, such as vasodilation. The balance of these vasoconstrictors and dilators maintains normal endothelial function, hence endothelial dysfunction is characterized by an inappropriate vasodilatation upon stimulation with agonists (such as acetylcholine (ACh)) or shear stress to release endothelium-derived vasodilators, including PGI_2, NO, and EDHF (Panza et al. 1993) (Fig.1.1). Among these molecules, Ang II and NO are the most effective targets of antihypertensive therapy; and therefore they were extensively studied during last decade.

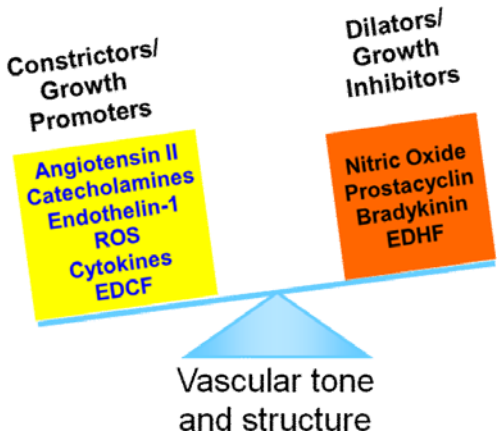

Fig.1.1. Imbalance in vaso-regulating factors induces endothelial dysfunction (Santilli et al. 2004)
Vascular tone and structure are maintained by the balance between constrictors and dilators. Ang II and NO represent major molecules for vasoregulation.

1.1.1. Nitric Oxide metabolism and signalling

NO is a central molecule for endothelial function. It is generated by a highly regulated family of enzymes called NO synthases (NOS) that utilize O_2, NADPH and tetrahydrobiopterin (BH4), Ca^{2+} and calmodulin as cofactors, L-arginine as substrates, and generates citrulline as a co-product, according to the equation:

$$2\ \text{L-Arginine} + 4\ O_2 + 3\ \text{NADPH} + 3\ H^+ \xrightarrow{\text{NOS}} 2\ \text{L-Citrulline} + 2\ \text{NO} + 4\ H_2O + 3\ NADP^+$$

NO has a half-life of only a few seconds *in vivo*. However, since it is soluble in both aqueous and lipid media, it readily diffuses through the cytoplasm and plasma membranes. In the extracellular

milieu, NO reacts with oxygen and water to form nitrates (NO_3^-) and nitrites (NO_2^-) (Murad 1998; Brown 1999), which became indirect markers for NO quantification.

In the vasculature, NO binds to the heme moiety of guanylate cyclase (GC), disrupting the planar form of the heme iron. The resulting conformational change activates the enzyme to produce the intracellular mediator cyclic GMP (cGMP), which is utilized as an intracellular amplifier and second messenger in a large range of physiological responses (Gerzer et al. 1981). It serves as NO receptor, and changes in cGMP level reflect the bioactivity of NO. Furthermore, cGMP-dependent protein kinase that phosphorylates and activates a calcium-sensitive potassium channel is a downstream mediator of vascular smooth muscle relaxation (Archer et al. 1994) (Fig. 1.2).

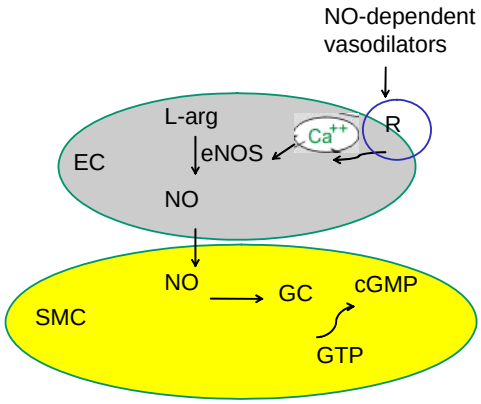

Fig. 1.2 NO synthesis and signal transduction
NO dependent vasodilators such as Ach, NO-mediated aortic relaxation is likely induced via receptor (R) mediated stimulation of Ca^{2+}-dependent NO production in the endothelium. NO, once liberated from the endothelium, diffuses towards the adjacent vascular smooth muscle cells and stimulates the activity of GC, an enzyme that catalyzes the chemical conversion of GTP to cGMP. cGMP probably serves as the first intracellular signal leading to NO-mediated vasodilation. EC, endothelial cell; SMC, smooth muscle cell.

1.1.1.1 Endothelial NOS (eNOS)

NOS are the key enzymes to synthesize NO. There are three isoforms of NOS, two of which (eNOS and neuronal NOS) are constitutively expressed and are acutely regulated by calcium/calmodulin and phosphorylation, whereas the third isoform of NOS (inducible NOS) is induced during inflammation and produces higher levels of NO for a longer period.

eNOS is expressed exclusively in endothelium. It exists in two distinct subcellular localizations: at caveolae of the plasma membrane and in the Golgi/perinuclear region of the cell. eNOS expression and activity are tightly governed both at the transcriptional and post-translational levels, by protein-protein interactions and by intracellular Ca^{2+} concentrations.

1.1.1.2 eNOS localization and caveolin-1

Targeting of eNOS to caveolae is required for proper eNOS function (Fig. 1.3). Caveolae are important structures in endothelial cells, which look like small spherical or egg-shaped static invaginations of the plasma membrane composed of caveolin protein. Caveolin-1 is localized to caveolae in the endothelium and associates with a number of regulatory molecules including eNOS. This localization could modulate eNOS activity by situating it in close physical proximity to the upstream signalling proteins (Shaul et al. 1996). Association of eNOS with caveolin-1 negatively regulates eNOS activity as it prevents calmodulin binding (Venema et al. 1997).

1.1.1.3 eNOS phosphorylation, Akt and Hsp 90

eNOS is known to be phosphorylated. Phosphorylation stimulates NOS activity at multiple sites, including Ser1177 and Ser635, and inhibits NOS activity at Thr495 and Ser116 (Bauer et al. 2003). Akt/Protein kinase B phosphorylates Ser1177 at the plasma membrane (Fig. 1.3), thus activating eNOS at basal levels and in response to agonists (Dimmeler et al. 1999; Fulton et al. 1999).

Akt has three isoforms: Akt 1, Akt 2, and Akt 3 (Datta et al. 1999). These isoforms have greater than 85% sequence identity and have the same structural organisation. Akt is a serine/threonine kinase with a pleckstrin homology domain that is activated in response to growth factors or cytokines by a mechanism involving phosphoinositide 3-kinase (PI3-K) and phosphoinositide-dependent kinase (PDK-1 and 2) (Franke et al. 1997; Kulik et al. 1997). Activation of Akt involves translocation from the cytosol (inactive) to the plasma membrane where activated PI3-K1 and 2 phosphorylate Akt on threonine 308 and serine 473, with both phosphorylations required for maximum Akt activation. Activated Akt phosphorylates intracellular proteins that include varieties of downstream signals and regulates growth, metabolism, survival, and cardiac function (Condorelli et al. 2002; Shiojima et al. 2002; Ananthakrishnan et al. 2005; DeBosch et al. 2006). Optimal Akt signalling promotes physiological growth and inhibits pathological hypertrophy.

Hsp 90 association is a prerequisite for subsequent Akt-mediated stimulation of eNOS. It is a member of the heat shock protein family of proteins that function as molecular chaperones. Hsp 90 is believed to function as a scaffold protein for Akt and eNOS (Garcia-Cardena et al. 1998; Sato et al. 2000). After binding, Hsp 90 and Akt synergistically activate eNOS (Fig. 1.3).

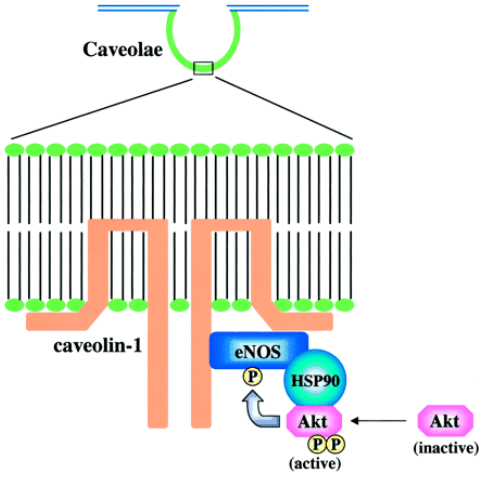

Fig. 1.3 Schematic illustration of Akt-Hsp 90-eNOS interaction at caveolae (Shiojima and Walsh 2002).
eNOS in caveolae is bound and inhibited by caveolin-1. eNOS can also be activated by phosphorylation, e.g. by the protein kinase Akt, and the eNOS/Akt interaction is thought to be fostered by Hsp 90.

1.1.2. Reactive oxygen species (ROS) generation and signalling

NO can be counteracted by molecules referred to as ROS. *In vivo* there is a fine tuned regulation system maintaining the balance between ROS and NO.

Any free radicals can be defined as ROS. A free radical is any atom such as oxygen, nitrogen with at least one unpaired electron in the outermost shell, superoxide anions ($O_2^{\cdot-}$), hydrogen peroxides (H_2O_2), and the extremely toxic hydroxyl radical (·OH). Free radicals are highly reactive due to the presence of these unpaired electrons. Physiologically, ROS are produced in a controlled manner at low concentrations and function as signalling molecules to maintain vascular integrity by regulating endothelial function and vascular contraction-relaxation (Touyz et al. 2003).

Oxidative stress, defined as an increase in the steady-state levels of ROS or inadequate removal of ROS, affects gene transcription, causes DNA strand break or chemical modifications, modifies proteins´ carbonyl or thiols and leads to lipid peroxidation (Griendling and Harrison 2001). ROS may react with DNA bases to produce oxidative DNA adducts. Such adducts have been associated with mutagenesis and carcinogenesis. ROS may directly damage DNA leading to the formation of the DNA adduct, 8-oxo-7,8-dihydro-2′-deoxyguanosine (8-oxo-dG). Indirect actions of ROS include lipid peroxidation of cellular membranes, resulting in the production of compounds (e.g. malondialdehyde) which are capable of forming DNA adducts such as a pyrimidopurinone adduct of deoxyguanosine (Marnett 2000). Thus, 8-oxo-dG and MDA are well developed markers for the measurements of ROS concentration.

ROS are involved in the pathogenesis of many cardiovascular diseases, including hypercholesterolemia, atherosclerosis, diabetes, and heart failure. Under pathological conditions, increased ROS bioactivity leads to endothelial dysfunction, increased contractility, VSMC growth, monocyte invasion, inflammation, and increased deposition of extracellular matrix proteins, important factors in hypertensive vascular damage (Taniyama and Griendling 2003). There is abundant evidence that $O_2^{\cdot-}$ is involved in various animal models of hypertension. Vascular $O_2^{\cdot-}$ is increased in the DOCA-salt induced rat model (Somers et al. 2000; Beswick et al. 2001), Ang II-infused Bl/6 mouse model (Rajagopalan et al. 1996; Landmesser et al. 2002), 1-kidney 1-clip rat renal hypertensive model (Dobrian et al. 2001). Consequently, to learn more about how ROS are produced and removed is very important.

1.1.2.1. Enzymatic sources of ROS

There are several enzymes involved in ROS generation (Fig. 1.4). Potential ROS sources include NAD(P)H oxidase, xanthine oxidase, cytochrome P450 based enzymes from mitochondria, dysfunctional NOS, metabolism of arachidonic acid by cyclooxygenase (COX) and lipoxygenase.

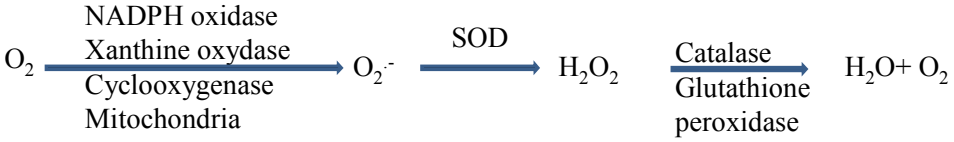

Fig. 1.4 ROS production and degradation pathways
$O_2^{\cdot-}$and H_2O_2, are the main ROS molecules. NADPH, Xanthine oxydase, cyclooxygenase, and mitochondria are involved in producing ROS; SOD and catalase compose the removing enzyme system for ROS.

1.1.2.2. NAD(P)H oxidase

Among various enzymes involved in the generation of ROS, NAD(P)H oxidase seems to be the major source of $O_2^{\cdot-}$ production in the vessel wall (Lassegue and Clempus 2003). It is a multi subunit enzyme catalysing $O_2^{\cdot-}$ production by the 1 electron reduction of oxygen using NAD(P)H as the electron donor:

$$2\ O_2 + NAD(P)H \rightarrow 2\ O_2^{\cdot-} + NAD(P) + H^+.$$

NAD(P)H oxidases have been demonstrated to be functional in all vascular layers, including the endothelium (Wolin 2000), the smooth muscle layer (Cai and Harrison 2000), and the adventitia (Uddin et al. 2003). Vascular NAD(P)H oxidase comprises at least 4 components: cell membrane–associated p22phox and gp91phox and cytosolic subunits, p47phox and p67phox (Babior 1999) (Fig. 1.5). Among them, gp91phox, also named Nox 2, is expressed in endothelium and adventitia, whereas its homologues Nox 1 and Nox 4 are expressed both in vascular smooth muscle cells and fibroblast cells, respectively (Table 1.1) (Sorescu et al. 2002).

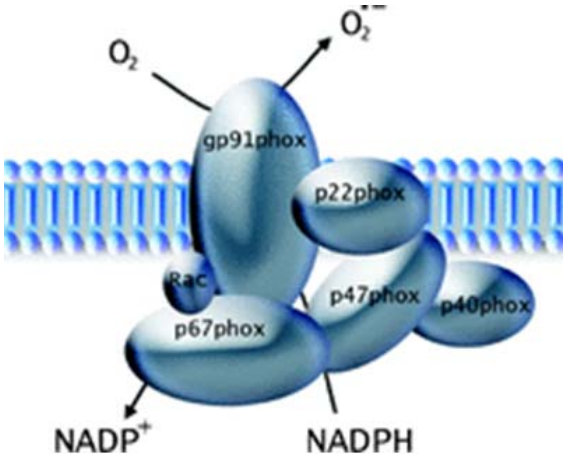

Fig. 1.5 NAD(P)H oxidase subunits (Babior 1999)
Vascular NAD(P)H oxidase comprises at least 4 components: cell membrane–associated p22phox and gp91phox forming the membrane bound cytochrome b558, and the cytosolic subunits, p47phox and p67phox. Binding of p67phox to cytochrome b558 induces a gradual conformational change of cytochrome b558, which then becomes capable of transferring electrons produced in the cytoplasm from NADPH to oxygen, reducing the latter to $O_2^{\cdot-}$. Rac disrupts p67/P40 phox binding.

Table 1.1 Tissue distribution of Nox homologues

	Tissue distribution
Nox 1 (Mox 1)	Colon, VSM, uterus and prostate.
Nox 2	Phagocyte, endothelium, cardiomyocytes, VSM (?) and lung.
Nox 3	Inner ear, kidney, liver, lung and spleen.
Nox 4 (Renox)	Kidney, VSM, endothelium, cardiomyocytes, bone, ovary, eye, placenta, skeletal muscle.
Nox 5	Lymphoid tissue, testis, prostate, breast and brain.

1.1.2.3. Cyclooxygenase (Cox) and prostaglandins

As it was already mentioned (1.1), thromboxane A_2 and PGI_2 are also a well known pair of vasoconstrictors and dilators. They belong to the family of prostaglandins (PG), which are highly active lipid mediators and physiological messengers.

PG are synthesized from the common precursor arachidonic acid (AA). The major enzymatic routes of AA metabolism in mammalian cells are the cycloxygenase (Cox) and the lipoxygenase pathway (LO) (Fig. 1.6).

The two isoforms of Cox, known as Cox 1 and Cox 2 are the key enzymes for the prostanoid metabolic pathway. Cox 1 represents the constitutive isoform, whereas Cox 2 is upregulated under inflammatory conditions. Cox catalyzes the rate-limiting initial step in the biosynthesis of PG from AA to generation of ROS (Needleman et al. 1986). PG are usually produced in smooth muscle cells of blood vessels. PGE_2 generally acts as a vasodilator, whereas PGF_{2a} commonly produces vasoconstriction by stimulating the Gq protein pathway. PGI_2 is produced in vascular endothelium. This prostanoid is a potent vasodilator and inhibitor of platelet adhesion to the endothelium. These actions of PG are similar to those of endothelium-derived NO.

On the other hand, the lipoxygenase pathway results in formation of hydroperoxyeicosatetranoic acids (HPETEs) and hydroxyeicosatetraenoic acids (HETEs).

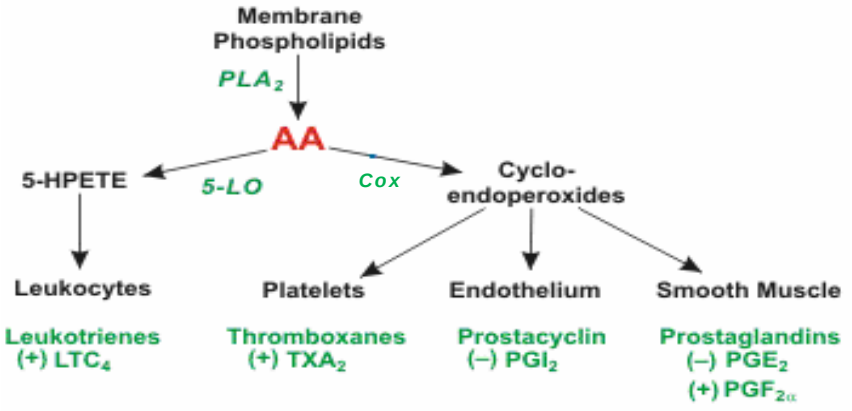

Fig. 1.6 Arachidonic acid metabolism (www.cvphysiology.com/AAmetabolism.gif)
AA, Arachidonic acid; PLA, phospholipase A; LO, lipoxygenase; Cox, cycloxygenase; (+), vasoconstriction; (-) vasodilation

A novel group of prostaglandin-like compounds isoprostanes are biosynthesised from esterified polyunsaturated fatty acid through a non-enzymatic free radical-catalyzed reaction independently of Cox. Several of these compounds possess potent biological activity, as evidenced mainly through their pulmonary and renal vasoconstrictive effects, and have short half-lives. F2-

isoprostanes are authentic biomarkers of lipid peroxidation and can be used as potential *in vivo* indicators of oxidant stress in various clinical conditions, as well as in evaluations of antioxidants or drugs for their free radical-scavenging properties (Basu 2004).

1.1.2.4. Antioxidant system

The effects of ROS generated within endothelial cells are dependent not only on the amount and sites of production but also on the processes that degrade or scavenge ROS. Organisms developed antioxidant systems to maintain the ROS balance (Fig. 1.4).

Reactive non-radical oxygen species such as H_2O_2 and singlet oxygen comprise the variety of reactive molecules that can cause damage to cells. Steady-state H_2O_2 levels in vascular tissue are tightly regulated by its endogenous scavengers catalase and glutathione peroxidase (Gpx1) (Aruoma OI 1998). Catalase is found primarily in peroxisomes and exclusively catalyzes the conversion of H_2O_2 to water. In vascular smooth muscle catalase possesses a higher Km for H_2O_2, compared to Gpx1, and may serve as an important intracellular defense against large amounts of H_2O_2 (Suttorp et al. 1986).

Another major antioxidant system against superoxide anion is superoxide dismutase (SOD), which acts to detoxify superoxide and releases H_2O. In mammalian tissue, three isoforms of SOD exist: the cytoplasmic Cu/ZnSOD, the mitochondrial MnSOD and the extracellular SOD. In the vessel wall, extracellular SOD functions as a major antioxidant enzyme in the extracellular space (Table 1.2).

Table. 1.2 Enzymes that degrade ROS (Schrader and Fahimi 2006)

Enzyme	Substrate	Enzyme is present in
(1) Catalase	H_2O_2	Cytoplasm (e.g., erythrocytes) and nucleus, mitochondria (rat heart)
(2) Glutathione peroxidase	H_2O_2	All cell compartments
(3) Mn SOD	$O_2^{\cdot -}$	Mitochondria
(4) Cu, Zn SOD	$O_2^{\cdot -}$	Cytoplasm
(5) ec SOD	$O_2^{\cdot -}$	Extracellular

The SOD mimetic 4-hydroxy 2,2,6,6,-tetramethyl piperidine 1-oxyl (tempol) lowers blood pressure in normotensive and hypertensive rats (Schnackenberg et al. 1998). Long-term tempol treatment attenuates hypertension development in several animal models of hypertension, and the

antihypertensive effects were proposed by an improvement of endothelium function via reduction of oxidative stress (Ortiz et al. 2001).

1.2. Structure and components of the renin angiotensin system (RAS)

The RAS is a peptide hormone family, which plays an important role in cardiovascular physiology and cell function. It is usually known as a hormonal and tissular system that releases Ang II and is involved in the regulation of blood pressure and salt and fluid homeostasis.
Renin and angiotensins are crucially involved in the control of blood pressure. Even being discovered more than 100 years ago, they still represent key targets for drugs combating cardiovascular disease.

1.2.1 Angiotensinogen (AOGEN) and angiotensin I (Ang I)

AOGEN, the high molecular weight protein precursor of angiotensins, mainly produced by the liver, is also synthesized and constitutively released in other tissues including the heart, vasculature, kidneys, and adipose tissue. Renin cleaves a decapeptide from AOGEN, which is called Ang I. Although Ang I is in itself an inactive compound, it is substrate for Ang II (Fig. 1.7).

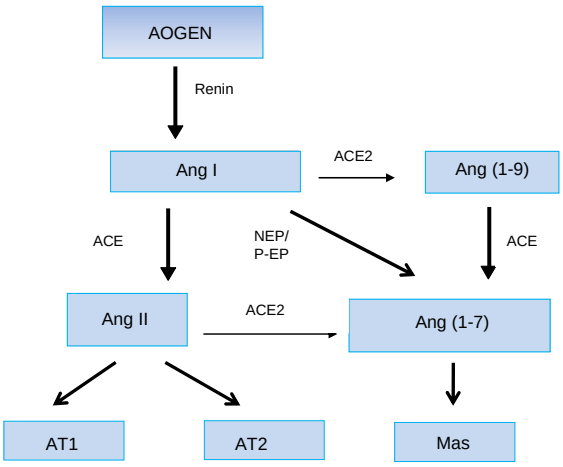

Fig. 1.7 Schematic presentation of RAS
Ang II, product of successive cleavage of AOGEN by renin and ACE, binds AT1- and AT2-receptors. Ang (1-7) produced from Ang I by NEP (neutral endopeptidase) and P-EP (prolyl-endopeptidase) or from Ang II by ACE2 binds Mas.

A transgenic mouse model overexpressing rat AOGEN was generated for research on the *in vivo* function of Ang II (Kimura et al. 1992). Mice are particularly sensitive to the transgenic AOGEN because this species is known to have low circulating AOGEN concentrations and mouse renin is capable of cleaving rat AOGEN (Oliver and Gross 1966). Three of these founder animals transmitted the transgene to their progeny and the transgenic lines, TGM (rAOGEN) 92, 102, and 123 were established. In TGM (rAOGEN) 123 the transgene was highly expressed in brain and liver. Total plasma AOGEN and plasma Ang II concentrations were about three times as high as those of negative control mice. TGM (rAOGEN) 123 mice also developed severe hypertension already at age of 2 months (Kimura et al. 1992) and exhibited end-organ damage (Kang et al. 2002). However, the other AOGEN transgenic lines were not characterized in details.

1.2.2 Systemic Ang II

1.2.2.1 Ang II generation

The generation of active angiotensin peptides is achieved by renin cleaving its only substrate AOGEN which is synthesized mainly in the liver resulting in the liberation of the inactive decapeptide Ang I. The active peptide Ang II is generated by the proteolytic ablation of the two carboxyterminal amino acids of Ang I by the mainly endothelium-associated ACE (Soubrier et al. 1993) (Fig. 1.7).

1.2.2.2 Physiological actions of Ang II

Ang II is a potent vasoactive peptide and its function is mediated through paracrine and autocrine actions. Ang II, the dominant effector of the RAS, regulates numerous physiological responses, including salt-water balance, blood pressure, vascular tone, and release of vasopressin, aldosterone secretion thus maintaining homostasis. It is well known that Ang II elicits its effects via two different receptor subtypes, AT1 receptor, which is expressed in all main target organs like kidney, heart, brain, adrenal cortex, and vessel wall and represents the receptor responsible for most actions of the peptide, and AT2 receptor, which is mainly restricted to embryogenesis, certain brain regions and the adrenal medulla but also presents at low levels in heart, kidney, and vessel wall.

1.2.2.3 Pathological actions of Ang II in the cardiovascular system

Ang II plays an important role in various cardiovascular diseases associated with VSMC, such as hypertension, atherosclerosis, and restenosis after interventional procedures. Hypertension injures blood vessels and thereby causes end-organ damage.
Pathophysiologically, hypertrophic and profibrotic actions of Ang II on cardiovascular system are of prime importance. The enhanced intracardiac Ang II formation in overloaded hearts is involved in coronary constriction, impairment of diastolic relaxation, myocyte enlargement and interstitial fibrosis, which aggravate the diastolic impairment (Holtz 1993).
Ang II also plays a role in the kidney, not only as a regulator of hemodynamics but also in the structural changes occurring in a variety of renal disorders (Gulati and Lall 1996).

1.2.3 Ang II in the brain

In addition to the circulating RAS, all major components of the RAS were found to coexist in tissues including the brain, heart, kidney, adrenal gland, and vasculature. This has led to the establishment of the concept of local RAS.
The brain RAS has been postulated more than 30 years ago (Ganten et al. 1971). It is distinctive from the other local tissue RAS, since it is physically separated from the endocrine one by the presence of the blood-brain barrier impeding the penetration of angiotensin from blood into the brain (Schelling et al. 1976). Circulating Ang II may transmit effects inside the brain through areas lacking the blood-brain barrier (Bader et al. 2001).

1.2.3.1. Animal model

Our group has generated a transgenic rat expressing an antisense construct against AOGEN exclusively in astrocytes, which led to a decrease in blood pressure (Schinke et al. 1999). This model provided new evidence for the implication of the brain RAS in hypertension (Baltatu and Bader 2003). Moreover, these animals also exhibit marked attenuation of left ventricular remodeling and dysfunction after myocardial infarction, demonstrating that the brain RAS has a substantial impact on left ventricular function and end-organ damage through locally produced angiotensins (Wang et al. 2004).

1.2.3.2. Central function of Ang II

Most of the known functions of the active angiotensin peptides in the brain are based on their actions on neurons, to regulate for instance the cardiovascular and fluid-electrolyte homeostasis (Bader et al. 2001), to modulate the autonomic nervous system (Fink 1997; DiBona and Sawin 1999), the hypothalamic-pituitary axis, vasopressin release (Aguilera and Kiss 1996), and the baroreflex sensitivity (Averill and Diz 2000) as well as to stimulate thirst (Denton et al. 1996; Fitzsimons 1998). In addition, other functions have been attributed to the brain RAS, such as influencing memory, cognition, stress, and addiction (Baltatu et al. 2000; Maul et al. 2001; McKinley et al. 2003).

1.2.3.3. Ang II in hypothalamic paraventricular nuclei (PVN)

The hypothalamus is an important center to regulate homeostasis. It has regulatory areas for thirst, hunger, body temperature, water balance, blood pressure, and links the nervous system to the endocrine system. The PVN is an important integrative site within the hypothalamus composed of magnocellular and parvocellular neurons. It is known to influence sympathetic nerve activity that is involved in blood volume regulation. Ang II was shown its functional links in this area. Direct microinjection of Ang II into the PVN causes dose-dependent elevations of blood pressure in rats (Bains et al. 1992). Acting as a neurotransmitter, PVN has been suggested to receive angiotensinergic input from the subfornical organ (SFO) with anatomical, neurochemical and electrophysiological evidence (Ferguson et al. 2001).

Not only Ang II but also AT1 receptors were predominantly expressed in all hypothalamic areas involved in the control of hormone production and release, particular in the PVN and median eminence (Tsutsumi and Saavedra 1991).

1.2.4 Ang (1-7)

In recent years it has become evident that the RAS has 2 major arms: a vasoconstrictor/proliferative in which the main mediator is Ang II, and a vasodilator/anti-proliferative, in which the major effector is Ang (1-7) acting on the G protein–coupled receptor (GPCR) Mas (Santos et al. 2003).

The heptapeptide Ang (1-7) is derived from Ang II and/or from Ang I. Its generation is catalyzed by endopeptidase P cleavage of Ang I (Wright and Harding 1997), or by the recently discovered

enzyme ACE2 converting Ang I to Ang (1-9). Then Ang (1-7) is produced by ACE cleavage of the dipeptide phenylalanine-histamine from Ang (1–9) (Vauquelin et al. 2002). Ang II also can be further metabolized to Ang (1-7) by ACE2 (Turner et al. 2002) (Fig. 1.7).

1.2.4.1. ACE2

ACE2 shares 42% sequence identity to the catalytic domain of ACE. In addition, ACE2 can convert Ang II into Ang (1-7). ACE2 shows 400 fold higher substrate preference for Ang II than for Ang I (Vickers et al. 2002). ACE2 is expressed in heart, kidney, liver and intestine (Donoghue et al. 2000). ACE2 may play a role as negative regulator of ACE. Furthermore, ACE2 acts as a tissue-specific negative feed-back regulator of the activated RAS. This action is probably mediated by Ang (1-7) and bradykinin (Pagliaro and Penna 2005), which is in agreement with the reduced ACE2 level in several rat models of hypertension (Yagil and Yagil 2003). Deficiency of functional ACE2 resulted in severe cardiac dysfunction associated with an accumulation of cardiac Ang II (Crackower et al. 2002). Chronic treatment with AT1 receptor antagonist induced ACE2 mRNA level in the SHR rats as well as increased Ang (1-7) level (Igase et al. 2005). ACE inhibitors promote Ang II antiproliferation by increasing the generation of Ang (1-7) in the vasculature (Tom et al. 2003).

1.2.4.2. Ang (1-7) function

In contrast to Ang II, Ang (1-7) is neither a dipsogen nor an aldosterone secretagogue, but similarly to Ang II, it releases vasopressin and prostaglandins in the brain (Schiavone et al. 1988). In addition, Ang (1-7) can improve the baroreceptor reflex and modulates the circadian rhythms of blood pressure and heart rate (Campagnole-Santos et al. 1992; Silva-Barcellos et al. 2001; Sampaio et al. 2007). Peripherally, the most important actions of Ang (1-7) appear to be related to the control of hydroelectrolyte balance (Santos and Campagnole-Santos 1994).

A. Vascular function

The blood vessels are an important site for the formation and biological actions of Ang (1-7) (Heitsch et al. 2001). In endothelial cells, Ang (1-7) stimulates prostaglandin release (Jaiswal et al. 1992), increases the release of nitric oxide (Porsti et al. 1994), augments the metabolic actions of bradykinin via inhibiting ACE activity (Abbas et al. 1997), and inhibits smooth muscle cell

growth (Freeman et al. 1996). Contrary to Ang II, which promotes thrombosis, Ang (1-7) acts as an antithrombotic agent in the venous thrombosis model in renal hypertensive rats (Kucharewicz et al. 2000).

B. Heart function

Ang (1-7) was protective against ischemia induced cardiac functional impairments and cardiac arrhythmias in isolated rat hearts (Ferreira et al. 2002). It was also shown to preserve cardiac function, coronary perfusion, and aortic endothelial function in a rat model for heart failure (Loot et al. 2002) and also reversed cardiac hypertrophy and fibrosis in rats (Iwata et al. 2005). Ang (1-7) overexpressing rats were more resistant than control animals to induction of cardiac hypertrophy by isoproterenol and had a reduced duration of reperfusion arrhythmias and improved post ischemic function in an isolated perfused heart model (Santos et al. 2004).
Since Ang (1–7) is elevated after treatment with ACE inhibitors or AT1 receptor blockers, Ang (1–7) may indirectly contribute to their beneficial effects on cardiac dysfunction and ventricular remodeling after myocardial infarction (Tallant et al. 2005). Therefore this peptide and its receptor are potential targets for the development of cardioprotective or anti-hypertensive agents.

1.2.5 Mas gene

1.2.5.1. Identification of *Mas* protooncogene

MAS was first discovered in 1986 and was originally described as a protooncogene due to its ability to transform NIH 3T3 cells in tumorigenicity assay in nude mice with DNA from a human epidermoid carcinoma cell line (Young et al. 1986). By in situ hybridization, (Rabin et al. 1987) mapped the human *MAS* gene to the distal half of chromosome 6q (6q24-q27), within a region frequently rearranged in malignant cells. Later on it was shown that activation of MAS additionally appears after transfection of human acute myelocytic leukemia DNA (Janssen et al. 1988) and human ovarian carcinoma DNA (van 't Veer et al. 1988). Most probably, the rearrangement of the 5'-noncoding sequences that appeared during transfection was responsible for the activation of MAS, which in turn led to the tumorigenicity in nude mice. Nevertheless, in all three primary tumors the MAS gene was not rearranged and had a weak focus-inducing activity in transfected NIH 3T3 cells. Further studies showed that Mas could promote the growth of rodent fibroblasts in serum-free medium (Andrawis and Abernethy 1992). In contrast,

overexpression of *Mas* in cones of retina induces cell death without tumor formation (Xu et al. 2000). Furthermore, experiments with transgenic mice overexpressing *Mas* ubiquitously and specifically in the brain did not reveal any tumor formation (our unpublished data), confirming that the *Mas* gene per se has no oncogenic activity. Therefore, most of the follow-up studies were focused on the elucidation of the physiological role of Mas and of the signalling pathways employed by this receptor.

1.2.5.2. Mas is a member of the GPCR family

The analysis of human MAS cDNA sequence revealed an open reading frame that codes for a 325 amino acid protein (Young et al. 1986). This protein has seven hydrophobic transmembrane domains, whereas N- and C-terminal ends are hydrophilic and shares strong sequence similarity with the GPCR subfamily of hormone-receptor proteins (Probst et al. 1992). More specifically, Mas belongs to the Class A Orphan GPCRs (http://www.gpcr.org/7tm/multali/multali.html). In fact, Mas was the first member of a GPCR subfamily, which include proteins sharing around 35% homology with Mas at the protein level. Besides the mas-related-gene (mrg) (Monnot et al. 1991) and the rat thoracic aorta gene (RTA) (Ross et al. 1990), the subfamily includes a group of approximately 50 GPCRs related to Mas, called Mrg (*Mas*-related genes), a subset of which is expressed in specific subpopulations of sensory neurons that detect painful stimuli (Dong et al. 2001; Burstein et al. 2006).

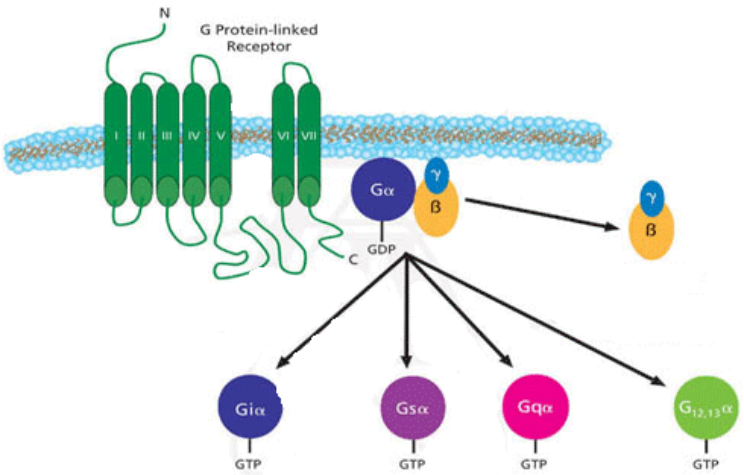

Fig. 1.8 GPCR structure and signalling
(http://nlp.postech.ac.kr/Research/POSBIOTM/content/intro.html)
GPCR are composed of 7 transmembrane domains. The G protein α subunit (Gα) cycles between an inactive GDP-bound form and an active GTP-bound form, where the inactive α subunit is bound to the receptor and to a βγ heterodimer (G β and Gγ). Upon ligand stimulation, the receptor stimulates GDP-GTP exchange to promote the formation of the GTP-bound βγ subunit. G proteins have been grouped into four subfamilies: Gs, Gi/o, Gq and G12 according to their down stream signalling effects.

Intracellular signalling of GPCRs is mediated by one or more members of the heterotrimeric G protein family (Fig. 1.8). The G protein α subunit (Gα) cycles between an inactive GDP-bound form and an active GTP-bound form, where the inactive α subunit is bound to the receptor and to a βγ heterodimer (Gβ and Gγ). Each subunit is further subgrouped into classes comprising at least 20 Gα, 6 Gß and 12 Gγ, thereby providing a variety of combinations between receptor subtypes to downstream G protein subunits. On the basis of sequence similarities in their Gα subunits, G proteins have been grouped into four subfamilies: Gs, Gi/o, Gq and G12. Whereas stimulatory (Gs) and inhibitory (Gi/o) G proteins are implicated in the regulation of adenylyl cyclase and the gating of ion channels, members of the Gq subfamily activate phospholipase C. Upon ligand stimulation, the receptor stimulates GDP-GTP exchange to promote the formation of the GTP-bound βγ subunit, which then dissociates from both the receptor and the GTP βγ dimer. Both the Gβγ and its subfamilies then mediate activation of downstream effectors, including activation (Gβγs) or inhibition (Gβγi) of adenylyl cyclase or activation of phospholipase C.

In addition to human, the *Mas* gene was isolated and characterized in rat and in mouse (Young et al. 1988; Metzger et al. 1995) The mouse and rat homologues show 97% identity between each other compared to 91% between mouse and human indicating that *Mas* is highly conserved, except in its hydrophilic amino-terminal domain. The recent advance in the sequencing of genomes of model organisms revealed that the *Mas* gene is also conserved in other species, including rhesus monkey, opossum, dog, and chicken, whereas in frog, zebrafish, and fugu there is no Mas homologue (http://ecrbrowser.dcode.org).

Mas gene structure as well as the regulation of *Mas* expression at the transcriptional level is relatively poorly studied. Like 90% of mammalian GPCRs, the open reading frame of *Mas* is not interrupted by introns (Jackson and Hanley 1989; Gentles and Karlin 1999), whereas at least in mouse several 5' untranslated exons are existing (Schweifer et al. 1997), and our unpublished data).

1.2.5.3. *Mas* expression pattern

A. Brain

Brain was the first organ where *Mas* was found to be highly expressed (Young et al. 1988). High amounts of *Mas* transcripts are present in the hippocampus and cerebral cortex of rat brain (Bunnemann et al. 1990). Martin et al. (1992) could show by *in situ* hybridization and RPA that *Mas* mRNA is expressed in a subpopulation of neurons in both the adult and developing rat central nervous system (CNS). In the adult CNS, *Mas* mRNA was most abundant in hippocampal

pyramidal neurons and dentate granule cells but also presented at low levels in the cortex and thalamus. Recently, *Mas* expression was also discovered in cardiovascular regions of the brain by Western blot and immunofluorescence (Becker et al. 2007). The study of *Mas* expression during rat ontogenesis showed that *Mas* is first expressed in the developing rat CNS at postnatal day 1. Even at this early stage in CNS development the pattern of *Mas* expression was similar to that seen in the adult (Martin et al. 1992). Furthermore, brief seizure episodes led to a significant and transient increase in *Mas* mRNA in the rat hippocampus, that may contribute to anatomical and physiological plasticity associated with intense activation of hippocampal pathways (Martin and Hockfield 1993).

In the mouse, the distribution of *Mas* mRNA in the brain is comparable to the rat being highest in the hippocampus and piriform cortex as detected by in situ hybridization (Metzger et al. 1995).

Kitaoka (Kitaoka et al. 1994) investigated the distribution of *MAS* expression in the rhesus macaque retina by *in situ* hybridization. They demonstrated a weak positive signal above the neurons of the retina, suggesting that *MAS* can be used as a possible marker for the retinal pigment epithelium.

B. Testis

We examined the ontogenetic profile of *Mas* expression and could demonstrate high levels of *Mas* mRNA in mouse and rat testis (Metzger et al. 1995; Alenina et al. 2002). *Mas* is also expressed in testis of rodents in a development-dependent manner (Bunnemann et al. 1990). Testicular *Mas* mRNA from rats was shown to be markedly increased during development beginning 5 weeks after birth and reaching their highest concentrations at 25 weeks of age (Metzger et al. 1995).

A similar profile of *Mas* expression in testis was also observed in mice: *Mas* mRNA is not detectable in testis of newborn animals, but its expression is dramatically upregulated, starting two weeks after birth and continuously increasing during puberty until 6 months of age when it becomes maximal (Alenina et al. 2002). Additional experiments using *in situ* hybridisation in 3 month-old mouse testis demonstrated a distinct expression of the *Mas* gene in Leydig and Sertoli cells, being much more pronounced in Leydig cells (Alenina et al. 2002). Interestingly, the well-controlled regulation of *Mas* expression in testis temporally coincides with the transformation of immature adult Leydig cells to mature cells. This period is also characterized by an increase in the testicular testosterone-secreting capacity of these cells. By the accomplishment of this transition, puberty is reached and overall testicular steroidogensis is approaching adult levels. All in all,

indicating that *Mas* is a marker for adult Leydig cells and may be involved in the function of this cell type.

C. Cardiovascular and other tissues

RT-PCR and RPA have discovered low levels of *Mas* expression also in other tissues of mice such as heart, kidney, lung, liver, spleen, tongue, and skeletal muscle (Villar and Pedersen 1994; Metzger et al. 1995). In the heart low levels of *Mas* transcripts were detected in cardiomyocytes and much higher concentrations in the endothelium of coronaries. Similarly *Mas* expression in the brain endothelium was shown before for cultured endothelial cells derived from rat cerebral resistance vessels (Kumar et al. 1996). In addition, *Mas* was detected with specific antibodies in the vessels of the corpus cavernosum (da Costa Goncalves et al. 2007). Altogether, these data indicate that *Mas* is expressed in the endothelial layer of different vessel types supporting an important role of this protein in the function of the endothelium.
Mas expression was also found in the smooth muscle of uterus and in bone marrow, whereas lung, liver and ovary were free of such transcripts.

1.2.5.4. Interaction of Mas with the RAS

The first attempts to clarify the function of Mas protein in *Xenopus* oocytes characterized it as Ang II receptor (Jackson et al. 1988). However, the activation of inward currents by Ang II in Mas-injected Xenopus oocytes was not inhibited by Ang II antagonists. In addition, the major Ang II receptors AT1 and AT2 were discovered afterwards and exhibited only 8% and 19% amino acid homology, respectively, to the Mas protein (Sasaki et al. 1991; Mukoyama et al. 1993). On the other hand, Ambroz *et al.* could show that the intracellular Ca^{2+} increase in Mas-transfected cells after Ang II treatment was only observed in cells expressing endogenous the AT1 receptor (Ambroz et al. 1991), and that *Mas* expression in the heart of rats showed its downregulation by AT1 receptor blockade (Ferrario et al. 2005). Thus, Mas seems to be a modulator of AT1 signaling.
Wolf (Wolf et al. 1992) could demonstrate that permanent transfection of a murine renal tubular cell line with Mas changed the hypertrophic actions of Ang II into a proliferative response.
Recently, it was shown that Mas can hetero-oligomerize with the AT1 receptor and inhibit the actions of Ang II being a physiological antagonist of the AT1 receptor (Kostenis et al. 2005). Possibly by this direct interaction, Mas is able to rescue binding and functionality of an AT1

receptor double mutant in CHO or COS7 cells (Santos et al. 2007). Furthermore, Sampaio *et al*. (Sampaio et al. 2007) recently showed in endothelial cells that Ang (1-7) via Mas counteracts Ang II and AT1 dependent c-Src activation and thereby ERK1/2 phosphorylation and the generation of ROS by NAD(P)H oxidase. Comparable results have been obtained in proximal tubular cells of the kidney (Su et al. 2006). Interestingly, both studies did not find a direct inhibitory activity of Ang (1-7) on ERK1/2 phosphorylation in contrast to the studies in cardiomyocytes mentioned above (Tallant et al. 2005).

Although Mas negatively influences the signalling of the AT1 receptor it induces an upregulation of receptor binding. This could be explained by a constitutive capacity of Mas activating the $G\alpha_{q/11}$ and stimulating protein kinase C-dependent phosphorylation of the AT1 receptor at its C-terminus (Canals et al. 2006).

Mas-knockout mice were also used to clarify the interaction between Mas and AT1. The distribution of cells expressing AT1 receptors in different limbic and thalamic brain structures in *Mas*-knockout and in wild type (WT) mice showed no significant alterations between the two strains by an immunohistochemical approach (Von Bohlen und Halbach et al. 2000). However within the amygdala, Ang II induced an increase in the field potentials in WT mice, while in *Mas*-knockout animals Ang II reduced them. Moreover, mice lacking the *Mas* gene showed enhanced Ang II mediated vasoconstriction in mesenteric microvessels (Peiro et al. 2007).

Recently, it was shown that AT1 might interact with AT2 (AbdAlla et al. 2001). They form stable heterodimers, causing increased activation of Gβγq and Gβγi, the two major signalling proteins triggered by AT1. Furthermore there is the evidence that Mas might functionally interact with both AT1 and AT2 receptors. When AT1 receptor was blocked, Ang (1–7) produced vasodilation in perfused mouse hearts. This effect could be blocked with an AT2 antagonist and was only seen in animals expressing the *Mas* gene. When AT2 alone was blocked, perfusion with Ang (1-7) produced a coronary vasoconstriction and it is not clear if this is mediated only by the AT1 receptor (Castro et al. 2005).

1.2.5.5. Signalling of Mas

Considerable efforts were made to find out which signal transduction pathways are employed by Mas. Zohn *et al*. (Zohn et al. 1998) suggested that Mas mediates the activation of GTP-binding protein Rac-dependent signalling pathway. Rac belongs to the Ras superfamily of GTPases. Mas and Rac 1 activated JNK and p38. Moreover, expression of Mas leads to activation of phospholipase C, indicating that Mas couples to the Gq/11 family of heterotrimeric G proteins,

hence stimulate PKC dependent phosphorylation of the AT1 receptor (Canals et al. 2006). One of the major pathways of Mas signalling in the cardiovascular system is the phosphorylation of Akt. Giani *et al*. (Giani et al. 2007) could show that this pathway is activated by Ang (1-7) in the heart and can be blocked by the antagonist A-779 indicating that the effect is mediated by Mas. Another study using cardiomyocytes showed an inhibition of MAP kinase activation by Ang (1-7) which could be blocked by antisense oligonucleotides against *Mas* (Tallant et al. 2005). Ang (1–7) reduces the growth of cardiomyocytes through activation of Mas in cultured neonatal rat myocytes.

1.2.5.6. *Mas*-knockout mice

Targeted deletion of the genomic region coding for the amino-terminal 253 amino acids of Mas including six transmembrane domains led to a loss of Mas expression (Walther et al. 1998). The homozygous *Mas*-deficient mice on the mixed 129xC57BL/6 genetic background were healthy, grew normally, and showed no obvious developmental abnormalities.

1.2.5.6.1. Mas is an Ang (1-7) receptor

Being discovered already in 1986, the direct function of Mas was unclear for more than a decade. Only after the generation of *Mas* knockout mice (Walther et al. 1998), it was possible to uncover the ligand binding to Mas. In these mice the binding of Ang (1-7) to kidney sections was abolished (Santos et al. 2003). Accordingly, *Mas*-deficient mice completely lack the antidiuretic action of Ang (1-7) after an acute water load. Furthermore, *Mas*-deficient aortas lose their Ang (1-7)-induced relaxation response. Coincident with this finding, AVE0991, a nonpeptide mimetic of Ang (1-7), induced an equipotent vasodilator effect in aortic rings like Ang (1-7) in WT mice. This effect could be blocked by two specific Ang (1-7) receptor antagonists, A-779 and D-Pro^7-Ang (1-7) (Lemos et al. 2005). As expected, AVE0991 (mimics the effects of Ang (1-7)) failed to induce vasodilation in *Mas*-deficient aortic rings. As observed previously for Ang (1-7), the antidiuretic effect of AVE0991 after water load was also blunted in *Mas*-knockout mice (Pinheiro et al. 2004).

In vitro studies confirmed that Ang (1-7) is a Mas ligand since it bound to *Mas*-transfected cells and elicited arachidonic acid release (Santos et al. 2003).

Collectively, these findings identify Mas as a functional receptor for Ang (1-7) and provide a clear molecular basis for the physiological actions of this peptide. Nevertheless, it can not be excluded that Mas may have additional ligands and that Ang (1-7) may have additional receptors.

1.2.5.6.2. Central autonomic control

Blood pressure variability (BPV) and heart rate variability (HRV) are relevant predictors of arterial hypertension and cardiovascular diseases in humans. Both anaesthetized *Mas*-knockout males and females (on the mixed genetic background) were normotensive and showed no alteration in baseline heart rate (Walther et al. 1998). However, in particular *Mas*-deficient females showed a strong reduction of HRV (Walther et al. 2000). Despite that the influence of *Mas*-deficiency on BPV was much lower than on HRV in females, a significant increase in BPV was observed in *Mas* knockout males. In addition, the autonomic balance was shifted in favour of the sympathetic tone in both sexes.

The baroreceptor reflex is an important factor in the homeostatic regulation of the cardiovascular system. It maintains the stability of blood pressure, and an impaired baroreflex might be a major cause of hypertension and end-organ damage (Shan et al. 1999). Apparently, there were sex specific differences in the sensitivity of the baroreflex between WT and *Mas*-knockout animals, which, however, did not reach statistical significance. Taken together, these results suggest that *Mas* is involved in central cardiovascular actions such as the control of the HRV, BPV, and spontaneous baroreflex fluctuations (Walther et al. 2000). These alterations are probably related to the described baroreflex-modulating actions of Ang (1-7) in the rostral ventral lateral medulla (RVLM) of the brain stem (Silva-Barcellos et al. 2004; Alzamora et al. 2006) and suggest a protective function of the Ang (1-7) /Mas axis in the central regulation of cardiovascular parameters.

1.2.5.6.3. Cardiac function in *Mas* knockout out mice

In vitro studies with isolated hearts of *Mas* knockout and WT mice were subjected to global ischemia, hearts from WT mice showed a significant decrease in systolic tension and an increase in diastolic tension. During reperfusion both parameters were increased. Depletion or blockade of Mas markedly attenuated these changes in isolated hearts (Castro et al. 2006). These results indicate that Mas plays an important protective role in cardiac function during

ischemia/reperfusion which is in keeping with the beneficial cardiac and coronary effects previously described for Ang (1-7).

In vivo, *Mas* deficiency impairs heart function and produces a marked change in the extracellular matrix toward a pro-fibrotic state. Systolic tension, +dT/dt, and –dT/dt were significantly lower in isolated hearts of Bl/6 *Mas* knockout mice. A decreased fractional shortening revealed by echocardiography, as well as posterior wall thickness in systole and left ventricle end-diastolic dimension, and a higher left ventricle end-systolic dimension. A markedly lower global ventricular function, as defined by a higher myocardial performance index, was observed. In addition, *Mas*-knockout mice presented a higher coronary perfusion pressure compared with control mice (Santos et al. 2006).

1.2.5.6.4. Endothelial function

Endothelial dysfunction is an initial step in the pathogenesis of cardiovascular diseases. Ang (1-7) mediated relaxation of isolated mesenteric arteries was equally impaired in both WT mice pretreated with A-779 and *Mas*-deficient mice (Peiro et al. 2007). Importantly, the response to the endothelium-dependent vasorelaxants, BK and ACh was comparably inhibited, while endothelium-independent vessel relaxation by sodium nitroprusside (SNP) was unaltered in these vessels. A-779-induced impairment of endothelial function was confirmed *in vitro*, since BK-mediated NO release was increased by Ang (1-7) and blunted by A-779 pretreatment in primary human endothelial cell cultures.

1.2.5.6.5. Brain phenotype in *Mas* knockout out mice

A. Morphology

Despite the high expression of *Mas* in the brain, no obvious alterations could be detected in the morphology of the hippocampus and its subregions indicating that the cytoarchitectural distribution patterns and the fine wiring of neuronal subtypes is not affected by *Mas* ablation.

B. Long term potentiation and memory

In addition to Ang II and IV, Ang (1–7) may also be involved in learning and memory since Ang (1–7) enhances long-term potentiation (LTP) in the hippocampus (Hellner et al. 2005). The dramatic improvement of LTP in the CA1 region of the hippocampus after theta-burst

stimulation, observed in *Mas*-knockout mice is in agreement with these data (Walther et al. 1998). A-779 blocked this LTP-enhancing effect of Ang (1–7) in WT mice and low concentrations of Ang (1–7) did not change the magnitude of CA1-LTP in *Mas*-deficient mice. Furthermore, *Mas* ablation leads to an improved maintenance of LTP in the dentate gyrus. Thus, Mas mediates Ang (1–7)'s LTP-promoting effect in the brain.

In contrast to its significant effects on LTP, which would classify *Mas* as a memory suppressor gene (Abel et al. 1998), its ablation and overexpression did not result in clear changes of spatial learning in both Morris Water Maze and Shuttle box experiment (Walther et al. 1998).

C. Anxiety

To check on changes in anxiety, *Mas*-deficient animals were examined in the Elevated-Plus Maze that is based upon the natural aversion of rodents for open spaces. Thus, mice exposed to the maze usually prefer the closed arms over the open arms. *Mas*-deficient male mice entered significantly less often the open arms of the maze and spent less time on this section than did the controls (Walther et al. 1998), whereas *Mas*-deficient females showed no differences (Walther et al. 2000). Thus, the behavioral data showed a significantly higher level of anxiety in *Mas*-deficient male mice, implicating that the lack of Mas protein influences anxiety in a sex specific manner.

1.2.5.6.6. Renal function in *Mas* knockout out mice

In water-loaded C57Bl/6 mice, AVE 0991 produced a significant reduction in urinary volume, associated with an increase in urinary osmolality. The Ang (1-7) antagonist, A-779, completely blocked the antidiuretic effect of AVE 0991. *Mas*-deficient mice completely lack the antidiuretic action of Ang (1-7) after an acute water load (Santos et al. 2003; Pinheiro et al. 2004).

1.2.5.6.7. Testis phenotype

In spite of the high expression of *Mas* in adult Leydig cells, which are essential for steroidogenesis and reproduction, *Mas*-deficient mice grew normally, were healthy and fertile, and had no alterations in the number of offspring in comparison to WT animals (Walther et al. 1998), indicating that *Mas* seems to be not essential for fertility or redundant systems may exist.

Despite increased relative weights of testes in *Mas*-knockout males, the number and motility of spermatocytes as well as testis morphology was unchanged.

1.2.5.6.8. Erectile dysfunction

Ang (1-7) potentiated the elevation of the corpus cavernosum pressure as well as NO release in rats. The facilitatory effect of Ang (1-7) was completely blunted by the specific Ang (1-7) receptor blocker A-779 and the NOS inhibitor N(omega)-nitro-L-arginine methyl ester (L-NAME). *In vivo* incubation of rat and mouse corpus cavernosum strips with Ang (1-7) resulted in an increase of NO release. This effect was completely abolished in *Mas*-deficient mice. Functionally, absence of Mas resulted in compromised erectile function due to penile fibrosis and severely depressed response to electrical stimulation. Furthermore, the attenuated erectile function of DOCA-salt hypertensive rats was fully restored by Ang (1-7) administration. Ang (1-7)-Mas axis seems to take a key role in erectile function (da Costa Goncalves et al. 2007).

1.3. Arginine vasopressin (AVP)

1.3.1. AVP generation and function

The nonapeptide hormone AVP gene is a highly expressed endogenous gene in hypothalamus, AVP is synthesized mainly in the magnocellular neurones of the supraoptic nucleus (SON) and the parvocellular neurons of the PVN of the hypothalamus (Vandesande et al. 1975). AVP is also synthesized in the suprachiasmatic nucleus of the hypothalamus and in some peripheral organs (Schmale et al. 1983; Robinson et al. 1988).

AVP can regulate adrenocorticotropic hormone secretion from the anterior pituitary (Plotsky et al. 1989). It is transported through axons, stored in the neurohypophysis, and then released into the peripheral circulation to regulate body fluid tonicity, and possibly cardiovascular function (Robertson 1976; Schrier and Bichet 1981). AVP is involved in the maintenance of homeostatic salt and water balance during dehydration by promoting water reabsorption in the kidney (Lolait et al. 1992).

1.3.2. AVP gene structure

The AVP gene is approximately 2 kb in size and consists of 3 exons and 2 introns, encoding a signal peptide, vasopressin, neurophysin II, and a carboxy-terminal glycopeptide (Schmale et al. 1983; Sausville et al. 1985) (Fig. 1.9).

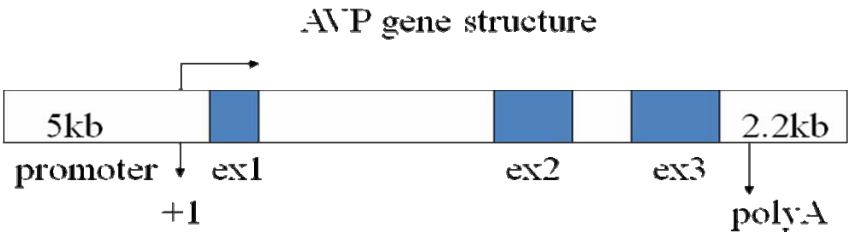

Fig. 1.9 Structure of the AVP gene
Ex 1, 2 and 3: exon 1, 2 and 3. +1, transcription starting point.

1.3.3. Stimulation of AVP expression by physiological stimuli

The activity of the AVP promoter can be increased by physiological stimuli. There are two ways to induce AVP expression. One way is water deprivation, which depletes the intracellular and extracellular compartments of water and consequently increases plasma osmolality and decreases intravascular volume. In water-deprived rats, peripheral RAS activity, circulating levels of AVP, and sympathoadrenal activity are all increased. Another way to increase the AVP gene expression was demonstrated by 7 days of salt loading (Murphy et al. 1989). Meneely and his collaborators have shown that chronic ingestion of excess sodium chloride alone would produce hypertension in rats which mimics human hypertension morphologically (Meneely et al. 1953). Its onset may occur at different intervals following the onset of salt-feeding, and its character may vary from mild to severe extent (Dahl 2005).

1.3.4. Use of AVP promoter for transgenic expression

The AVP gene is peculiarly expressed in hypothalamus by its specific promoter targeting activity (Zeng et al. 1994). Regulation of AVP expression *in vivo* is differential: it can be stimulated by osmotic and hypovolemic stimuli in magnocellular neurons of the SON and PVN (Burbach et al. 1984; Davis et al. 1986; Sawchenko 1987). AVP messenger RNA (mRNA) content is increased after water deprivation in hyperosmolar rats (Zingg et al. 1986). However, the mechanisms of transcriptional regulation of the AVP gene within the cell are not well known.

For exploring the AVP promoter as a transgenic tool, several investigations were conducted to find regulatory elements responsible for the tissue-specificity of AVP expression *in vivo*. First attempts to test the AVP promoter used transgenic mice models (Ang et al. 1993). Genomic regions were identified that are sufficient for the appropriate tissue-specific expression and physiological regulation of the AVP gene. The expression of a 13.4 kb AVP genomic fragment containing 9 kb of 5' upstream sequence, the AVP coding sequence and 1.5 kb of sequence 3' of the structural gene was restricted to discrete groups of hypothalamic neurons in three lines.

In parallel to this work, a transgenic mouse containing a shorter genomic clone of the rat AVP gene was developed. The rat AVP transgene was shown to have similar tissue distribution of expression as the endogenous mouse AVP gene. But expression of the transgenic AVP mRNA was also found in the lung and pancreas of the transgenic mice, sites of known ectopic expression of AVP. Moreover the transgene could be stimulated by 72 h of water deprivation (Grant et al. 1993).

Another successful model of a transgene consisting of the rat AVP structural gene contained a reporter gene in exon III, flanked by 5 kb of upstream and 3 kb of downstream sequences. It was expressed in vasopressinergic, but not oxytocinergic, magnocellular neurons of transgenic rats. The transgene response to osmotic challenge exceeded that of the endogenous gene by 10–15 folds (Zeng et al. 1994).

Not only longer 5´ upstream sequence exhibited adequate promoter activity. In small cell lung carcinoma cell system, the promoter activity of 1.5 kb construct was significantly increased by endothelin 3 or high osmolality. Thus, the 5' flanking sequence between -1500 and -532 contains the elements responsible for osmotic and non-osmotic stimulation of AVP gene transcription (Kim et al. 1996).

Further investigation used a construct containing 3.8 kb of the 5' flanking region and all the exons and introns in the mouse AVP gene fused at the end of exon 3 to a reporter gene. The results revealed that cis–elements responsible for the cell-specific expression of the AVP gene were located 2.1 kb 3´ downstream of exon 3 of the AVP gene (Jeong et al. 2001), comparable results were shown that 3 kb 5’ promoter region and 0.2 kb of 3’ UTR sequences were responsible for transgenic expression (Davies et al. 2003). In the case of the other 2 constructs of 5 kb and 11 kb of upstream sequences used for transgenic mice, low basal expression was seen in the neurons of the SON and PVN, and transgene expression was increased markedly in these cells following dehydration.

To combine all the data, it was decided to use 5 kb 5’ promoter region and all exons and introns of the rat AVP gene in this project.

1.4. Biological peptide pump

To investigate effects of angiotensin peptides, the novel technology of a biological peptide pump was developed in the group of Reudelhuber (Methot et al. 2001) (Fig.1.10).

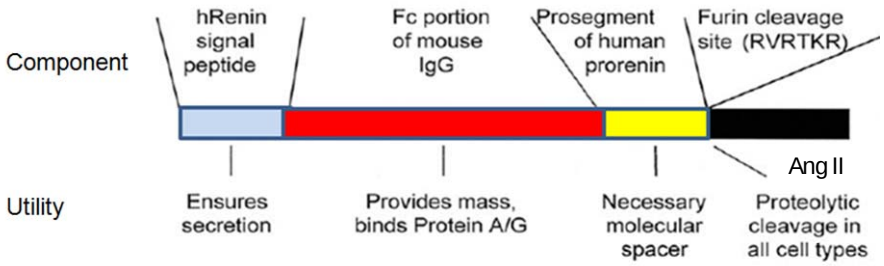

Fig. 1.10 Scheme of the fusion protein
The human prorenin signal peptide is linked to a portion of the mouse heavy chain constant region of IgG2b. The IgG2b fragment is linked to a portion of the human prorenin prosegment containing a cleavage site at its carboxyl terminus for furin which allow the release of the peptide of interest (eg. Ang II).

The essential features of this fusion protein are as follows: A signal peptide from human prorenin, which ensures that the protein will enter the endoplasmic reticulum for secretion from the cell, is linked to a portion of the mouse heavy chain constant region of IgG2b.

Normally, the heavy chains of immunoglobulins form disulfide bridged dimers in the secretory pathway where they bind to a protein called BiP, while binding the light chain. The Ig fragment chosen does not contain either the intermolecular disulfide bridge or the BiP-binding region, therefore, this fragment is primarily secreted as a monomer (Jutras et al. 2000). The immunoglobulin portion of the molecule does not only provide mass for the efficient production of the protein precursor in the secretory pathway, but it also greatly facilitates expression of a broad assortment of linked peptides (Brechler et al. 1996), perhaps because it adopts a stable conformation, thereby avoiding the degradation of poorly folded proteins, which is known to occur in the secretory pathway (Ellgaard et al. 1999). Another advantage of using this portion of the mouse IgG molecule is that it contains a protein A-binding region, making it possible to easily purify the fusion protein from cell culture supernatants. The immunoglobulin fragment is linked to the peptide of interest by a portion of the human prorenin prosegment containing a cleavage site at its carboxyl terminus for a protease. This “molecular spacer” is necessary to expose the protease processing site for the cleavage, which results in the release of the peptide. The prorenin prosegment was used because it is predicted to form a number of α-helical coils (Heinrikson et al. 1989), which would increase its flexibility.

The angiotensin peptide used in this study is released by a single cleavage, by the processing protease furin, leading to the constitutive secretion of the released peptide. Furin is a serine protease related to bacterial subtilisin and the yeast kexin proteases as a mammalian homolog. It is a membrane-bound protease that remains primarily in the trans-Golgi network of the secretory pathway of virtually all mammalian cells (Molloy et al. 1999). The peptide cleavage site designed in the fusion protein is suitable to furin by modifying the natural prorenin prosegment cleavage site (PMKR to RVRTKR; Fig.1.10). After cleavage, the encoded peptide is released in the secretory pathway and secreted by the cell.

The first application of this strategy was for creating transgenic mice, which utilized this fusion protein to release Ang II from cardiomyocytes (van Kats et al. 2001). Expression of the transgene resulted in high Ang II levels in the heart and release of the peptide into the circulation. High circulating Ang II led to hypertension and structural remodeling (ventricular enlargement and cardiac fibrosis) of the heart in this model. That elevated cardiac Ang II levels alone did not directly induce cardiac hypertrophy but increased interstitial fibrosis was concluded from this study.

By applying this transgenic strategy, Lochard and colleagues (Lochard et al. 2003) restored Ang II expression exclusively in the brain of AOGEN-deficient mice. In this system, Ang II was released from an artificial protein during secretion. With these animals, they demonstrated that brain-specific Ang II could correct the hydronephrosis and partially renal dysfunction normally observed in AOGEN-deficient mice.

In addition, the same strategy was applied to overexpress Ang (1-7) under CMV promoter control in transgenic rats (Santos et al. 2004). The model showed doubling of circulating Ang (1-7) level. Furthermore, transgenic rats were more resistant than control rats to induction of cardiac hypertrophy by isoproterenol.

1.5. Aims of the thesis

Although the RAS has been studied for more than 100 years, there are still open questions. To address the *in vivo* function of Ang II, a novel transgenic mouse model (TGM L102) with systemic overexpression of AOGEN was going to be characterized in this thesis. In particular, hemodynamic parameters and end organ damage should be examined.

Moreover, a novel transgenic rat model with brain specific Ang II overexpression should be generated, to clarify the role of the brain Ang II in the regulation of hypertension.

Counteracting the effects of Ang II, Ang (1-7) and its receptor Mas have broadened our view on the RAS. However, how Mas and Ang (1-7) regulate vascular function is still an unsolved question. *Mas* is expressed in vascular endothelium, which at the same time is an important site for Ang (1-7) generation. In rats, short-term Ang (1-7) infusion improves *in vivo* endothelial function primarily via NO release. On the other hand, Ang (1-7) attenuates Ang II-induced ROS generation in endothelial cells. This knowledge lead to the hypothesis that Mas could be involved in the balance between NO and ROS and may therefore be an important mediator of cardiovascular regulation. Previous attempts to study the cardiovascular function of Mas were limited by the heterogeneous genetic background of the *Mas*-deficient animals used. Therefore, *Mas*-deficient mice should be backcrossed for 7 generations onto the FVB/N and Bl/6 background. In these animals, the cardiovascular actions and the signalling pathways of Mas should be studied and gene expression profiling should be employed to uncover down stream mediator of Mas.

2. Materials

2. Materials

2.1. Reagent

2.1.1. Chemicals

Acrylamide (40%, 20:1)	Carl Roth	Karlsruhe, Germany
acetylcholine(ACh)	Sigma	München, Germany
Agar	Difco	Kansas City, USA
Agarose	Gibco	Betheseda, USA
Ammonium acetate	Sigma	München, Germany
Ammonium persulfate	Sigma	München, Germany
Ampicillin	Serva	Heidelberg, Germany
Bacto-Tryptone	Difco	Kansas City, USA
Bacto-Agar	Difco	Kansas City, USA
Bacto-Yeast-Extract	Difco	Kansas City, USA
Bis-Acrylamide	Serva	Heidelberg, Germany
Bromophenol blue	Sigma	München, Gramany
BSA	Biomol	Hamburg, Germany
Butylated hydroxytoluene	Sigma	München, Germany
Chloroform	Merck	Darmstadt, Germany
Diethyl pyrocarbonat (DEPC)	Sigma	München, Germany
Dimethyl sulfoxid (DMSO)	Merck	Darmstadt, Germany
Dithiothreitol	Sigma	München, Germany
dNTP (100 mM)	Amersham	Braunschweig, Germany
λ-DNA/HindIII/EcoRI marker	Fermentas	Vilnius, Lithuania
Eosin Y certified	Sigma	München, Germany
Ethylendiamine-glycol-bis-(ß-amino, ethylether)-tetraacetic acid (EGTA)	Carl Roth	Karlsruhe, Germany
Ethylendiamine-tetraacetic acid (EDTA)	Sigma	München, Germany
Ethanol	Merck	Darmstadt, Germany
Ethidium bromide	Serva	Heidelberg, Germany
Formaldehyde	Merck	Darmstadt, Germany
Formamide	Fluka	New Ulm, Germany
Glycerol	Sigma	München, Germany

Glacial acetic acid	Sigma	München, Germany
Hexamers	Gibco	Betheseda, USA
Haematoxylin (Mayers ämalaunlösung)	Merck	Darmstadt,Germany
H_2SO_4	Merck	Darmstadt,Germany
Hydrochloric acid	Carl Roth	Karlsruhe, Germany
IPTG	Biomol	Hamburg, Germany
Isopropanol	Carl Roth	Karlsruhe, Germany
Kanamycin	Sigma	Taufkirchen, Germany
Ketavet (ketamine 100 mg/ml)	Pharmacia	Erlangen, Germany
KSCN	Sigma	München, Germany
L-NAME	Sigma	München, Germany
Paraformaldehyde	Sigma	München, Germany
Phenol	Sigma	München, Germany
Phenol-Chloroform-Isoamylalcohol	Carl Roth	Karlsruhe, Germany
Phenylmethylsulfonyl fluoride	Carl Roth	Karlsruhe, Germany
Proteinase K	Boehringer	Mannheim, Germany
Rompun (xylazine 2%)	Bayer	Leverkusen, Germany
SDS	Serva	Heidelberg, Germany
Skimmed milk powder	Carl Roth	Karlsruhe, Germany
Sodium acetate	Merck	Darmstadt,Germany
Sodium chloride Sodium dihydrogen	Merck	Darmstadt,Germany
phosphate monohydrate	Merck	Darmstadt,Germany
Sodium dihydrogen phosphate dihydrate	Merck	Darmstadt,Germany
Sodium hydrogen phosphate heptahydrate	Merck	Darmstadt,Germany
Sodium dodecylsulphate	Carl Roth	Karlsruhe, Germany
Sodium nitroprusside	Sigma	München, Germany
Sodium nitrite	Sigma	München, Germany
Thiobarbituric acid	Sigma	München, Germany
TEMED	Gibco	Betheseda, USA
Triton X-100	Serva	Heidelberg, Germany
Tris	Sigma	München, Germany
TRIzol reagent	Gibco	Betheseda, USA
Trichloroacetic acid	Sigma	München, Germany

Urea	Sigma	München, Germany
X-Gal	Biomol	Hamburg;Germany
ΦX174-DNA/HaeIII-Marker	Fermentas	Vilnius, Lithuania
Xylene	Merck	Darmstadt, Germany
Xylencyanol	Bio-Rad	München, Germany
2-Mercaptoethanol	Sigma	München, Germany
2, 3-diaminonaphthalene	Sigma	München, Germany

2.1.2. Enzymes

DNase A	Roche	Basel, Switzerland
DNase I (RNase-free)	Roche	Basel, Switzerland
MMLV	Gibco	Betheseda, USA
DNA ligase	Gibco	Betheseda, USA
Proteinase K	Sigma	München, Germany
Restriction enzymes	Amersham	Freiburg, Germany
RNase A	Roche	Basel, Switzerland
RNasin	Promega	Madison, USA
T4 -DNA-Ligase	Promega	Madison, USA
Taq-DNA-Polymerase	Gibco/BRL	Betheseda, USA

2.1.3. Primary antibodies

Gp91 phox	BD Biosicence # 611415	Heidelberg, Germany
Caveolin-1	Cell Signaling #3238	Frankfurt, Germany
ß-actin	Cell Signaling #4967	Frankfurt, Germany
Akt	Cell Signaling #9272	Frankfurt, Germany
Hsp90	Cell Signaling #4874	Frankfurt, Germany
HRP anti-mouse IgG	Pierce	Bonn, Germany
HRP anti-rabbit IgG	Pierce	Bonn, Germany
Cytochrome C	Santa Cruz Biotechnology	Heidelberg, Germany
Caspase 3	Cell Signaling	Frankfurt, Germany

2.1.4. Kits:

Ambion RPA II kit	AMS Biotechnology	Whitney, UK
QIAquick Gel Extract Kit	Qiagen	Hilden, Germany
Plasmid Maxi Kit	Qiagen	Hilden, Germany
Transcription Kit	Stratagene	La Jolla, USA
Ambion mMessage mMachine Kit	AMS Biotechnology	Whitney, UK
Platinum® SYBR® Green qPCR	Invitrogen	Hilden, Germany
RNeasy Mini Kit	Qiagen	Hilden, Germany
In Situ Cell Death Detection Kit	Roche	Mannheim, Germany
Nitrate/Nitrite Colorimetric Assay Kit	Cayman Chemical	Michigan, USA
8-Isoprostane ELISA Kit	Cayman Chemical	Michigan, USA
Fluka SOD Assay Kit BioChemika	Sigma	München, Germany
SuperSignal West Pico Chemiluminescent Substrate	Pierce	Bonn, Germany
[α-^{32}P] γUTP (800 Ci/mmol)	Amersham	Freiburg, Germany
Quickspin™ columns, Sephadex G-50	Boehringer	Mannheim, Germany

2.2. Equipment

2.2.1. Equipment for molecular biology:

Aga gel Minin	Biometra	Göttingen, Germany
Agarose gel electrophoresis apparatus	Biometra	Niedersachsen, Germany
Analytic balance	Sartorius Analytic	Göttingen, Germany
Bio-imaging Analyzer BAS 2000	FUJIX	Tokyo, Japan
Centrifuge 5415C	Eppendorf	Hamburg, Germany
Centrifuge Sorvall RC 5C	Heraeus	Hanau, Germany
Electrophoresis-apparatus GNA 200	Pharmacia Biotech	Freiburg, Germany
Electrophoresis-power Mini Power PACK P20	Biometra	Göttingen, Germany
Gel-dryer D62	Biometra	Göttingen, Germany
Electroporator 2510	Eppendorf	Hamburg, Germany
Heating bath GFL 1083	Heidolf	Burgwedel, Germany
I cycler	Bio-rad	München, Germany

Incubator (bacteria culture) B6120	Heraeus	Hanau, Germany
Liquid scintillation system Beckman LS6000SC	Beckman	Minnesota**,** USA
Magnetic stirrer Modell MR 3001	Eppendorf	Hamburg, Germany
Master cycler gradient	Biozym	Oldendorf, Germany
Membrane filter (0.22 µm, 0.45 µm)	Millipore	Morlsheim, Germany
Microscope	Leica	Wetzlar, Germany
Mini-Protean®3 Electrophoretic Cell	Bio-rad	München, Germany
Mini Trans-Blot® Electrophoretic transfer Cel	Bio-rad	München, Germany
Mixer Thermomixer compact	Eppendorf	Hamburg, Germany
Peltier thermal Cycler PTC-200	Biozym	Oldendorf, Germany
Power supply for the gel chamber	Appligene	Illkirch , France
PowerLab	ADInstruments	Castle Hill, Australia
Quartz-cuvettes	Hellma	Mühlheim, Germany
Quickspin™ columns, Sephadex G-50	Roche	Basel, Switzerland
Saran film	Roth	Karlsruhe, Germany
Slab gel dryer: SGD4050	Appligene	Illkirch , France
Strips for the PCR	Biozym	Oldendorf, Germany
Superfrost plus slides	Menzel Glaeser	Braunschweig, Germany
Thermomixer 5437	Eppendorf	Hamburg, Germany
UV/ visible spectrophotometer	Appligene	Illkirch , France
UV Stratalinker 1800	Stratagene	La Jolla, USA
Vortex: VibroFix	Janke & Kunkel-IKA	Heitersheim, Germany
Vertical polyacrylamide gel electrophoresis apparatus	Sigma	München, Germany
Whatman 3MM paper	Whatman	Madison, USA

2.2.2. Equipment for blood pressure measurement

Pressure cuff	Technical and Scientific Equipments	Bad Homburg, Germany
Process control unit series 209000	Technical and Scientific Equipments	Bad Homburg, Germany
Pulse transducer (ID=9 mm)	Technical and Scientific Equipments	Bad Homburg, Germany
Inverted Microscope	Leica	Wetzlar, Germany
Manipulator	Eppendorf	Hamburg, Germany

Software TSE-BMON	TSE	Bad Homburg, Germany
Surgical instruments	TSE	Bad Homburg, Germany
Catheters PE10 and PE50	Clay Adams	Sparks, USA

2.3. Solutions and buffers

Acidic Alcohol	4 ml concentrated HCl 95% ethanol
Ampicillin	50 µg/ml H2O
Blocking buffer**:**	5 % BSA in TBS buffer
DEPC H_2O	0.1% Diethyl-Pyrocarbonat in H_2O bidest 37ºC over night, autoclave
dNTP-Mix (5 mM)	5 mM dATP 5 mM dGTP 5 mM dCTP 5 mM dTTP in TE buffer
Ear buffer	100 mM Tris pH 8.5 5 mM EDTA 200 mM NaCl 0.2% SDS
Eosin solution	dissolved in 60% Ethanol (4:1)
Ethidium bromide	1 mg/ml H_2O bidest
GTE-buffer	50 mM Glucose 10 mM EDTA 25 mM Tris-HCl (pH 8.0)
IPTG	200 mg/ml, in H_2O bidest
Loading buffer	40% sucrose 0.05% bromphenolblue 0.05% xylencyanol in TE buffer
Lysis buffer	50 mM Tris-HCl (pH 8.0) 100 mM NaCl 100 mM EDTA 1% SDS

Neutralization solution	1.5 M NaCl 1 M Tris-HCl (pH 7.0)
PBS buffer	130 mM NaCl 7 mM Na_2 HPO4 4 mM NaH_2 HPO4
PMSF	100 mM phenylmethylsulfonylfluoride in isopropanol
Protein Extraction Buffer	10 mM Tris, pH 7.4 1mM EDTA 250mM NaCl 0.1% NP-40 1mM PMSF 1×Protase inhibitor cocktail 0.5mM Sodium orthovanadate
Proteinase K	10 mg/ml in H_2O bidest
Paraformaldehyde	4% paraformaldehyde in 1x PBS
RNase A, stock	4 mg/ml in H_2O bidest
SDS/Running Buffer	25 mM Tris 192 mM Glycine 1% SDS
SET (20x) pH 7.2	3 M NaCl 0.4 M Tris 20 mM EDTA
Solution E1	50 mM Tris pH 8.0 10 mM EDTA 100 µg/ml RNase
Solution E2	200 mM NaOH 1% SDS
Solution E3	3.1 M Potassium acetate pH 5.5
TAE-Buffer (50x)	200 mM Tris 200 mM acetic acid 5 mM EDTA pH 8.0
TBE-buffer (5x)	445 mM Tris-HCl 445 mM Boric acid 10 mM EDTA
TBST (10x)	10 mM Tris-HCl, pH 8,0, 1.5 M NaCl,

	2 % Tween 20
TE-buffer (1x)	10 mM Tris-HCl (pH 8.0) 1 mM EDTA
TE/RNase-buffer	20 µg/ml RNase A in TE buffer
Transfer Buffer	20 mM Tris pH 8.0 150 mM Glycine 20% methanol
Van Gieson's Solution	20.0ml Acid fuchsin, 1% 25.0ml Picric acid, saturated
Washing solution	0.2x SET 0.2% SDS
Weigert's Iron Hematoxylin	
Solution A	1.0g Hematoxylin 100.0ml Ethyl alcohol, 95%
Solution B	4.0ml Ferric chloride 29% 95.0ml Distilled water 1.0ml Hydrochloric acid, concentrated

Working Solution Mix A and B in equal parts. The mixture turns a rich deep blue-violet and is best prepared fresh each time, but it will keep and can be used for several days, sometimes as long as a month.

X-Gal solution	50 mg/800 µl DMSO

2.4. Media, antibiotics, and agar-plates

LB Medium (pH 7.5)	1% bacto-trypton 0.5% yeast extract 0.5% NaCl
LB-Agar	1% bacto-trypton 0.5% yeast extract 0.5% NaCl 1.5% agar

The LB medium was prepared with distilled water, autoclaved, and stored at 4°C.

Antibiotics

Master solution for ampicillin was prepared as 50 mg/ml, sterile filtered and stored at -20°C. The antibiotic was added after the autoclaved medium has cooled down to a temperature lower than 55°C with a final concentration 50 µg/ml.

Amp / IPTG / X-Gal plates

LB-agar with 100 µg/ml ampicillin, 4 µg/ml IPTG and 50 µg /ml X-Gal was poured into Petri dishes. The dishes were stored at 4°C.

2.5. Gels

1% agarose gel	1 g agarose 100 ml 1xTAE 50 µl EtBr(1 mg/ ml)
5% PAA-gel (for RPA)	28 g urea 12 ml 5x TBE 480 µl APS 10 ml AA/BAA (20:1) 64 µl Temed

12% SDS-PAGE

Running gel	0.375 M Tris-HCl, pH 8.8 0.1% (w/v) SDS 12%/0.8% w/v Acrylamide/Bis-acrylamide 0.1% (w/v) ammonium persulfate (APS) TEMED (1 µl per ml of gel)
5% Stacking gel	0.125 M Tris-HCl, pH 6.8 0.1% (w/v) SDS 5%/0.8% w/v Acrylamide/Bis-acrylamide 0.1% (w/v) ammonium persulfate (APS) TEMED (1 µl per ml of gel)

2.6. Anesthesia

Mice were anasthetized by an intraperitoneal injection of 17 µl of anesthetic solution per 1g mouse body weight.

Anesthetic solution	10% (v/v) Ketaet (ketamine) 0.02% (v/v) Romazine (xylazine) in saline

2.7. Sterilization of solutions and equipments

All solutions, which are not heat sensitive, were sterilized at 121°C, for 105 Pa for 60 min in an autoclave. Heat sensitive solutions were filtered through a disposable sterile filter (0.22 to 0.45

µm pore size). Plastic ware was autoclaved as above. Glassware was sterilized overnight in an oven at 220°C.

2.8. Vectors used for the cloning and sequence analysis

pGEM-T	Promega	Wisconsin, USA
pcDNA3.1(-)	Invitrogen	Carlsbad, California, USA
pBSK(+)	Invitrogen	Carlsbad, California,USA
Topo	Invitrogen	Carlsbad, California,USA

2.9. Synthetic oligonucleotides Primers (Biotez; Berlin-Buch, Germany)

A. The following primers were used for PCR

Symbol Sequence (5´→ 3´)

AVP5‘ 5’-GGACTCTAGCGGCCGTCTGC-3’
AVPEx15 5’-CTGAACGCGTGGCGAGGATAGGTGGGCACTGCGTGCAG-3’
AVPEx13 5’-TCCGACGCGTAGCTGAGACAGGTACCACTG-3’
AVPEx25 5’-GCAGCAGATGCCCGCGGCAG-3’
AVPEx23 5’-TGCCGCGGGCATCTGCTGCAGCGGTGG-3’
AVPEx35 5’-ACGGAAGCTTGTGTCCCAGCCAGCTG-3’
AVPEx33 5’-TCCGTCGACTCTGCCAAGCCCGGGTCTAC-3’
AVP3‘ 5’-TCTGCATATGTGTGTCCCAATCTCACCAGG-3’
Ig 5 5’-CATCACCCATCGAGAGAACC-3’
Ren 23 5’-GGGACCAAGCCTGGCCATGTCC-3’

OLIGO Ang II C
GATCAAGAGTGCGCACTAAACGCGACCGCGTATACATCCACCCCTTTTAGTCGACAC
ATG

OLIGO Ang II D
TGTCGACTAAAAGGGGTGGATGTATACGCGGTCGCGTTTAGTGCGCACTCTT

B. The following primers were used for real time PCR:

eNOS
fw primer: 5'-CCT TCC GCT ACC AGC CAG A-3'
rev primer: 5'-CAG AGA TCT TCA CTG CAT TGG CTA-3'

ß-actin
fw primer: 5'- CTG GCC TCA CTG TCC ACC TT-3'
rev primer: 5'- CGG ACT CAT CGT ACT CCT GCT T-3'

HPRT1
fw primer: 5'- TGA CAC TGG TAA AAC AAT GCA-3'
rev primer: 5'- GGT CCT TTT CAC CAG CAA GCT-3'

Akt1
fw primer: 5'-ATCGTGTGGCAGGATGTGTA-3'
rev primer: 5'- AGCTGTGAACTCCTCATCGAA-3'

Akt2
fw primer: 5'-AGCTCACTCAAGCTAGGTGACAG-3'
rev primer: 5'-GCCTCCAGGTCTTGATGTATTC-3'

Nox 2
fw primer: 5'- GTG ATA ATG CCA CCA GTC TGA-3'
rev primer: 5'-CAG GTC TGC AAA CCA CTC A -3'

Nox 4
fw primer: 5'- GCC CCA GTG TAT CAG CAT TAG -3'
rev primer: 5'- AGT GGA CAC CAA ATG TTG CTT -3'

Cox 1
fw primer: 5'-CTGCGGCTCTTCAAGGAT -3'
rev primer: 5'-GTGGGTAGCGCATCAACA -3'

Cox 2

fw primer: 5’- TCATCAGTT TTTCAAGACAGATC -3’

rev primer: 5’- ACCTGATATTTCAATTTTCCATCC -3’

ACE 2

fw primer: 5’-ATGTAGAACGTACCTTCGCAGAG-3’

rev primer: 5’-GGGCTGATGTAGGAAGGGTA-3’

Gfer (Affymetrix ID: 160269_at)

fw primer: 5’-CTG CGA GGA ATG TGC GGA AGA-3’

rev primer: 5’-TGC CCA GCT TCC GAT TCA CC-3’

StAR (Affymetrix ID: 92213_at)

fw primer: 5’-AGC AGG GAG AGG TGG CTA TG-3’

rev primer: 5’-ACC ACC TCC AAG CGA AAC AC-3’

3ß-HSD6 (Affymetrix ID: 102729_f_at)

fw primer: 5’-AGA TCA GGG TCC TGG ACA AGT-3’

rev primer: 5’-TCC TCA GGT ACT GGG TGT CAA-3’

3ß-HSD3ß1 (Affymetrix ID: 103072_at)

fw primer: 5’-TGT GGG CCA GAG GAT CAT-3’

rev primer: 5’-TGT CTC CTT CCA ACA CTG TCA-3’

C. RT-PCR primers for transgenic AVP-AngII rats

Primer 5 5’-GCATCTGCTGCAGCGATG-3’

Primer 3 5’-GGGAGATCATGAGTACATCC-3’

Primer 4 5’- TGCCAGGAGGAGAACTACC-3’

AVP 5´ 5’-GCATTTGTGCAGCGGTG-3’

Primer 3 nest 5'-GAG GGA AGA TGA AGA CGG A- 3'

2.10. Probes for RPA

Table 3.1. Probes used in RPA

Probe	Linearization Enzyme	Transcriptase	Length	Antisense RNA length
rL32(ribosomal protein L32)	XbaI	T7	144 bp	127 bp
mAOGEN	AccI	T7	850 bp	400 bp
rAOGEN	EcoRI	T7	800 bp	350 bp
AVP Probe A	SacII	sp6	573 bp	336bp IgG2b and 71bp human renin protected fragment.
AVP Probe B	XmaI	sp6	510 bp	331bp
Rgs2	SacII	T3	187 bp	162 bp
Adam19	SacII	sp6	256 bp	236 bp
Col6a3	Spe I	T7	207 bp	209 bp
Hsd3b6	XhoI	T3	425 bp	394 bp
Star	KpnI	T7	380 bp	307 bp
Cpxm2	SacII	sp6	260 bp	239 bp
Collagen III	HindIII	sp6	476bp	500bp

3. Methods

3. Methods

3.1. Molecular biology

3.1.1. DNA

3.1.1.1. Isolation of DNA

3.1.1.1.1. Isolation of genomic DNA for southern blot

One cm of the tail from a mouse was incubated in 700 µl of lysis buffer containing 35 µl proteinase K (10 mg/ml) at 55°C overnight with shaking. In the morning the samples were incubated in ice for 10 min, then mixed with 300 µl of 6 M NaCl, and kept on ice for 5 more min. After centrifugation (14 000 rpm, 4ºC, 10 min) the aqueous phase was transferred into a new tube and incubated for 15 min at 37°C with 5 µl of RNase A (4 mg/ml). DNA was precipitated by adding 1 ml of isopropanol and centrifuged (14 000 rpm, 4ºC, 15 min). The pellet was washed with 75% ethanol, dried and resolved in 100-200 µl of TE-buffer. The concentration of extracted DNA was estimated as described (3.1.1.6.). DNA was kept at -20ºC.

3.1.1.1.2. Isolation of genomic DNA from mouse ear or tail biopsies for PCR

2-5 mm mouse ear or tail tip was cut off and put into 1.5 ml microcentrifuge tube. 100 µl of ear buffer was added. The sample was incubated at 55°C overnight with shaking (800 rpm). On the second day, the tube was incubated at 95°C for 10 minutes to inactivate the proteinase K. Afterwards 750 ul TE/RNase were added and 2 µl of the template were used for the PCR.

3.1.1.1.3. Isolation of plasmid DNA

A. Mini preparation

Three ml of LB medium with 50 µg/ml ampicillin was inoculated with a single E.coli colony and incubated overnight at 37°C with shaking. Two ml of this culture was centrifuged at 14000 rpm for 1 min. The pellet was resuspended in 300 µl of solution E1. Cells were lysed by adding 300 µl of solutions E2. Equal amount of solution E3 was added to the tube, and mixed immediately by inverting. Cell debris and chromosomal DNA were pelleted by centrifugation at 14 000 rpm, RT for 5 minutes. The supernatant was transferred into a new tube and 0.6 ml of isopropanol was added to precipitate the DNA. After centrifugation (14 000 rpm, RT, 10 mins) and washing with 70% ethanol, air- dried pellet was resuspended in 50 µl TE buffer. 2-5 µl of DNA was taken for the further digestion. DNA was kept at -20°C.

B. Maxi preparation

Plasmid DNA was isolated from 200 ml of LB medium plus ampicillin using Qiagen Plasmid Maxi Kit according to the manufacturer's instruction. The DNA was usually dissolved in 200-600 µl of TE buffer and kept at-20°C.

3.1.1.2. Southern blot hybridization analysis

A. DNA gel electrophoresis and blotting

DNA was digested over night with appropriate enzymes in volume of 30-40 µl. 100 ml of 1% agarose gel with 1 µl ethidium bromide (10 mg/ml) were prepared with 1× TAE and poured into an 8.3× 18 cm electrophoresis platform. 5 µl of PCR products were mixed with 1 µl 6× loading buffer and loaded into the wells. The gel was run at 120 V for 1 h and then photographed before blotting. The gel was rinsed in sterile water and placed into a clean plastic box containing 300 ml denaturing buffer. The box was shaken slowly on a platform shaker for 20 min at room temperature. The DNA was transferred onto nylon membrane with denaturing buffer by the capillary transfer method (Dunn and Sambrook 1980). After overnight transfer in denaturing solution, the membrane was neutralized by gently shaking in 0.05 M Na_2HPO4 for 5 min, air dried and DNA was fixed by exposing to UV light for 2 min in UV stratalinker 2400 (Stratagene).

B. Probe labeling by random hexamer priming

The labeling was carried out using the Prime-It-Labeling Kit (Stratagene, USA). Purified PCR products were labeled by random hexamer priming (Feinberg and Vogelstein 1984), which is based on a DNA polymerization reaction primed by random hexanucleotides binding to the template. About 120 ng of DNA (14.5 µl) were denatured at 95°C for 5 min and chilled on ice. Then 25.5 µl labeling mixture, 18 µl LS, 3 µl ATG (100 µM mix of dATP, dGTP, dTTP), 1.5 µl BSA (acetylated, 10 mg/ml), 0.5 µl Klenow enzyme (5 U/µl), and 2.5 µl [α-^{32}P] dCTP (10 µCi/µl), were added to the denatured samples and the labeling reaction was incubated for 2 h at 37°C. The probe was purified with Microspin^{TM} G50 Column (Pharmacia) before hybridization.

C. Hybridization

Filters were prehybridizated at 65°C for 2 h using 20 ml of hybridization buffer (1 M NaCl, 1% SDS, 10 mM Tris HCl), then buffer was replaced with 10 ml hybridization buffer containing the denatured probe. Hybridization was performed at 65°C overnight. Filters were washed twice at 65°C for 20 min first with 100 ml of wash solution I, followed with 100 ml of wash solution II. Filters were dried briefly on Whatman paper, sealed in plastic foil (Saran wrap) and exposed to X-ray film (Kodak X-OMAT) for 1 to 2 days. The films were developed using Agfa curix 60.

3.1.1.3. PCR reaction conditions

PCR reaction was performed in 45 µl reaction volume depending on the amount of PCR product needed. DNA template was mixed in ice with:

5 µl Taq polymerase buffer (10 xes)
2 µl dNTPs (5 mMs)
1.8 µl $MgCl_2$
1µl of each primer (50 ng/µl)
0.3 µl Taq Polymerase (5 Us/ml)
In total volume of 50 µl filled up with H_2O bidest.

The mixture was covered with mineral oil and the reaction mixture was subjected to the following program in the Peltier thermal Cycler PTC-200 (Biozym):
The PCR products were analyzed by 1-2% agarose gel electrophoresis

3.1.1.4. Genotyping of transgenic animals

The genotyping of offspring was performed by means of PCR (3.1.1.3) using sequence specific primers. Two µl of DNA solution, prepared from ear biopsies (3.1.1.1.2) were taken for the PCR reaction. Different pairs of primers, summarized in Table 3.2., were used for the genotyping of *Mas*-knock out animals and AVP-Ang II transgenic rats.

Table 3.2 PCR, used for genotyping of *Mas*-knockout and AVP-Ang II transgenic rat

Primers	Amplified fragment	Size of PCR product	Annealing temperature	Purpose
MAS10 MAS14	*Mas*	~500 bp	63°C	Presence of wild-type *Mas* allele
MAS12 NEOPVU	3' end of *Mas*, fused with Neo^R	~500 bp	63°C	Presence of knockout *Mas* allele
IgG5 Ren23	IgG2b	~500 bp	58°C	Presence of transgenic mouse IgG in rats

3.1.1.5. DNA extraction from agarose gel

PCR fragments, which were used for cloning, labeling, and microinjections were gel extracted using QIAquick Gel Extract Kit (Qiagen). The extraction procedures recommended by the supplier were followed.

3.1.1.6. Measurement of nucleic acid concentration

The quantity of DNA was measured photometrically by measuring absorption of the samples at 260 nm. DNA quality (i.e. contamination with salt and protein) was checked by the measurements at 230, 280, and 320 nm. The concentration was calculated according to the formula:

C= (E 260 – E 320) x f x c

C= concentration of sample (µg/µl)

E 260 = absorption at 260 nm

E 320 = absorption at 320 nm

f = dilution factor

C=0.05 µg/µl for double stranded DNA

C=0.04 µg/µl for RNA

C=0.03 µg/µl for single stranded DNA

3.1.1.7. Ligation of DNA fragments

The ligation of an insert into a vector was carried out in the following reaction mix:

30 ng vector DNA
50-100 ng insert DNA
1 µl ligation buffer (10x)
1 µl T4 DNA ligase (5 U/µl)
in a total volume of 10 µl, filled up with H_2O bidest.

The ligations were carried out at 16°C overnight.

3.1.1.8. DNA transformation in bacteria

A. Preparation of competent *E.coli* bacteria

LB medium (100 ml) was inoculated with a single colony of E.coli (strain DH5α) and the culture was grown at 37°C to OD 0.6. Bacteria were centrifuged (2600g, 2°C for 15 min) and the pellet was resuspended in 250 ml of sterile ice-cold 10% glycerol. The bacteria were centrifuged again and resuspended in 10 and then in 1 ml ice-cold 10% glycerol. 40 µl of cells were aliquoted into precooled eppendorf-tubes, frozen in liquid nitrogen and keep at -70°C.

.

B. Electro-transformation

After ligation the DNA was used to transform bacteria using the electroporator, which was set to voltage 1350V. Electro-competent cells were thawed on ice. Ligation reaction (2-5ul) was added to 40 µl cells in an eppendorf tube and mixed well. Then, the cells/DNA mix was transferred to the electro-cuvette (pre-chilled), the cells were pulsed once; after the gene pulser beeps, LB medium was quickly transferred to the cuvette, and the mixture was gently pipeted up and down. LB/cells were transferred back to culture tube. Tubes were then incubated at 37°C with shaking for 50 min. For cell seeding, 135 µl of each transformation culture was plated onto LB (L-Broth growth media for bacteria) plates containing ampicillin, IPTG and X-Gal (isopropyl-beta-Dthiogalactopyranoside and 5-bromo-4-chloro-3-indolyl-ß-D-galactoside; for ingredients see chapter 2.3). Cells were grown on the plates by overnight (16-24 hours) incubation at 37°C. Using this method, approximately 20- 50 colonies per plate could be seen in the experiments, and generally the white colonies contained the target inserts.

3.1.1.9. TA-cloning

Taq and other polymerases have a terminal transferase activity that results in the non-templated addition of a single nucleotide to the 3'-ends of PCR products. In the presence of all 4 dNTPs, dA is preferentially added. This terminal transferase activity is the basis of the TA- cloning strategy. For the cloning of PCR products, pGEM-T Vector system that has 5`T overhangs was used.

3.1.1.10. DNA sequencing

The DNA samples were submitted to automatic sequencing using the thermo sequenase fluorescent-labeled primer reaction. The sequencing was performed by Invitek (Berlin-Buch, Germany).

3.1.1.11. Construct for AVP-Ang II transgenic rats

To clone the AVP gene, a 4.7 kb 5′ UTR fragment was amplified with primers AVP5 and AVPEx15, a 1.4 kb exon 1-2 fragment was amplified with primers AVPEx13 and AVPEx25, a 0.4 kb exon 2-3 fragment was amplified with primers AVPEx23 and AVPEx35, a 2.3 kb ex3 fragment was amplified with primers AVPEx33 and AVP3′. Thereby, all the ATGs codons were mutated to avoid the endogenous AVP protein being translated, so that the amplified sequences only serve as transcriptional regulator. Each of these fragments was ligated into pGEM-T vector or Topo vector. Afterwards, the pGEM-T vector containing the exon 2-3 fragment was cut and ligated with a 1 kb HindIII and SalI fragment plasmid Pskph, (a gift of T. Reudelhuber, Montreal, Canada (Methot et al. 2001)) containing the sequence coding for Ang II. Then, the exon1-2 fragment was cut and cloned in with MluI and SacII. Thereafter, the 5′ UTR fragment was inserted with EagI and MluI, and at last the ex3 fragment containing the AVP polyadenylation site was ligated with SalI and NdeI (Fig. 3.1).

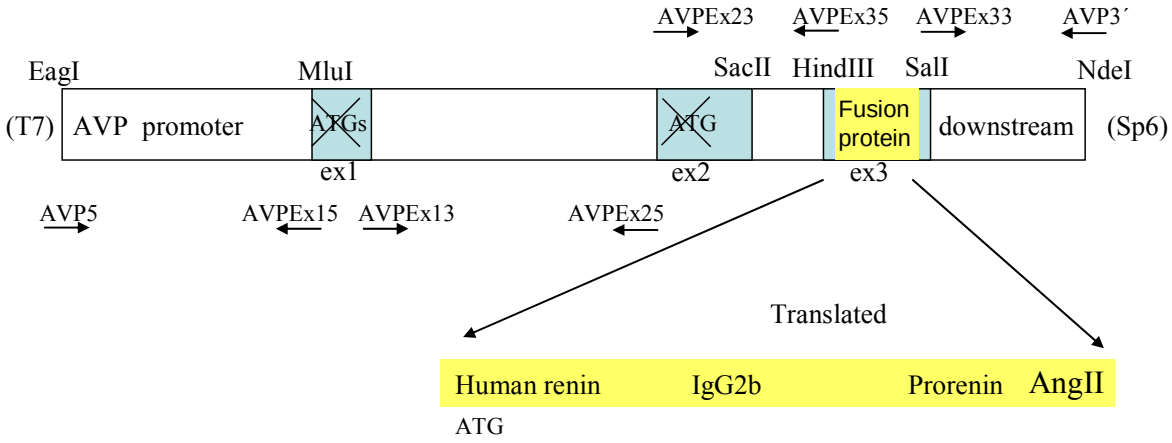

Fig. 3.1 Scheme of AVP-Ang II

3.1.1.12. Preparation of DNA for microinjection

13.8 kb construct was digested with EagI and SalI to release the insert. After restriction digestion the DNA fragment was isolated from the agarose gel using a QIAquick Gel Extract Kit (3.1.1.5). The DNA was taken up in microinjection buffer, adjusted to a concentration of 3 ng/µl and filtrated through a 0.22 µm filter.

All animal experiments were carried out in accordance with local and national ethical guidelines. DNA (2 ng/µl) was microinjected into the male pronucleus of fertilised one-cell SD rat oocytes and eggs were transferred into the oviducts of pseudopregnant females. DNA from tail biopsies from the progeny was analyzed by PCR.

3.1.1.13. Apoptosis detection

In situ detection of DNA fragmentation was made by the TUNEL method according to the procedures in (In Situ Cell Death Detection Kit, Fluorescein). In brief, cardiac and renal sections (5 µm) were deparaffinized, hydrated, and treated with proteinase K. Terminal deoxynucleotidyl transferase (TdT) enzyme was applied on the specimens and incubated at 37°C for 1 hour. Finally, the slides were mounted.

3.1.2. RNA

3.1.2.1. Isolation of total RNA from mouse tissue

Total tissue RNA was isolated using TRIzol reagent (Gibco) according to the manufacturer's instruction. 100-200 mg tissue sample was homogenized in 1 ml of TRIzol reagent by using a homogenizer. The lysate was transferred into an eppendorf tube. The homogenate was incubated at RT for 5 min to permit the complete dissociation of nucleoprotein complexes, and then 0.2 ml of chloroform was added. After vigorous vortexing, the homogenate was incubated at RT for another 15 min. After centrifugation of the samples at 12000 rpm for 30 mins at 4°C, the colorless upper aqueous phase was transferred into a new tube. The RNA was precipitated by adding 0.5 ml of isopropanol. Finally, the pellet was washed with 75% ethanol, dissolved in 80-100 µl of DEPC H_2O. The concentration of extracted RNA was measured as described in (3. 1.1.6). Isolated RNA was kept at -80°C.

3.1.2.2. Reverse transcription (RT)

2-5 µg of total RNA was mixed with 5 µl of random hexamer primers (20 µM) in a volume of 15 µl DEPC H_2O. To avoid formation of RNA secondary structures, which might interfere with the synthesis, the mixture was heated to 80°C for 3 min, and then quickly chilled on ice. After a brief centrifugation, the following was added to the mixture:

6 µl 5x First strand buffer
3 µl 0.1 M DTT
3 µl 5 mM dNTPs
1 µl RNasin (10 U/µl)
2 µl M-MLV (200 U/µl)

The content of the tube was mixed gently and incubated at 37°C for 1h. The reaction was inactivated by heating at 80°C for 10 min. After the cDNA synthesis is completed, 5 to 10 µl of reaction was used as template for a PCR.

3.1.2.3. Nested PCR Amplification

Nested PCR was used due to its high sensitivity to amplify the rare RT-PCR products. The first-round PCR amplification was performed in a 25 µl reaction volume containing 2 µl DNA sample, using the pair of oligonucleotides: primer 4 and 3. The expected product was a 530 bp

fragment. The second-round PCR amplification was carried out by using 1 µl of the first-round PCR products as templates in 25 µl reactions. Primer pair was as follows: AVP 5´and primer 3 nest. The resultant product was expected to be a 270 bp fragment.

3.1.2.4. RNase Protection Assay

Targeted gene expression was analyzed by Ribonuclease Protection Assay (RPA) using commercially available Ambion RPA II kits (AMS Biotechnology), according to the protocol of the manufacturer.

A. Probe labelling

The probe was prepared by linearization of the plasmid DNA, purified from agarose gel (3.1.1.5) and dissolved in DEPC H_2O. The labeled antisense RNA probe was synthesized by T7, or T3, or SP6 RNA polymerase in the presence of [α -32 Ps] (UTP using an RNA transcription kit (Stratagene, USA). To perform in vitro transcription 0.5 µ g of DNA was mixed with:

1 µl rATP
1 µl rCTP
1 µl rGTP
5 µl Transcription buffer
1 µl RNasin
1 µl DTT
3 µl [α -32 Ps] UTP (800 Cis/mM)
1 µl of T7, or T3 or Sp6- polymerase
In final volume of 25 µl (DEPC H_2O)

After incubation at 37°C for 1 h, 1 µl of RNase- free DNase I was added to digest the DNA template. To clean the probe from free unincorporated nucleotides, the total reaction mixture of 25 µl was purified with Quick- Spin- column Sephadex G50 (Roche, Basel, Switzerland) according to the protocol of the manufacturer. The activity of the probe was measured by the scintillation counter LS600SC (Beckman, Minnesota, USA).

B. RNA-RNA hybridization

50 µg total RNA and 10 µg of yeast as a control were used for RPA. RNA samples were hybridized with approximately 20,000 cpm of the radio-labeled antisense probe and 10,000 cpm of the L32, probe as a housekeeping gene. The hybridized fragments, once protected from RNase

A/T1 mix digestion, were separated by electrophoresis on a denaturing gel (5% polyacrylamide, 8 M urea) and analyzed using a FUJIX BAS 2000 Phospho-Imager system. Quantitative analysis was performed by measuring the intensity of the bands normalized by the intensity of the rl32 bands.

3.1.2.5. Affymetrix gene expression analysis

The affymetrix gene chip features a cassette enclosing the oligomer microarray and a 250 µl chamber for hybridization, washing and staining. mRNA is converted to cDNA by reverse transcription from a primer that incorporates the T7 promoter, which allows subsequent in vitro transcription using T7RNA polymerase to amplify each cDNA into a cRNA population. This amplification by transcription boosts the sensitivity for rare mRNAs while maintaining the original relative ratio of each message in the population, and also allows for the incorporation of biotinylated CTP and UTP. The cRNA is fragmented, hybridized to the chip and stained with streptavidinphycoerythrin, which attaches fluorescent labels through high affinity interaction with the biotin tags. A scanning confocal microscope detects laser-excited fluorescence from hybridized cRNA. The sensitivity is sufficient enough to detect rare transcripts present at less than 0.1 (on average) copies per cell in yeast (Wodicka et al. 1997). The simple procedure to prepare the target is shown in Fig 3.3.

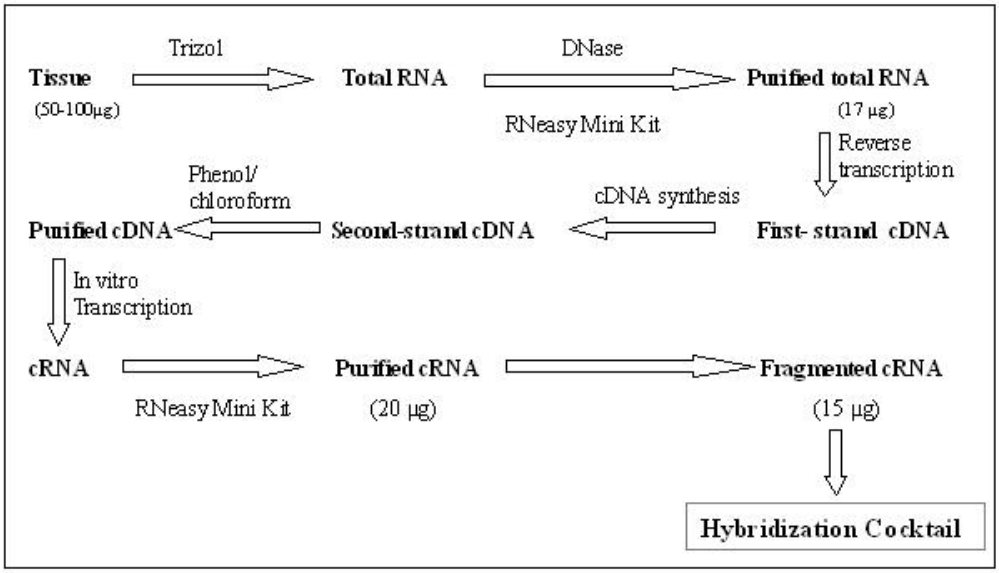

Fig. 3.3. Procedures to prepare the target for hybridization with Affymetrix chip

3. Methods

A. RNA clean-up

43 µl of total RNA (20-30 µg) was mixed with 2 µl of DNAase (1 U/µl, from Promega) and 5 µl of 10 × RQ1 DNase buffer and incubated at 37°C for 20 min. After digestion, clean-up was performed using RNeasy kit from QIAGEN. Samples were adjusted to a volume of 100 µl with RNase-free water. 350 µl of RNeasy lysis buffer was added to the sample and mixed thoroughly. 250 µl of absolute ethanol was added to the lysate and mixed well by pipetting, 700 µl of sample was applied to RNeasy mini spin column sitting in a collection tube. Purified RNA were eluted with 30 µl of RNase- free water after the RNeasy columns were washed for twice with buffer RPE from kit. The RNA yield was quantified by spectrophotometric analysis using the convention that 1 OD at 260 nm equals 40 µg RNA per ml. The integrity and size distribution of total RNA was verified on 1.2% formaldehyde agarose gel.

B. Synthesis of double strand cDNA from total RNA

Twenty micrograms of total RNA were used to synthesize double-stranded cDNA with a SuperScript kit (Invitrogen), incorporating a T7 promoter sequence by using oligodT–T7 primer.

C. cDNA Purification using Phenol/chloroform extraction

The final cDNA synthesis preparation was purified using phenol/chloroform according to the method described in gene chip expression analysis technique manual. 193.5 µl of synthesis preparation was mixed with 200 µl of phenol, vortexed for 10 seconds (sec). The upper water phase was transferred to a new tube after the tubes were centrifuged for 15 sec. 50 µl of TE (10 mM Tris, 1 mM EDTA, pH 8.0) was added to the phenolic phase, vortexed for 10 sec and centrifuged for 15 sec. The upper water phase was transferred to the same tube. The water phase was extracted once with Phenol/chloroform/isoamyl alcohol (25:24:1) and twice with chloroform/isoamyl alcohol (24:1). 2 µl of 5 mg/ml glycogen, 120 µl 5 M NH_4AC and 500 µl 100% ethanol were added to each sample. The samples were stored at -20°C for 1 h and centrifuged at high speed for 10 min. The pellets were washed using 300 µl of 70% ethanol. The purified cDNA was dissolved in 1.5 µl of DEPC treated water.

D. Synthesis of Biotin-Labeled cRNA

cRNAs were prepared by an *in vitro* transcription reaction using T7 megascript Kit. 18.5 µl of labeling mixture (2 µl 75 mM ATP, 2 µl 75 mM GTP, 1.5 µl 75 mM CTP, 1.5 µl 75 mM UTP, 3.75 µl 10 mM Bio-11-CTP, 3.75 µl 10 mM Bio-16-UTP, 2 µl 10× T7 Buffer and 2 µl 10× T7

Enzyme) were added to 1.5 µl of purified cDNA. After the samples were incubated at 37 °C for 5 h in a thermocycler, the reaction mixtures were purified using RNeasy Mini kit. 2 µl of cRNA from each sample was used measuring the concentration and purity of cRNA spectrophotometrically. The convention that 1 OD at 260 nm equals 40 µg/ml RNA was applied, maintain the A260/A280 ratio close to 2.0 for pure cRNA.

E. Fragmentation of the cRNA and preparation of the hybridization cocktail

The samples including 32 µl of cRNA (20 µg) with 8 µl of 5× fragmentation reaction were incubated at 94 °C for 35 min in a thermocycler. Then 2 µl of the reaction was checked on 1.2% agarose gel. The standard fragmentation procedure should produce a distribution of RNA fragment sizes from approximately 35 to 200 bases. The fragmented cRNA was stored at -80°C until ready to perform the hybridization. Hybridization cocktails were prepared by mixing 30 µl (15 µg total cRNA) fragmented cRNA from each target, 2.5 µl control Oligonucleotide B2 (5 nM), 5.0 µl Herring sperm DNA (10 mg/ ml), 6.25 µl BSA (20 mg/ ml), 125 µl 2× MES, and 81 µl H_2O.

F. Hybridization of Affymetrix chips

The mouse Genome U74Av2 Set monitors the expression of more than 12,000 genes and EST clusters. Fragmented, biotinylated anti-sense cRNA was prepared from mRNA, and hybridized to the probe array for 16 h at 45°C while rotating at 60 rpm. The levels of hybridization were measured with the HP Gene Array scanner after the array was stained with streptavidin-phycoerythrin (SAPE).

G. Washing, Staining, and Scanning probe arrays

Affymetrix chips were washed and stained according to Affymetrix chip expression analysis technical manual. Washing and staining of the chips were controlled by microarray suite software. After washing and staining, the probe array was removed and checked for large bubbles or air pocket. If bubbles were present, the array was refilled with non-stringent buffer. The probe arrays were kept at 4 °C in the dark until scanning was performed. Images were scanned using a GeneArray scanner (Agilent Technologies, Palo Alto, CA).

3.1.2.6. Quantitative Real Time RT-PCR using SYBR Green PCR Master Mix

Real-time PCR was performed in a 25µl reaction (10 µl diluted cDNA; 250-300 nM each primer; 1X SYBR Green Master mix (Qiagen Quantite SYBR) using a Bio-Rad I Cycler. Four samples were measured in each experimental group in duplicate.

Due to the nonspecific nature of SYBR Green detection, any double stranded DNA will be detected. Nonspecific product formations are checked by dissociation curve or gel analysis. All quantitations were normalized to the endogenous control ß-actin to account for variability in the initial concentration.

The relative quantitation for a target gene was calculated following:

♦ The mean threshold cycle (C_T) value was the average of the replicate wells run for each sample.

♦ ΔC_T was the difference between the mean C_T values of target samples between endogenous controls.

♦ $\Delta\Delta C_T$ was the difference between the mean ΔC_T values of the samples (such as cDNA samples from knock out mice) for each target gene and the mean ΔC_T of the calibrator (cDNA samples from wild type mice) for the target.

♦ The relative quantitation value was expressed as $2^{-\Delta\Delta CT}$.

3.1.3. Protein

3.1.3.1. Preparation of protein extract

Frozen tissue was crashed to powder with liquid nitrogen in a mortar and pestle. The powder was transferred to eppendorf tubes and incubated on ice for 30 minutes in protein extraction buffer (2.3). After centrifugating for 10 minutes at 10,000×g, total protein concentration of the supernatant was determined by Bradford protein assay.

3.1.3.2. SDS-PAGE and Western Blot

The extract proteins prepared from mice aorta tissue of *Mas* knock out and wild type mice and ventricles of TGM L102 were separated and transferred to nitrocellulose membranes and probed with antibodies. 30 µg of protein for each sample were mixed with loading buffer, denatured at 94°C for 5 min and cooled on ice. 10-12% resolving gel and 5% stacking gel were prepared

using Bio-rad Mini-Protean®3 Electrophoretic Cell. After removing the comb, the protein samples were loaded on the gel, and the gel was run at 140 V. A transfer sandwich consisting of the protein gel and a nitrocellulose membrane was assembled. The proteins were electrophoretically transferred from the gel to a nitrocellulose membrane for 1 h at 320 mA constant current in the precooled transfer buffer using Bio-rad Mini Trans-Blot® Electrophoretic transfer Cell. The membrane was placed in a plastic box, washed for 5 min with wash buffer TBST and allowed to air dry at room temperature. The membrane was blocked in blocking solution (1× TBS, 5% Non-Fat milk or BSA) for an hour at room temperature. The membrane was washed twice for 5 min with TBST. The diluted primary antibody Akt (1:1000), Hsp90 (1:1000), gp91phox (1:1000), caveolin-1 (1:1000), caspase 3 (1:1000), Cyt (1:1000), in 5% milk or BSA/TBS-T was added and incubated overnight at 4°C. The membrane was washed once for 15 min, and then four times for 5 min with TBS-T. The diluted HRP-labeled second antibody in 5% milk/TBS-T (1:2000) was added and incubated for 1 h at room temperature. The membrane was washed once for 15 min, and then four times for 5 min with TBS-T. The membrane was incubated in the chemiluminescence reagent (0.125 ml of chemiluminescence regent per cm^2 of membrane) prepared by mixing equal volumes of the enhanced luminol reagent and oxidizing reagent for one minute while shaking. The excess chemiluminescence regent was removed by draining and the membrane was placed in a plastic sheet protector. The membrane was exposed to Kodak X-OMAT film for 30 sec and film was developed. An optimum exposure was determined according the quality of the developed film.

3.1.3.3. Histochemistry

Heart, kidney, and lung from mice were fixed in PBS containing 4% paraformaldehyde, dehydrated, embedded in paraffin, and cut into sections 5 μm in thickness. The sections were deparaffinized and rehydrated, then stained with hematoxylin for 3 minutes, and after washing in water, stained with eosin for 30 seconds, and then fixed in ethanol and Xylene.

Sections were stained with collagen-specific Van Gieson stain to determine the fibrosis. Paraffin sections were deparaffinized with xylene and hydrated with graded ethanol. The sections were subsequently placed in Weigert's iron hematoxylin solution for 20 minutes, rinsed for 10 minutes, and placed in van Gieson's stain for 5 minutes (All the chemicals and facilities were provided by Department of Veterinary Medicine, Free University of Berlin). Subsequently, the slides were placed in 95% ethanol and dehydrated with 100% ethanol. Connective tissue and

muscle areas were identified according to their respective gray level, where as collagen fibers appeared red, myocytes yellow, and interstitial space white.

3.1.3.4. Superoxide dismutase (SOD) activity

SOD in aorta homogenates was measured with the SOD Assay Kit (Fluka SOD Assay Kit BioChemika). This method uses xanthine and xanthine oxidase as a superoxide generator, and a highly water-soluble tetrazolium salt, WST-1 (2-(4-iodophenyl)-3-(4- nitrophenyl)-5-(2,4-disulfophenyl)-2H-tetrazolium, monosodium salt), as a superoxide indicator. Absorbance was measured spectrophotometrically at 450 nm. SOD activity was calculated using a standard curve according to the manufacturer's instructions and was expressed as units per mg of protein.

3.1.3.5. Catalase activity

Catalase activity in aorta was measured spectrophotometrically as the rate of the decomposition of H_2O_2 as described elsewhere. The thoracic aorta was washed by perfusion through the left ventricle with 0.9% NaCl containing 0.16 mg/ml heparin to remove erythrocytes. Aortic rings free from fat and connective tissue were homogenized and sonicated in 50 mM phosphate buffer, pH 7.0, containing 0.1 % Triton X-100, 1 mM EDTA, 10 µg/ml aprotinin and 0.1 mM phenylmethylsulfonyl fluoride (PMSF). A small aliquot (10 µl) was removed for protein determination. After centrifugation (16,800 g for 10 minutes at 4ºC) the supernatant was assayed for enzyme activity. Fifty µl of the supernatant, 800 µl phosphate buffer, pH 7.0, and either 50 µl H_2O or 50 µl 10 mM sodium azide were combined on ice. The reaction was initiated by adding 100 µl of 60 mM H_2O_2 in 50 mM phosphate buffer, and was allowed to proceed on ice. At 2 min and 10 min, 100 µl aliquots were withdrawn and quenched in 5 ml of a solution containing 0.24 M H_2SO_4 and 2 mM $FeSO_4$. After this, 400 µl KSCN (0.2 mM final concentration) was added, and the absorbance of each sample was measured at 460 nm. One unit of catalase activity was calculated kinetically at 2 time points and defined as the rate constant of the first-order reaction (k). Relative activity was expressed as k/mg protein.

3.2. Animals

All animal experimental protocols were in compliance with the Guide for the Care and Use of Laboratory Animals published by the OPRR (Office for Protection against Research Risks) of

the US National Institutes of Health, Washington, D.C. (NIH Publication No. 85-23, revised 1985). Local German authorities approved the studies with standards corresponding to those prescribed by the American Physiological Society. Mice were maintained in IVC (Techniplast, Deutschland) cages under standardized conditions with an artificial 12-h dark–light cycle (light: 6:00 a.m. – 6:00 p.ms.; dark: 6:00 p.m. - 6:00 a.m.), at a constant temperature (20-22^{o}C) with free access to standard chow (0.25% sodium; SSNIFF Spezialitäten, Soest, Germany) and drinking water *ad libitum*. To obtain *Mas* gene-deleted mice on a pure genetic background, we bred heterozygous *Mas*-knockout animals (mixed genetic background, 129xC57Bl/6) to the FVB/N and Bl/6 mouse lines (Charles River, Sulzfeld, Germany) for 7 generations. C57Bl/6 and FVB/N were ordered from Charles River (Sulzbach, Germany).

3.2.1. Breeding strategy and treatment for transgenic rats

Positive transgenic founders (F0) were first coupled with wild type (w/w) SD rats leading to the birth of heterozygous (+/w) F1 transgenic offspring. In order to get homozygous (+/+) transgenic rats, positive males (+/w) of the F1 generation were coupled with positive F1 females (+/w). Positive F2 mice, that could be both homo- and heterozygous were mated with wild type (w/w) rats. In case all F3 pups were positive, the F2 transgenic parent was homozygous.
Groups of rats were given diets (rat chow; Dyets Inc., Bethlehem, PA) with varying salt content (normal salt [NS], 0.4% NaCl; high salt [HS], 8% NaCl (Ssniff EF R/M high sodium) during a 2-week experimental period together with regular drinking water.

3.2.2. Phenotyping of transgenic animals

3.2.2.1. Measurement of relative heart weight

Mice were killed by cervical dislocation and were opened from the abdomen to the chest. The hearts were immediately excised and put into saline to get rid of blood. All the hearts were removed of the atria and weighed. Relative organ weight was determined as % of body weight:
Relative organ weight (%) = organ weight (mg) /mouse body weight (mg) x100%

3.2.2.2. Tail cuff measurement of blood pressure in rats

Blood pressure was measured by tail-cuff plethysmography (BP 2000, Apex) under light ether anesthesia. Multiple measurements were made by the same operator at each time point, as a rule

between 10:00 and 14:00, and the mean value was taken as the representative blood pressure level.

3.2.2.3. Telemetric blood pressure measurement in mice

All experiments were performed in adult (12-14 week old) male FVB/N-*Mas*-deficient and FVB/N-WT mice.

The telemetric techniques were performed by a core facility at the MDC and are described in detail elsewhere (Obst et al. 2004). Initial recordings of blood pressure were begun 10 days after the surgery, when the mice had regained their circadian blood pressure and heart rate rhythm, while surgical and anesthesia-induced changes had abated. Heart rate was computed from the pulse intervalls of blood pressure recordings. Miniosmotic pumps containing tempol (50 mg/kg/day) were implanted intraperitoneally. After an additional 7 days of recovery, blood pressure and heart rate values were recorded in tempol-treated FVB/N-*Mas*-deficient and WT mice. Data were sampled from the TA11PA-C10 device every 5 min for 10 sec continuously day and night with a sampling rate of 1000 Hz and stored on a hard disk using the DATAQUEST software (A.R.T. 2.1, Data Sciences International). Data for the day/night-time blood pressure and heart rate pressure were averaged from 6 am to 6 pm and *vice a versa*.

3.2.2.4. Assessment of endothelial function and invasive catheter measurement of blood pressure

Animals were anesthetized by intraperitoneal (i.p.) ketamine (100 mg/kg) and xylazine (10 mg/kg), and modified cannulas (PE-10) were inserted into abdominal aorta through the femoral artery and exteriorized at the animals' necks. After 48 hr, BP and HR were recorded with a transducer (MLT 1050 model) connected to a computer system for data acquisition and analysis (PowerLab, ADInstruments) in freely moving animals. After 1-2 hours BP recording, the animals were anesthetized and a catheter (4 mm length, 0.1 mm inner diameter, and 0.25 mm outer diameter coupled to 3-cm-long PE-10 tubes) was placed into the descending aorta through the left carotid artery for drug infusion. Endothelial function in anesthetized mice was evaluated by measuring changes in mean BP in response to bolus intra-aortic ACh and sodium nitroprusside (SNP) administration. The substances were given in 1 µl per 10 g bodyweight at the following doses: 25, 50, 100, and 200 ng/kg for ACh and 1, 3, and 10 µg/kg for SNP. To correct the differences in vascular smooth muscle reactivity, the response to ACh was normalized by the

SNP-response (10 µg/kg) according to the formula Δ MAP(ACh) / Δ MAP(SNP). In control experiments eNOS activity was blocked by pre-treatment with L-NAME (30 mg/kg, intravenously). All hemodynamic data were collected and analyzed on a computer using Chart version 5 in Powerlab. Substances were dissolved in isotonic saline (0.9% NaCl) immediately before use.

In order to rule out possible effects of anesthetics, endothelial function was also assessed in conscious mice. Seventy-two hours before experiments, the mice were anesthetized and modified catheters (PE-10 insert in PE-50) were placed into the abdominal aorta via the femoral artery for the measurement of arterial pressure and in the femoral vein for drug infusion. Another catheter (4 mm length, 0.1 mm inner diameter, and 0.25 mm outer diameter coupled to 3-cm long PE-10 tubes) was placed in the descending aorta. The ends of catheters were tunneled subcutaneously, exteriorized, and sutured between the scapulae. During the recovery period (24-48 hours after surgery), catheters were flushed with heparinized saline (10 IU/ml) (1-3 µl/g bodyweight). The mice were tested in a conscious, unrestrained state. Endothelial function was evaluated as described above for anesthetized mice.

3.2.2.5. Assessment of renal function

Renal excretory function in conscious mice was assessed by using metabolic cages equipped with a funnel system, which separated urine from feces. The mice were conditioned for 2 days in metabolic cages with free access to drinking bottles containing water, which were refilled each morning. After conditioning (1 day), 24-hours urine volume and water intake were monitored under baseline conditions, meanwhile, sampling was conducted for 24 hours. Collected urine was kept at -80°C. The concentrations of albumin and creatinine in urine were measured by Labor Diagnostik (Leipzig, Germany).

3.2.2.6. Measurement RAS components concentration in mouse plasma

About 0.5 ml of blood was collected from each mouse, transferred to a 1.5 ml tube containing 25 µl of 10 mM EDTA and protein cocktail and mixed within 30 sec. Plasma was obtained by centrifugation at 5 000 rpm for 5 min and stored at –80°C.

The RAS components measurements were performed by core facility at the MDC and are described in detail elsewhere (Bohlender et al. 1996). Plasma renin activity was determined with

100 µl of plasma using an indirect enzyme-kinetic assay based on the release of Ang I from excess AOGEN by adding bilaterally nephrectomized rat plasma without any residual renin activity containing constant substrate concentrations (Bohlender et al. 1998). Ang I and Ang II concentration in plasma was measured by direct radioimmunoassay.

3.2.2.7. Spectrophotometric Assays for Nitrite/Nitrate (Griess assay)

Before measurement, urine was diluted 1:50 and 80 µl of sample was used to determine total nitrate and nitrite level by a Nitrate/Nitrite Colorimetric Assay Kit (Cayman Chemical) according to the manufacturer's protocol. In brief, nitrate was first converted to nitrite by nitrate reductase; thereafter samples were incubated with Griess reagent and absorbance was measured at 540 nm using a spectrophotometer (SPEKOL 11, Zeiss, Germany). Each sample was run as a technical duplicate.

3.2.2.8. Nitrite determination by reaction with 2, 3-di-aminonaphthalene (DAN)

To collect the blood, mice were decapitated and the collected blood was transferred to a tube containing 10% EDTA solution. After centrifugation (1000 xg for 10 minutes) plasma was mixed with 2, 3-diaminonaphthalene (50 µg/ml in 0.62 N HCl) to form fluorescent products. Ten minutes later, the reaction was stopped by the addition of 20 µl of 2.8 N NaOH. The amount of fluorescent products was determined using a fluorometer (Fluoroskan II; Dainippon Pharmaceutical, Osaka, Japan) with excitation at 365 nm and emission at 405 nm and data were normalized by protein concentration. Sodium nitrite was used as a standard. Each sample was run as a technical triplicate.

3.2.2.9. cGMP measurement

Intracellular cGMP was released with 1 ml 6% (w/v) trichloroacetic acid (TCA), which was subsequently removed by extraction with water-saturated diethyl ether. The cGMP was then acetylated and measured by radioimmunoassay. cGMP values were normalized by protein concentration. Determination of cGMP was performed by RIA as described in ref (Langenickel et al. 2004).

3.2.2.10. Thiobarbituric acid reactants (TBARS)

Snap-frozen tissue was crushed in a prechilled mortar. One-hundred µl homogenate was mixed with 100 µl of 16.2 % SDS solution. After the addition of 1250 µl of thiobarbituric acid (TBA), samples were incubated at 95°C for 1 hr and centrifuged at 956 x g for 15 min at RT. Absorbance was then read at 532 nm and normalized by protein concentration.

3.2.2.11. Measurement of urinary isoprostane

Mice were placed in metabolic cages to collect urine over 24 hours for a consecutive 2 days. Samples were collected in the presence of 0.1% butylated hydroxytoluene and were stored at -80°C. An aliquot was stored for creatinine measurement. The concentration of isoprostane was measured by a 8-Isoprostane ELISA Kit (Cayman Chemical) according to the manufacturer's protocol.

3.3. Statistical Methods

All data are expressed as the mean ± SE. For Affymetrix data and real time PCR, expression values were compared between WT and *Mas*-knockout mice using Student's t test and $p<0.05$ was considered to indicate significantly different expression between the two groups of mice. To find the functional groups of genes overrepresented in the set of genes differentially expressed in testes of *Mas*-deficient vs. control mice, a chi-squared test was used.

Comparisons between individual pairs of means were made using unpaired two tailed Student's t-test. For the category phenotypic data, the Mann-Whitney U-test that is the non-parametric equivalent to the t-test was used. The nonparametric Wilcoxon test was used to compare two paired groups. The three groups were compared using one-way analysis of variance Values of $p<0.05$ (two-tailed) were considered statistically significant.

4. Results

4.1. *Mas*-deficient mice

4.1.1. Elevated blood pressure in FVB/N but not Bl/6 *Mas*-deficient mice

Previous studies on *Mas*-deficient mice have been performed on a mixed 129/Bl/6 genetic background and these mice were normotensive (Walther et al. 2000). To obtain more reliable results, *Mas*-deficient mice were backcrossed for 7 generations to the FVB/N (FV) and C57Bl/6 (Bl/6) genetic background. We first investigated basal cardiovascular parameters in these animals by invasive catheter in conscious mice. As seen in *Mas*-deficient mice on a mixed genetic background mean arterial pressure (MAP) on a pure C57Bl/6 *Mas*-deficient (Bl/6 *Mas*) background was not different from controls (106.0 ± 0.6 in Bl/6 *Mas vs.* 101.0 ± 0.7 mmHg in Bl/6, $p>0.05$) (Fig. 4.1C). In contrast, MAP in FVB/N *Mas*-deficient (FV *Mas*) mice was significantly elevated compared to controls (MAP 120.1 ± 1.80 in FV *Mas vs.* 100.8 ± 2.06 mmHg in FV, $n=7$, $p<0.001$). These data were confirmed by telemetry measurement (Fig. 4.1B, $p<0.01$). FV *Mas* mice showed a normal day/night rhythm of blood pressure (108.0 ± 0.3 vs. 101.0 ± 0.1 mmHg ($p<0.05$) during the day and 112.0 ± 0.3 vs. 106.0 ± 0.1 mmHg ($p<0.05$) during the night) (Fig. 4.1A, B).

Heart rate was significantly lower in FV *Mas* than in FV mice, but also showed a normal rhythm (day: 523.1 ± 5.1 in FV *Mas vs.* 563.2 ± 5.3 in FV, $p<0.001$; night: 556.4 ± 9.9 in FV *Mas vs.* 601.0 ± 9.1 beats/min in FV, $p<0.01$) (Fig. 4.1D). Again, heart rate in Bl/6 *Mas* was not different from Bl/6 mice (612.6 ± 22.14 in Bl/6 *Mas vs.* 596.6 ± 23.58 in Bl/6, $p>0.05$) (Fig. 4.1E).

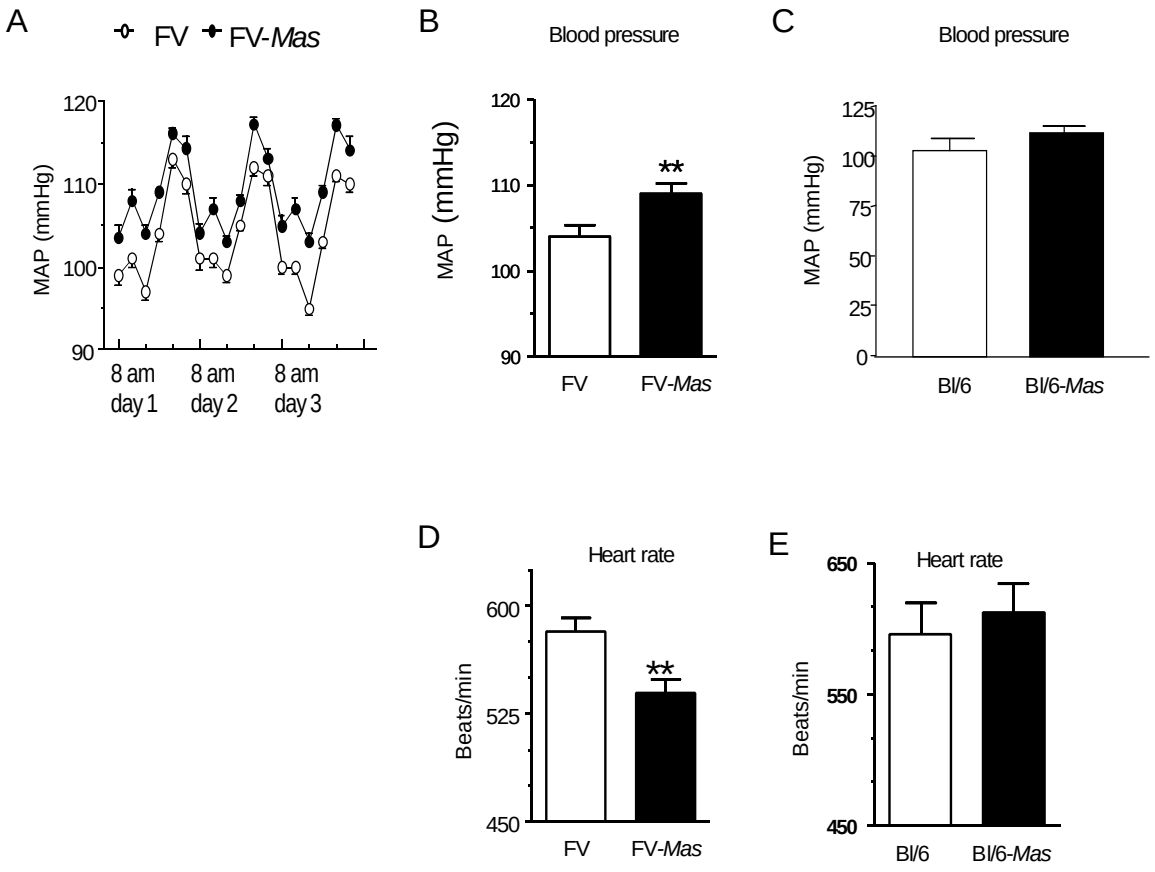

Fig. 4.1. Basal cardiovascular parameters in *Mas*-deficient mice
(A) Circadian variations in MAP (B) Telemetric MAP averaged over 3 days for FV*Mas* (n=7) and FV mice (n=6). (C) HR averaged over 3 days for FV *Mas* (n=7) and FV (n=6) mice. (D, E) MAP and HR in conscious Bl/6 *Mas* (n=6) and Bl/6 (n=5) mice. Data represent mean ± SEM, **p<0.01 (Student's t-test)

4.1.2. Impaired endothelial relaxation response in *Mas*-deficient mice

To further examine the functional consequences of *Mas* deletion we studied vascular reactivity *in vivo* in *Mas*-deficient mice. We first evaluated endothelial function in anesthetized mice by bolus intra-aortic administration of the endothelium-dependent vasodilator ACh. The vasodilatory response to ACh was markedly decreased in both FV *Mas* mice compared to FV over the dose range of 50-200 ng/kg (Fig. 4.2A, $p<0.001$); as well as in Bl/6 *Mas* mice (Fig. 4.2G, $p<0.01$). In contrast, endothelium-independent response measured by administration of SNP was slightly increased in FV *Mas* mice ($p<0.05$) (Fig. 4.2B).

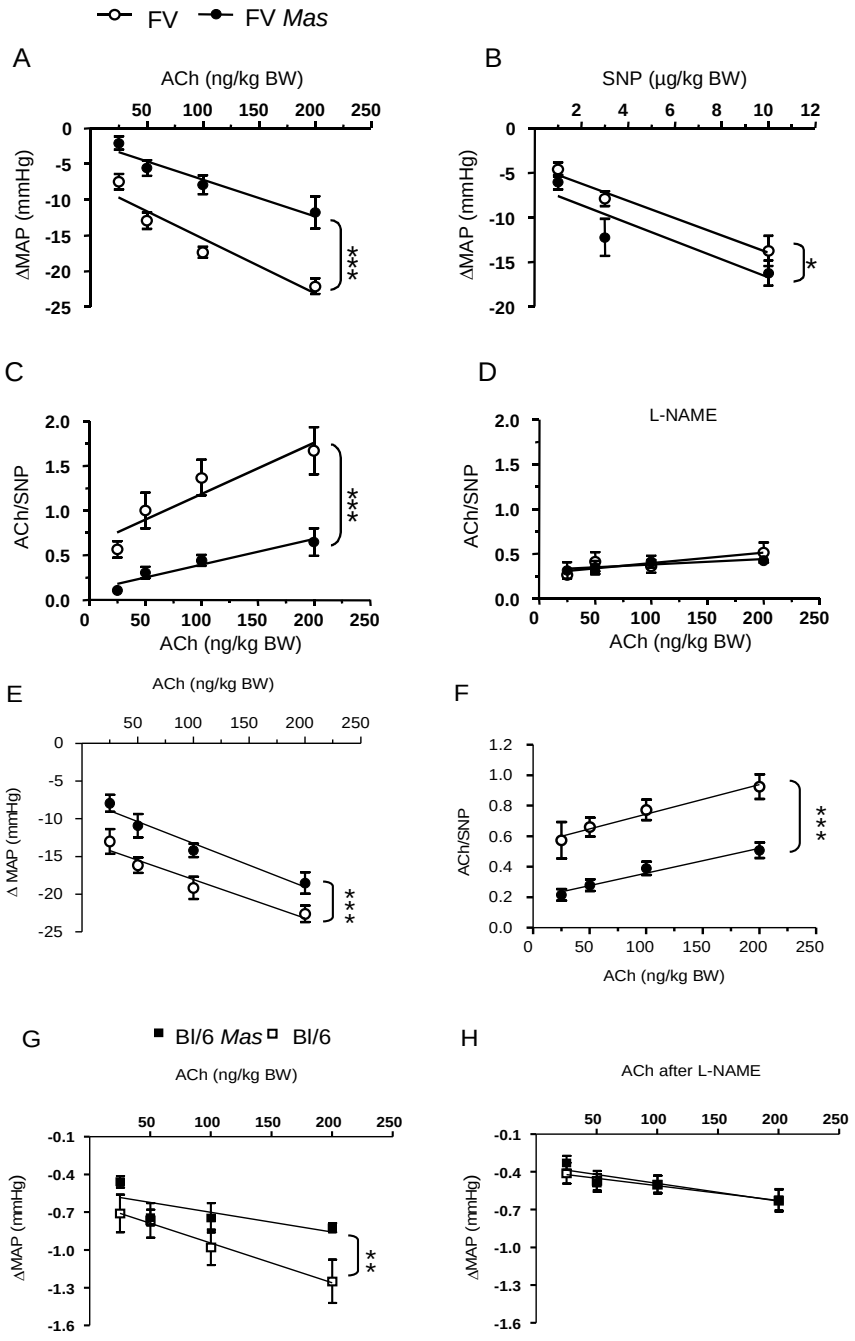

Fig. 4.2. Endothelial function in *Mas*-deficient mice

(A) Vascular response to increasing concentrations of ACh in anesthetized FV *Mas* and FV mice. (B) SNP in anesthetized FV *Mas* (n=5) and FV (n=6) mice. (C) Vascular response to ACh normalized by SNP in anesthetized FV *Mas* and FV mice. (D) Vascular response to ACh normalized by SNP after L-NAME treatment in anesthetized FV *Mas* and FV mice. Data represent mean ± SEM. Similar data were obtained in two independent experiments. (E) Vascular response to increasing concentrations of ACh in conscious FV *Mas* (n=8) and FV (n=11) mice. (F) Vascular response to ACh normalized by SNP. Data represent mean ± SEM.) (G) Vascular response to increasing concentrations of ACh in anesthetized Bl/6 *Mas* (n=5) and *Bl/6* (n=6) mice. (H) Vascular response to ACh after L-NAME treatment in anesthetized Bl/6 *Mas* (n=5) and *Bl/6* (n=6) mice. *p<0.05 **p<0.01, ***p<0.001 (two-way ANOVA)

Normalization of the ACh response by the SNP effect reinforced the evidence that endothelium-dependent vascular reactivity was impaired in FV *Mas* mice ($p<0.001$) (Fig. 4.2C). The difference was completely blunted after administration of the NOS inhibitor L-NAME (Fig. 4.2D, H) in both lines. The same results were achieved in conscious animals (Fig. 4.2E, F) confirming the fact that *Mas* deletion impairs endothelial function in mice.

4.1.3. RAS in *Mas*-deficient mice

To observe if *Mas* gene deletion changes main components of the RAS, we measured plasma renin activity and Ang I and II concentrations. There was 5 times higher plasma renin activity (Fig. 4.3A, $p<0.01$) and nearly 2 times higher Ang I concentration (Fig. 4.3B, $p<0.01$) in FV than Bl/6 mice, but no differences between *Mas*-deficient mice and any WT. No alterations in Ang I and II were observed either (Fig. 4.3B, C).

ACE2 is involved in the generation of Ang (1-7), its expression level may be affected by Mas. However, in *Mas*-deficient mice did not show any change in ACE2 mRNA in aorta as measured by real time PCR, but the ACE2 expression level in FV mice was significantly higher than in Bl/6 mice (Fig. 4.3D, $p<0.05$).

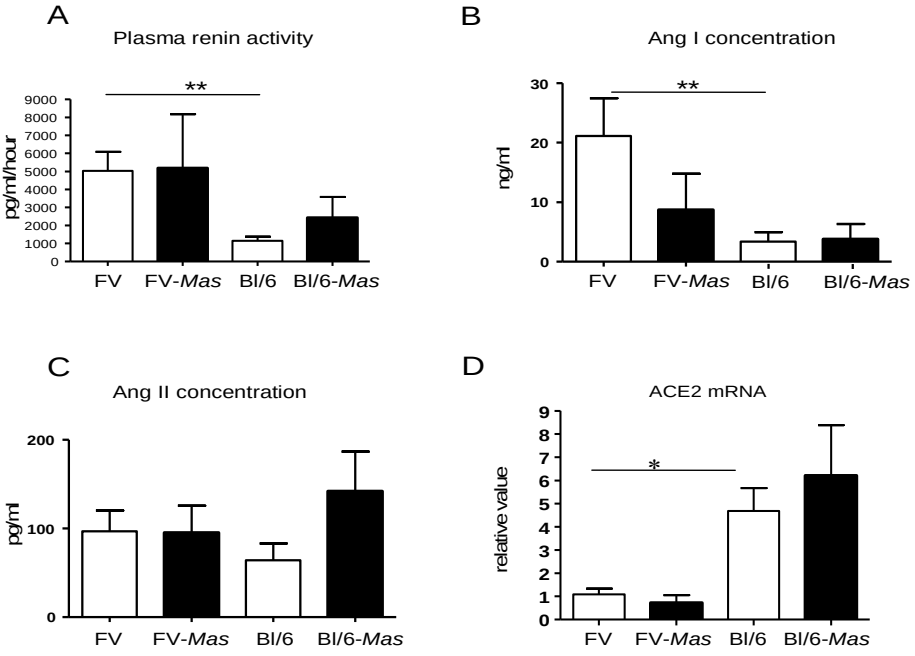

Fig. 4.3. Plasma renin activity, Ang I and II and ACE2 mRNA levels
(A) Plasma renin activity FV *Mas* (n=3) and FV (n=5) mice, Bl/6 *Mas* (n=6) and Bl6 (n=7) mice (B) Ang I concentration in plasma, FV*Mas* (n=7) and FV (n=4) mice, Bl/6 *Mas* (n=7) and Bl/6 (n=7) mice (C) Ang II concentration in plasma, FV *Mas* (n=8) and FV (n=6) mice, Bl/6 *Mas* (n=7) and Bl/6 (n=8) mice (D) Real-time RT-PCR detection of ACE2 mRNA in aorta. Expression level was normalized to the respective ß-actin level. FV*Mas* (n=6), FV (n=5). Bl/6 *Mas* (n=4), Bl/6 (n=3). Data represent mean ± SEM, *p<0.05, **p<0.01

4.1.4. Reduced NO-bioavailability in *Mas*-deficient mice

To understand the mechanisms involved in elevated blood pressure and impaired endothelial function, we tested whether these effects were caused by alterations in NO levels in *Mas*-deficient mice. Most of the NO is oxidized to nitrite/nitrate, and the concentrations of these anions have been used as quantitative indices of NO production. The simplest and most widely used technique is spectrophotometric measurement of nitrite using the Griess reaction (Viinikka 1996). But this method has a detection limit for nitrite, which is 1.0-5.0 µM in biological fluids. Fluorometric measurement uses 2,3-diaminonaphthalene (DAN), which reacts with nitrite to form the fluorescent compound 2,3-naphthotriazole, is 50 times more sensitive than the Griess assay. Therefore we applied both methods to measure NOx.

In both genetic backgrounds urinary NOx were markedly decreased in *Mas*-deficient mice (Fig. 4.4A, $p<0.001$). In addition, FV *Mas* mice presented a lower plasma nitrite-concentration in comparison to controls as detected by the fluorometric assay (Fig. 4.4B, $p<0.01$). However, the difference in Bl/6 mice did not reach statistical significance (Fig. 4.4B). Since the main source of plasma NO is eNOS, we determined if eNOS expression was altered in *Mas*-deficient mice by real time RT-PCR. Using ß-actin as a reference gene, we found that eNOS was down regulated in FV *Mas* mice (Fig. 4.4C, $p<0.01$). Bl/6 *Mas* mice exhibited the same tendency (Fig. 4.4C). Relative quantification of eNOS mRNA normalized by HPRT1 as a reference gene showed that eNOS is down regulated in aortas of Bl/6 *Mas* mice (Fig. 4.4D, $p<0.01$) and FV *Mas* mice showed the same tendency (Fig. 4.4D).

Altogether, our findings showed that the bioavailability of NO is disturbed in *Mas*-deficient mice.

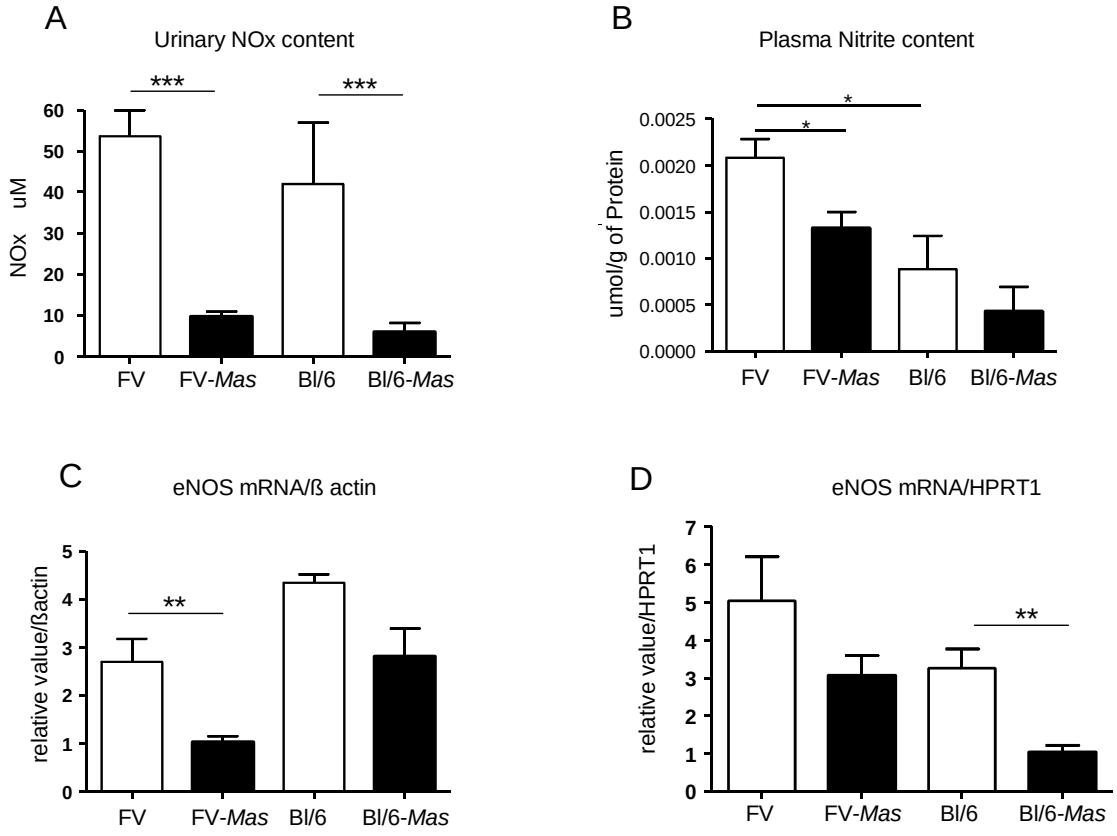

Fig. 4.4. NOx levels and eNOS expression
(A) Urinary NOx content in *Mas*-deficient and WT mice by Griess assay, (all groups n=6) (B) Plasma nitrite content in *Mas*-deficient and WT mice (n=8 per group) measured by a fluorescence method (C) Real-time RT-PCR detection of eNOS mRNA in aortas. Expression of eNOS was normalized to the respective ß-actin expression; FV *Mas* (n=6), FV (n=5), Bl/6 *Mas* (n=4), Bl/6 (n=3). (D) Expression of eNOS in aortas was normalized to the respective HPRT1 expression for each sample; FV *Mas* (n=3), FV (n=3). Bl/6 *Mas* (n=6), Bl/6 (n=5). *p<0.05, **p<0.01, ***p<0.001 (Student's t-test). Similar data were obtained in two independent experiments.

4.1.5. eNOS interacting proteins in *Mas*-deficient mice

eNOS is associated with caveolin-1 in caveolae and its activity is negatively regulated by this protein. Therefore, caveolin-1 expression was checked by immunofluores and western blot. No difference in caveolin-1 levels was found in the aorta of FV *Mas* compared to FV mice (Fig. 4.5A, B). However, since the caveolin-1 signal was detected in a mixed cell population, these data could be misleading concerning the caveolin-1 levels in the endothelial cells.

Akt-mediated phosphorylation activates eNOS and Akt acts as a positive regulator. Akt 1 and Akt 2 mRNA expression levels exhibited upregulation in aorta of Bl/6 *Mas* mice compared to WT as detected by real time PCR (Fig. 4.5C, D, $p<0.05$). Correspondingly, the Akt protein level was also increased in Bl/6 *Mas* mice as detected by western blot (Fig. 4.5E, F).

Hsp 90 as a scaffold protein connecting Akt and eNOS. We observed upregulation of Hsp 90 levels in aortas of Bl/6 *Mas* mice (Fig. 4.5F).

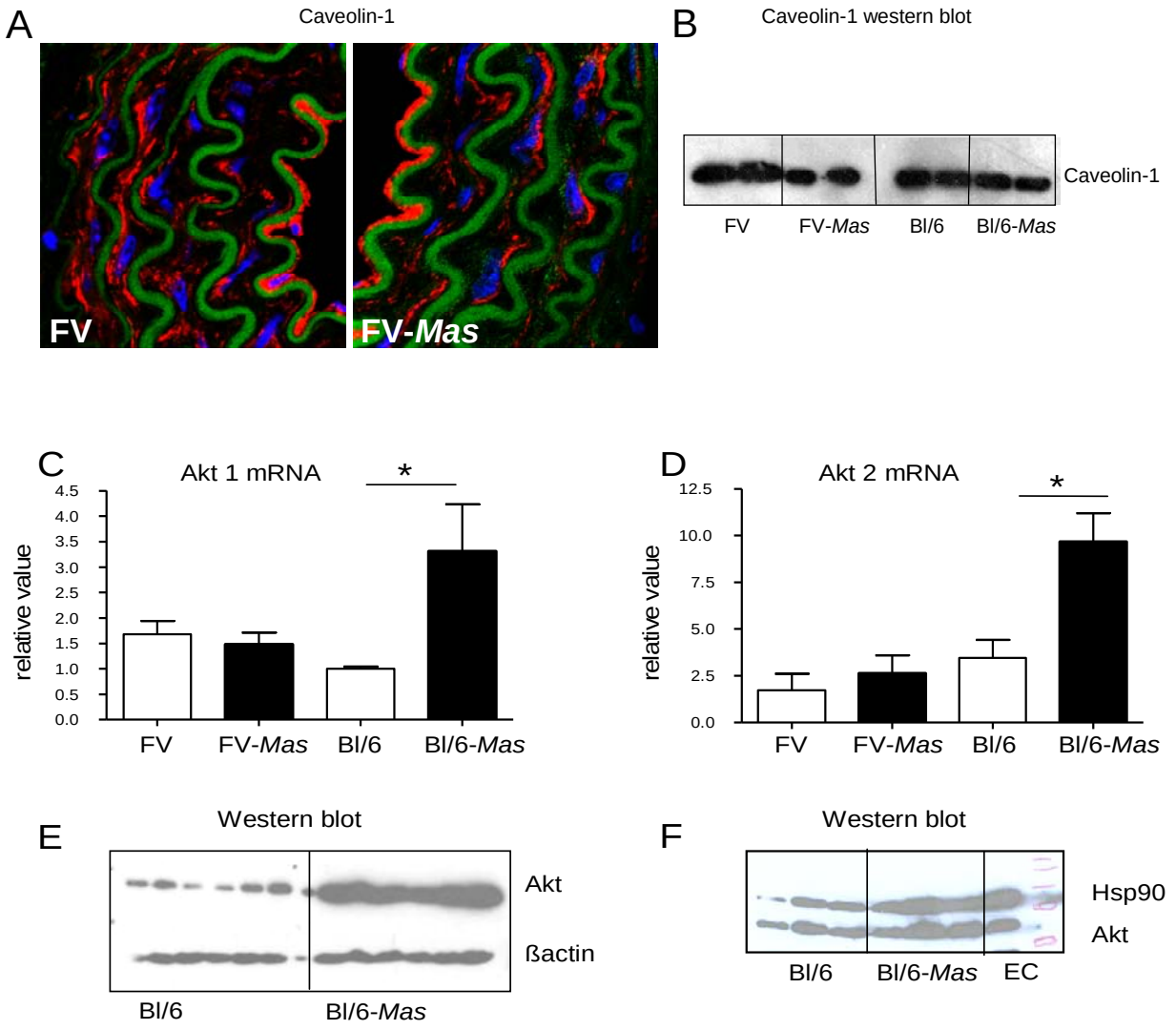

Fig. 4.5. Expression of Caveolin-1, Akt and Hsp 90
(A) Representative aorta slices from FV *Mas* and WT mice (n=3) stained with anti-caveolin-1 antibody (1:100 dilution). (B) Western blot for caveolin-1, 40 µg of proteins of aortic homogenates from FV, Bl/6 and FV *Mas* and Bl/6 *Mas* mice (n=2) were separated on 12% SDS-PAGE gel. Caveolin-1 was visualized using a polyclonal rabbit anti-caveolin-1 antibody (1:1000 dilution). (C, D) Akt 1 and Akt 2 mRNA expression levels were detected by real time PCR. n=4. (E) Western blot for Akt, 40 µg of proteins of aortic homogenates from Bl/6 *Mas* and Bl/6 mice were separated on 12% SDS-PAGE gel, Akt and ßactin were visualized with Akt (1:1000) and ß actin (1:2500) antibody. (n=6). (F) Western blot of aortic homogenates with Hsp 90 (1:1000) and Akt (1:1000) antibody, (n=3). EC, endothelial cell extract used as positive control.

4.1.6. cGMP in the aorta of *Mas*-deficient mice

cGMP is the most reliable marker to determine the release of biologically active NO. It was found that the concentration of cGMP was lower in the aorta of Bl/6 *Mas* mice compared to WT (Fig. 4.6, $p<0.01$).

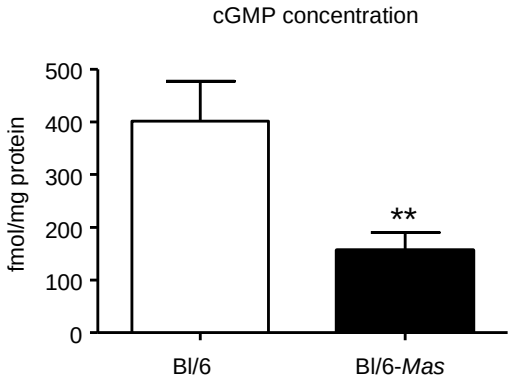

Fig. 4.6. Concentration of cGMP in aorta
cGMP content in aortic homogenates of Bl/6 *Mas* (n=6) and Bl6 (n=6) mice. Values are normalized by protein concentration, **p<0.01

4.1.7. Oxidative stress in *Mas*-deficient mice

NO acts as an endogenous antioxidant by quenching $O_2^{\cdot-}$ and provides a protective function against ROS action. The balance between NO and superoxide is important for the fine control of the vascular tone (Cai and Harrison 2000). To check for the involvement of oxidative stress in the altered regulation of blood pressure and endothelial function observed in *Mas*-deficient mice, we measured thiobarbituric acid reactive substances (TBARS) level, namely malondialdehyde (MDA), which is an indicator of oxidative stress. This method is most widely used for studying lipid peroxidation and is based on the reaction of MDA with thiobarbituric acid (TBA), in which one molecule of MDA reacts with two molecules of TBA to form a stable pink to red color that absorbs maximally at 532 nm (Sinnhuber et al. 1983; Nair and Turner 1984).

TBARS were significantly increased in the aorta homogenates of FV *Mas* mice compared to controls (Fig. 4.7A, $p<0.01$). The same result was found for the plasma sample (Fig. 4.7B, $p<0.05$). In contrast, no difference between Bl/6 *Mas* mice and controls was observed. Interestingly, the TBARS level in plasma of Bl/6 mice was higher than in FV mice (Fig. 4.7B, $p<0.05$).

Isoprostanes are known in vivo markers for oxidative stress. They have been regarded as a more sensitive and stable biomarker than MDA (Lykkesfeldt 2007). The 24-h urinary F2-isoprostanes excretion was 2 times higher in Bl/6 *Mas* mice in comparison to Bl/6 mice (7.09±2.82 ng/mg creatinine (Cr) vs 3.60±1.19 ng/mg Cr, respectively). Additionally Bl/6 mice displayed higher isoprostane excretion than FV (1.16±0.37 ng/mg Cr) (Fig. 4.7D, $p<0.001$). Urinary isoprostane could be influenced by kidney function. Therefore, urinary albumin and creatinine were measured to correct isoprostane values. There were no differences in urine albumin and creatinine between *Mas*-deficient and control mice. Unexpectedly, FV mice exhibited higher creatinine (Fig. 4.7C, $p<0.01$) and albumin excretion concentration in comparison to Bl/6 mice (Fig. 4.7E, $p<0.001$). Since there was significantly less urine volume in FV than Bl/6 mice (Fig. 4.7F, $p<0.01$), the daily excretion of albumin and creatinine was not different between the two mouse strains anymore (Fig. 4.7G, H).

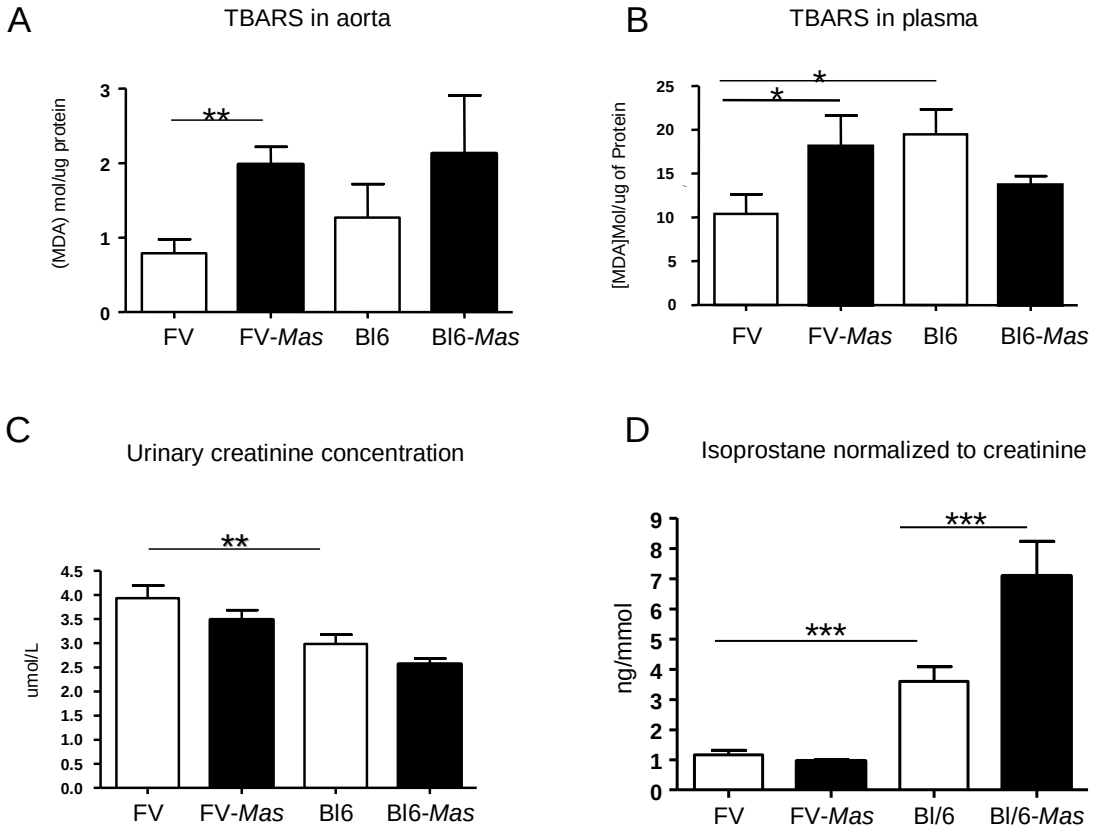

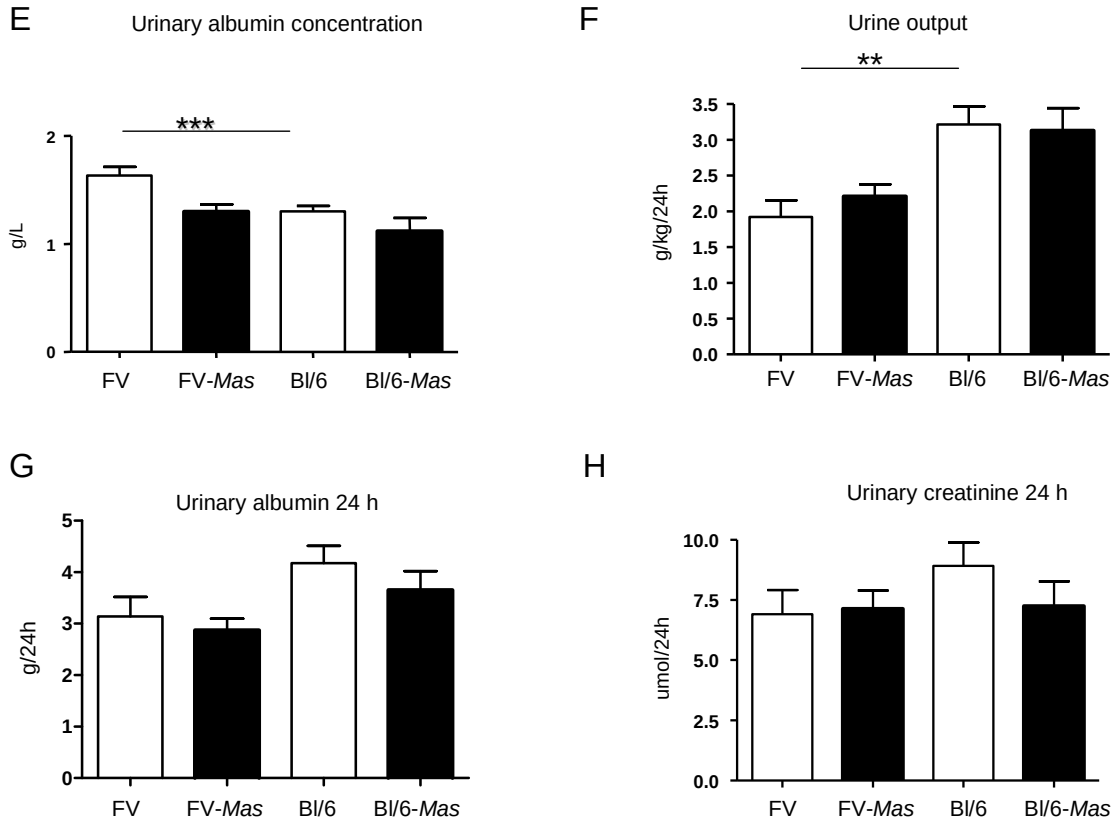

Fig. 4.7. Oxidative stress markers and kidney function
(A) Concentration of the TBARS in aorta of 2 lines of *Mas*-deficient (n=4) and WT (n=5) mice. (B) TBARS in plasma of *Mas*-deficient (n=4) and WT (n=5) mice. Similar data were obtained in two independent experiments. (C) Urinary creatinine concentration, each group (n=6). (D) Urinary isoprostane excretion. Isoprostane concentration normalized by creatinine concentration, (all groups n=6) (E) Urinary albumin concentration. (each group n=6). (F) Urine output, (all groups n=6), (G and H) Urinary albumin and creatinine in 24-h urine collections. *p<0.05, **p<0.01, ***p<0.001 (Student's t-test).

4.1.8. ROS generation in *Mas*-deficient mice

To identify the probable source of the augmented ROS levels observed in *Mas*-deficient mice, we analyzed expression and activity of enzymes involved in the generation and metabolism of ROS. NAD(P)H oxidase isoforms (Nox 1-5) are involved in augmented $O_2^{\cdot-}$ production in hypertension. Since Nox 2 and Nox 4 are highly expressed in vascular tissues, we determined the expression levels of both isoforms. There was a markedly increased Nox 2 mRNA level in aortas of Bl/6 *Mas* mice, but, oppositely, Nox 2 levels were decreased in FV *Mas* mice (Fig. 4.8A, $p<0.05$) and Nox 4 mRNA levels were decreased compared to Bl/6 mice (Fig. 4.8B). Nox 2 protein content determined by western blotting was higher in both FV *Mas* and Bl/6 *Mas* mice than in their WT controls (Fig. 4.8C, D).

Cyclooxygenase (Cox-1 and Cox-2) are the key enzymes for the prostanoid metabolic pathway to regulate endothelial function. There were no differences in the expression level of these genes between *Mas*-deficient mice and controls in both Bl/6 and FV lines, but Cox-1 mRNA expression in FV mice was higher than in Bl/6 mice (Fig. 4.8E, F, $p<0.05$).

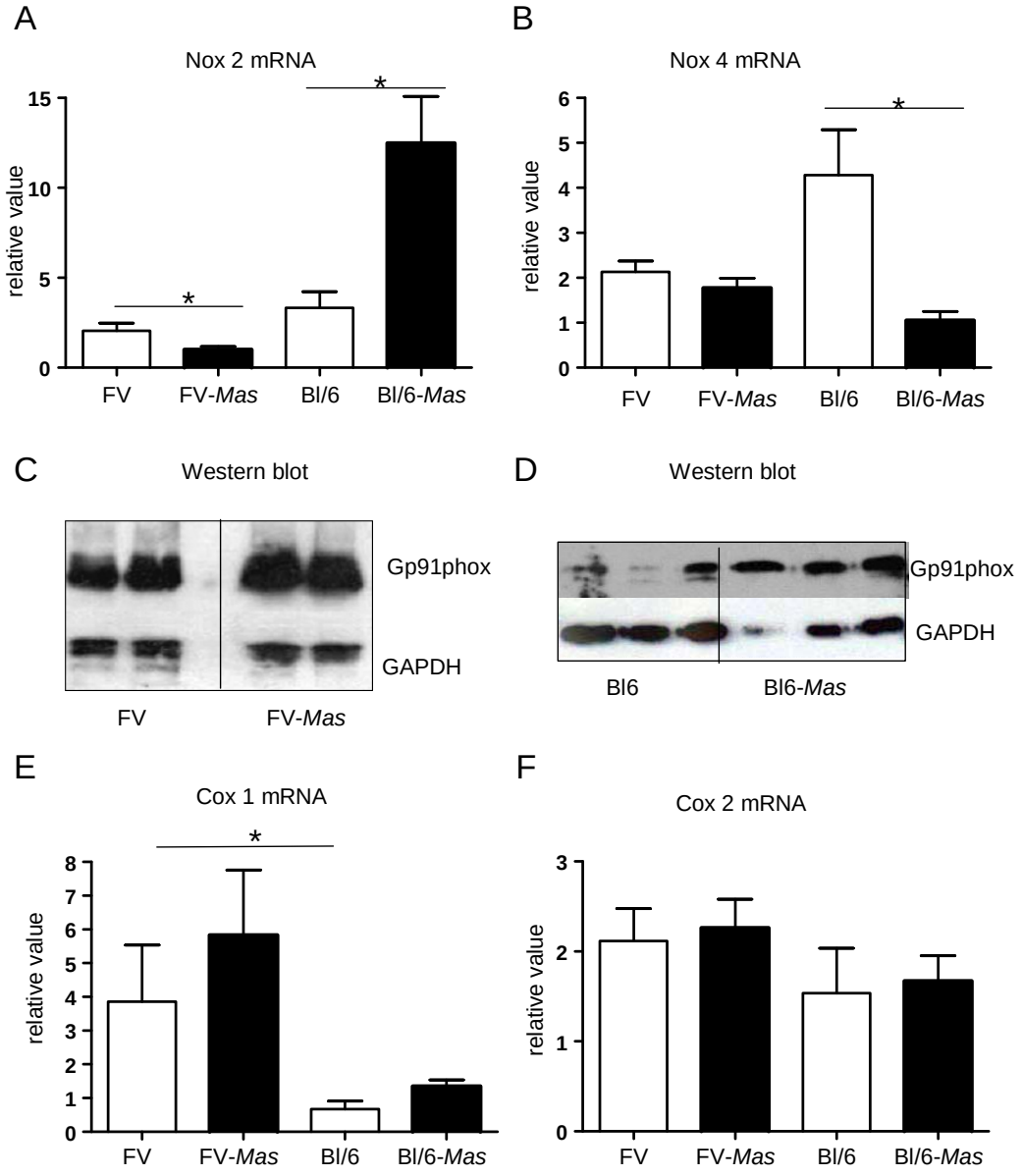

Fig. 4.8. ROS generation

(A and B) Real-time RT-PCR detection of Nox 2 (A) and Nox 4 (B) mRNA normalized to the respective ß-actin mRNA content. Nox2: FV *Mas* (n=12), FV (n=8). Bl/6 *Mas* (n=7), Bl/6 (n=7). Nox4: FV *Mas* (n=4), FV (n=7), Bl/6 *Mas* (n=4), Bl/6 (n=4). (C and D) Representative western blot for the gp91phox subunit of NAD(P)H oxidase in the aortic homogenate of *Mas*-deficient and WT mice. Similar data were obtained in two independent experiments. (E and F) Real time PCR detection of Cox 1 and Cox 2 mRNA expressions in aorta. Cox 1: FV *Mas* (n=5), FV (n=3), Bl/6 *Mas* (n=4), Bl6 (n=3). Cox 2: FV *Mas* (n=11) and FV (n=9) mice, Bl/6 *Mas* (n=7), Bl/6 (n=6). *$p<0.05$.

4.1.9. ROS degradation in *Mas*-deficient mice

SOD, catalase and glutathione peroxidase comprise the main enzymes systems for the degradation of ROS. To test whether increased ROS are due to altered degradation of ROS, we measured SOD and catalase activity in aorta tissue extract. Both SOD and catalase activities were reduced in FV *Mas* mice compared to FV animals but not in the Bl/6 mice (Fig. 4.9A, B). These results suggest that oxidative stress observed in FV *Mas* mice is due to inefficiency of the endogenous antioxidant mechanisms in scavenging ROS and probably to an NAD(P)H-oxidase dependent ROS overproduction. Additionally, both SOD and catalase activities were reduced in Bl/6 mice compared to FV mice (Fig. 4.9A, B, $p<0.01$).

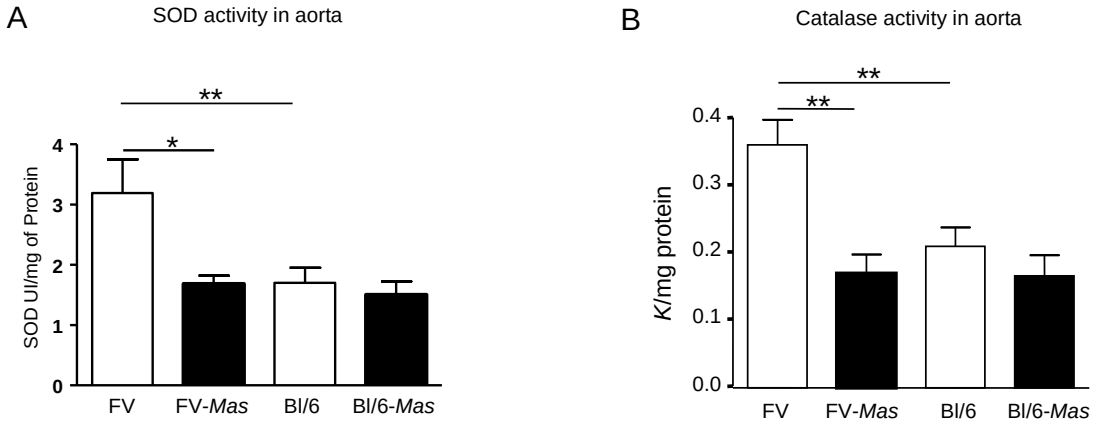

Fig. 4.9. ROS degrading enzymes
(A) SOD and (B) Catalase activity in aorta of *Mas*-deficient (n=4) and WT (n=5) mice. *p<0.05, **p<0.01 (Student's t-test). Similar data were obtained in two independent experiments.

4.1.10. Effect of tempol on blood pressure in FV *Mas*-deficient mice

To elucidate if the ROS increase is related to the elevated blood pressure in FV *Mas*-deficient mice, we studied the effect of tempol (SOD mimetic) on blood pressure in FV lines. Tempol did not change heart rate (data not shown) but reduced MAP in both *Mas*-deficient and WT mice (Fig. 4.10A). However, the reduction was significantly more pronounced in *Mas*-deficient mice (MAP: -7.0 ± 1.0 vs. -2.8 ± 0.9) (Fig. 4.10B, $p<0.01$). These results suggest that increased ROS may be involved in the increased blood pressure observed in *Mas*-deficient mice.

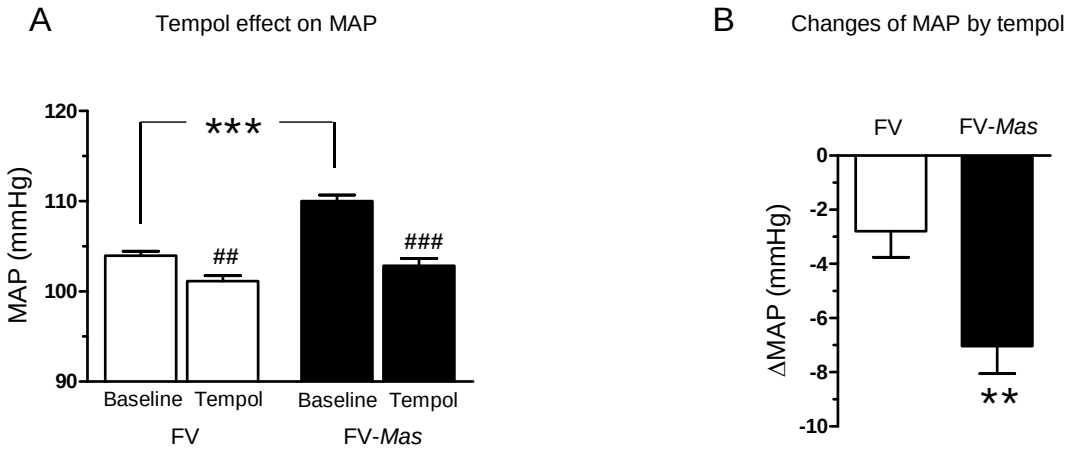

Fig. 4.10. Tempol effect on cardiovascular parameters
(A) Mean arterial blood pressure (MAP) before and after tempol treatment (50 mg/kg/day) in FV *Mas* (n=21) and FV (n=22) mice. (B) Changes of MAP (Δ MAP) by tempol in FV *Mas* and FV mice; $^{\#\#}p<0.01$, $^{\#\#\#}p<0.001$ tempol-treatment vs. baseline; $^{**}p<0.01$. ***p<0.001 (FV *Mas vs* FV) (one-way ANOVA followed by Bonferroni's post-test)

4.1.11. Alterations in gene expression in the hearts of Bl/6 *Mas*-deficient mice

In order to find genes of which the expression is changed in hearts of Bl/6 *Mas* mice in comparison to Bl/6 controls, the cRNA of hearts in Bl/6 and Bl/6 *Mas* deficient mice was probed with 12488 transcripts of Affymetrix Murine Genome U74Av2 GeneChip. 269 transcripts were identified to be differentially expressed: 87 genes were downregulated in *Mas*-deficient mice, $p<0.05$, while 182 genes were upregulated, $p<0.05$ (Appendix, Table 1 and 2). Noticeably, 3 genes in the PI3K-Akt pathway were upregulated. Akt 1 KO/WT =1.78, p= 0.035, Akt 2 KO/WT =1.13, p= 0.001, Pdk1 KO/WT =1.23, p= 0.04, corresponding to our real time PCR data, which showed increased expression level of Akt 1 and Akt 2 in aorta (Fig. 4.5C, D). Thus, Akt expression is upregulated by *Mas* deletion in cardiovascular tissues.

A. Gene ontology mining analysis

In order to identify pathways affected by deletion of *Mas* in the heart, we subjected the set of 269 differentially expressed genes to gene ontology mining analysis. The ontology branch "Biological Processes Analysis" revealed that genes involved in Notch signalling pathway (2 genes of 2) were enriched in this group of transcripts. By "Cellular Component Analysis" genes

related to MHC protein complex (6 genes of 37, Chi Sq. 33.25, P=8.57E-9) and muscle thin filament (2 genes of 5, Chi Sq. 32.67, P=1.16E-8) were detected.

B. Verification of microarray data by RPA

Some of the genes which were found to be differentially expressed in *Mas*-deficient mice were evaluated by RPA:

Rgs2 (Regulator of G-protein signalling 2) gene expression was found reduced by Affymetrix KO/WT= 0.49, P=0.0020. This reduction was confirmed by RPA KO/WT =0.49, p= 0.001 (Fig. 4.11A).

Adam19 (A disintegrin and metalloproteinase domain 19 (meltrin beta)) gene expression was found increased by Affymetrix KO/WT=2.85, p=0.024. The data was confirmed by RPA KO/WT=1.69, p= 0.03 (Fig. 4.11B).

Cpxm2 Carboxypeptidase X 2 (M14 family) (belonging to the metallocarboxypeptidase gene family) gene expression was found upregulated by Affymetrix KO/WT = 2.07, p=0.024. We could see a trend of increase by RPA but it was not significant, KO/WT =1.27, p= 0.15 (Fig. 4.11C).

Col6a3 (Procollagen**,** type VI, alpha 3) gene expression showed a trend of upregulation by Affymetrix KO/WT= 1.48, p=0.056 which was not confirmed by RPA in Bl/6 *Mas* and Bl/6 mice (Fig. 4.11D).

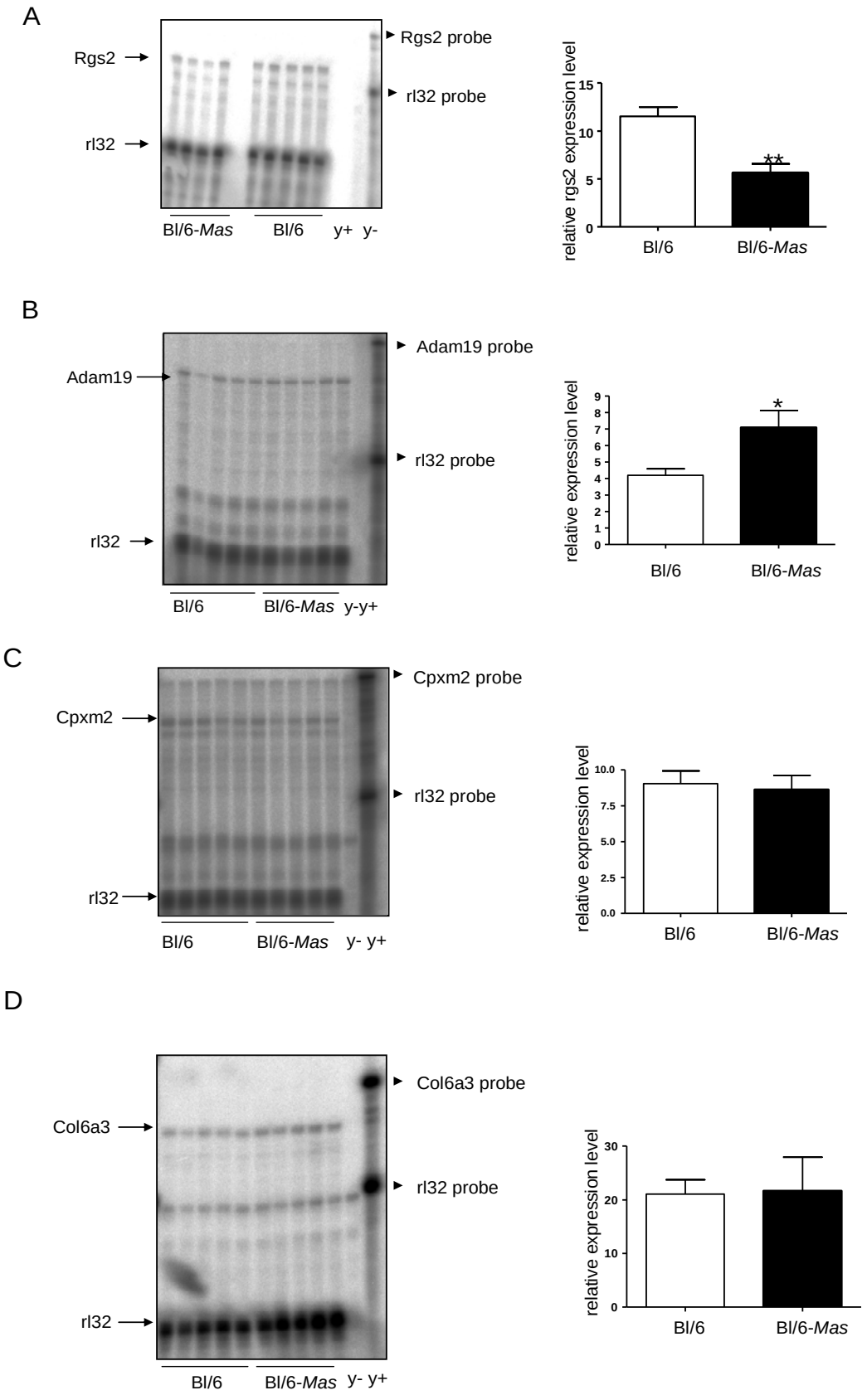

Fig. 4.11. Gene expression detected by RPA in the hearts of Bl/6 *Mas* mice.

(A) Expression of rgs2, (Bl/6 *Mas* (n=4) and Bl/6 (n=5)). (B) Expression of Adam19 (Bl/6 *Mas* and Bl/6, n=5) (C) Expression of Cpxm2 (Bl/6 *Mas* and Bl/6, n=5) (D) Expression of Col6a3 (Bl/6 *Mas* and Bl/6, n=5). rl 32 probe was used as housekeeping gene expression control. y+, yeast RNA with RNase digestion, y-, yeast RNA without RNase digestion. * $p<0.05$, ** $p<0.01$

4.1.12. Alterations in gene expression in the testis of Bl/6 *Mas*-deficient mice

In order to find genes of which the expression is changed in testes of Bl/6 *Mas* mice in comparison to Bl/6 controls, we used the Affymetrix Murine Genome U74Av2 GeneChip and probed 12488 transcripts. After validation of the microarray data, we identified 132 transcripts that were differentially expressed in the testis between *Mas*-deficient and WT mice. 65 genes were upregulated in Bl/6 *Mas* mice (Appendix, Table 3) and 67 genes were downregulated (Appendix, Table 4), whereby 10 (7.5%) of the identified transcripts were changed more then 2 fold. As expected, the *Mas* gene itself was downregulated (KO/WT=0.41, P=0.013, Table 4). The residual expression most probably originates from the 3'-region of the *Mas* gene, which was not deleted in *Mas*-deficient mice (Walther et al. 1998) and is identified by the Affymetrix gene chip array.

A. Gene ontology mining analysis

In order to identify pathways affected by deletion of *Mas* in testis, we subjected the set of 132 differentially expressed genes to gene ontology mining analysis. In the ontology branch "Cellular Components", genes belonging to the intracellular membrane-bound organelles, were overrepresented in the set of significantly affected genes (59 genes of 132, Chi Sq. 9.59, P=0.0024), being most pronounced in the subpopulation of genes with activities in mitochondria (18 genes of 132, Chi Sq: 16.69, P=0.00005), including genes important for steroidogenesis. In the ontology branch "Biological Processes", the group of genes involved in organelle organization and biogenesis were significantly affected (15 genes of 132, Chi Sq. 5.41, P=0.027), including two genes which are active in mitochondria (Pex11b, ID: 103814_at and Mrpl23, ID: 92646_at, Table 4). The ontology analysis in the branch "Molecular Function" revealed overrepresentation of genes involved in ion binding in the set of 132 genes analyzed (14 genes of 132, Chi Sq. 6.79, P=0.012).

B. Verification of microarray data by real time PCR and RPA

Quantitative reverse-transcription polymerase chain reaction is often used to confirm findings from microarray data (Qin et al. 2006).

To confirm the Affymetrix microarray dataset, four genes (StAR, ID: 92213_at; 3ß-HSD1, ID: 103072_at; 3ß-HSD6, ID: 102729_f_at; and Gfer, ID: 160269_at) were selected for real-time PCR analysis, comparing WT vs. *Mas*-deficient mice. The expression of StAR was decreased in *Mas*-deficient mice to 58% of WT expression level (Fig. 4.12A, $P<0.05$), corresponding to the Affymetrix results (KO/WT=0.59, P=0.0052, Table 1). Moreover; 3ß-HSD1 was increased to 161% (Fig. 4.12B, $P<0.05$) and 3ß-HSD6 expression was decreased to 49% (Fig. 4.12C, $P<0.01$) of WT expression, both confirming the microarray data (3ß-HSD1: KO/WT=1.67, P=0.0057, Table 3; 3ß-HSD6: KO/WT=0.35, P=0.0076, Table 4).

One exception was Gfer, being 4 fold upregulated in the Affymetrix data (KO/WT=3.98, P=0.04), whereas its expression in *Mas*-deficient mice was found to be decreased to 74% of WT expression level in 3 independent real time PCRs (Fig. 4.12D, $P<0.05$).

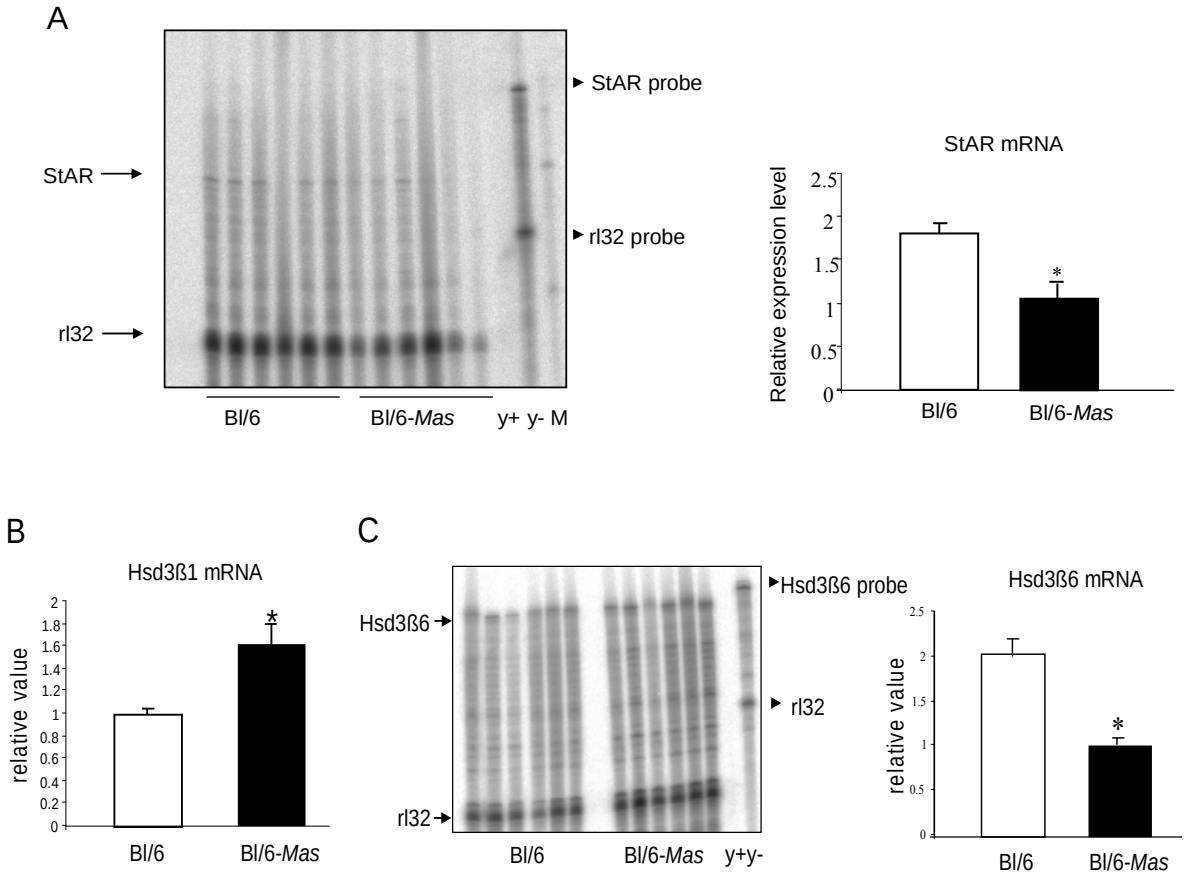

Fig. 4.12. Gene expression in the testes of Bl/6 *Mas* mice.

(A) Expression of StAR, left panel RPA, y+, yeast RNA with RNase digestion, y-, yeast RNA without RNase digestion. rl 32 probe was used as housekeeping gene expression control. Bl/6 *Mas* (n=6) and Bl/6 (n=6), right panel: real time PCR, Bl/6 *Mas* (n=4) and Bl/6 (n=4). (B) Expression of Hsd3ß1 by real time PCR in Bl/6 *Mas* mice (n=5) (C) Expression of Hsd3ß6 in Bl/6 *Mas* mice, left panel RPA (n=6); right panel real time PCR (n=4). (D) Expression of Gfer in Bl/6 *Mas* mice by real time PCR in Bl/6 *Mas* mice (n=4), * $p<0.05$.

4.2. TGM L102 mice

The whole rat angiotensinogen gene cut with EcoRI and HindIII was microinjected into pronuclei of a fertilized egg from NMRI mouse (Fig. 4.13A). 3 transgenic lines L123, L102 and L92 (TGM L123, L102 and L92) lines were produced (Kimura et al. 1992). L123 line has already been characterized exhibiting hypertension and fibrosis in heart and kidney (Kang et al. 2002). In this thesis, L102 was analyzed.

4.2.1. Genotyping and Southern blot for TGM L102 mice

Transgenic mice could be identified using PCR by a 800 bp band (Fig. 4.13B). Additionally, results of the PCR were verified by southern blot. Genomic DNA was digested by EcoRI, and after hybridization with a specific probe we could detect bands only in the male and female L102 mice, but not in the WT animals (Fig. 4.13C).

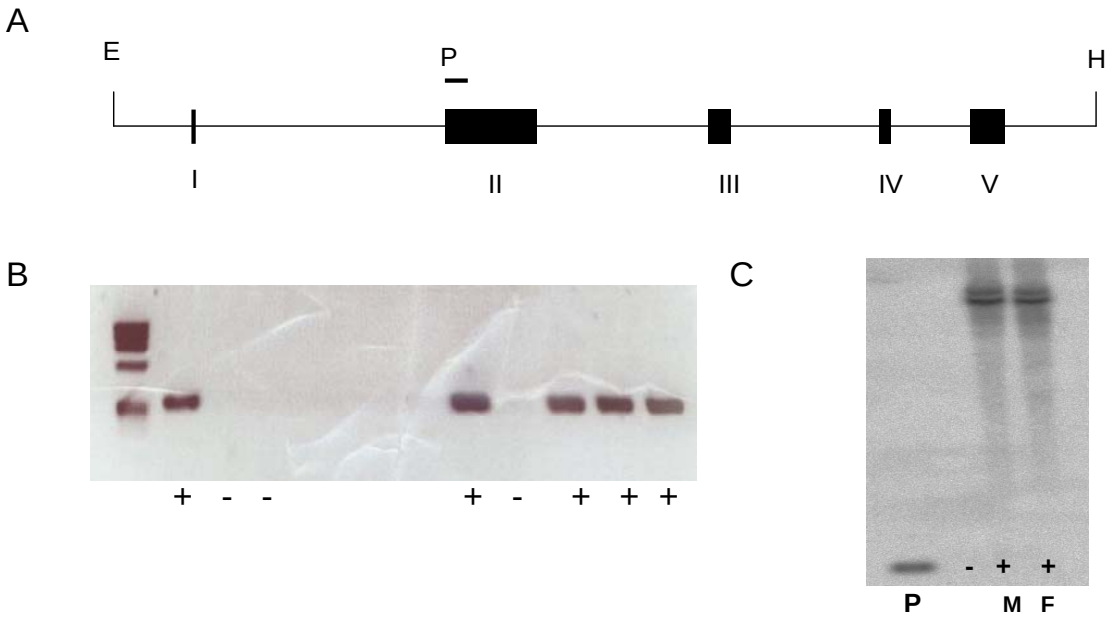

Fig. 4.13. Genotyping and Southern blot
(A) DNA construct for the generation of the transgenic mice, rat AOGEN gene fragment used for for microinjection, I-V represent 5 exons of rat AOGEN gene. E: EcoRI, H: HindIII, P: probe, a fragment of rat AOGEN exon 2 used as southern probe. (B) Genotyping by PCR (C) Genotyping by southern blot, 15 µg of genomic DNA was digested with EcoRI and hybridized with P, P was run as a positive control. M: male; F: female. +: L102; -: NMRI.

4.2.2. Transgenic and endogenous AOGEN expression in TGM L102 mice

Using separate mouse and rat AOGEN probes, 2 protected bands could be detected in RPA representing the endogenous and transgenic AOGEN expression. The rat AOGEN transgene was expressed highly in the liver and brain, also detectable in the heart, kidney and lung, and like the endogenous mouse AOGEN gene expression (Fig. 4.14).

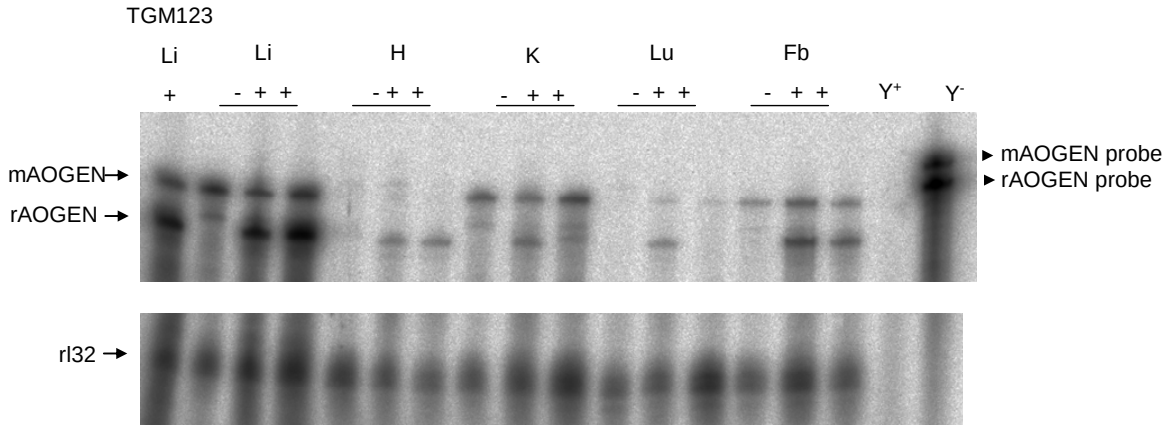

Fig. 4.14. Transgenic and endogenous AOGEN expression in different organs of 3 months old mice

Li: liver, H: heart, Lu: lung, K, kidney, Fb: forebrain, +: L102, -: NMRI. Y+, yeast RNA with RNase digestion, Y-, yeast RNA without RNase digestion. mAOGEN and rAOGEN: protected RNA hybridized with probe, rl 32 probe was used as housekeeping gene expression control. TGM123 Li: liver mRNA from the line of TGM L123, as a positive control.

4.2.3. Cardiovascular parameters in one year old TGM L102 mice

By the invasive catheter method conscious mice were assessed for cardiovascular parameters. The MAP reached 136.7 ± 6.7 mmHg in the transgenic mice vs 108.7 ± 5.0 mmHg in the NMRI (Fig. 4.15A), whereby systolic pressure of 4 animals reached levels of more than 190 mmHg. Heart rate was similar in L102 and control mice (Fig 4.15B). The rise in blood pressure was paralleled by cardiac hypertrophy (ventricle/ body weight ratio: L102: 4.4±0.3 mg/g, WT: 2.9±0.04 mg/g) (Fig. 4.15C, $p<0.001$).

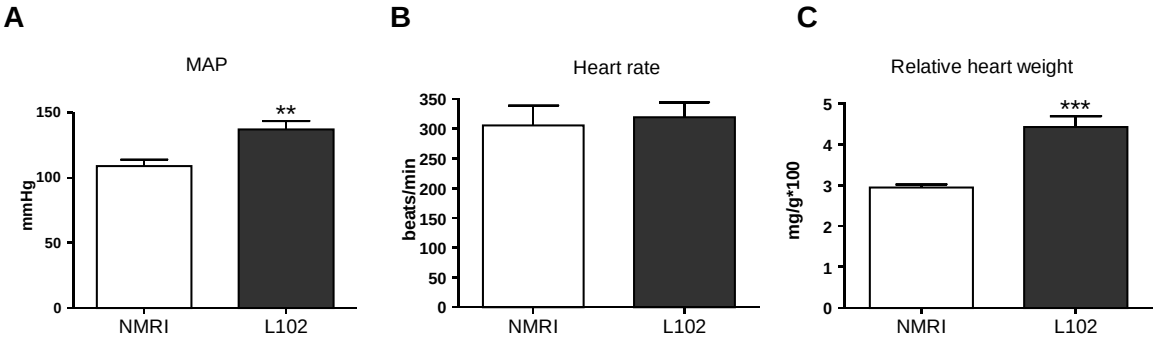

Fig. 4.15. Measurement of basal cardiovascular parameters in one year old mice
(A) MAP (L102 n=8, NMRI n=7) (B) Heart rate (C) Relative heart weight. Data represent mean ± SEM, **p<0.01, ***p<0.001 (Student's t-test)

4.2.4. Fibrosis staining of heart, lung and kidney in TGM L102 mice

Van Gieson staining is a useful stain to detect elastic material particularly in vascular malformations. This method stains collagen pale red, other tissue elements yellow, and nuclei brown. By this method, intense fibrosis was found in perivascular and interstitial tissues of heart, lung, and kidney in TGM L102 mice, in contrast to the WT mice (Fig. 4.16).

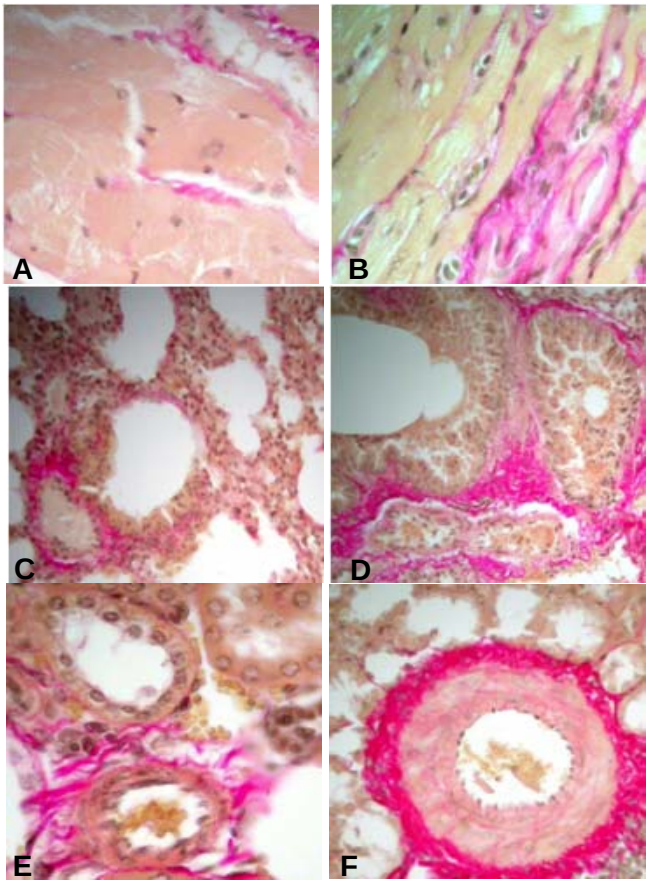

Fig. 4.16. Van Gieson staining
Representative slices of (A) Heart, (C) Lung, and (E) Kidney of NMRI mice and (B) Heart, (D) Lung, and (F) Kidney of TGML102 mice

4.2.5. Collagen III gene expression in the heart of TGM L102 mice

Histochemistry detected marked fibrosis in the tissues of L102 mice. Collagens comprise the most important family of structural macromolecules of the extracellular matrix upregulated in fibrosis. Therefore we determined collagen III expression level and detected higher collagen III expression in the hearts of L102 (Fig. 4.17, $p<0.05$).

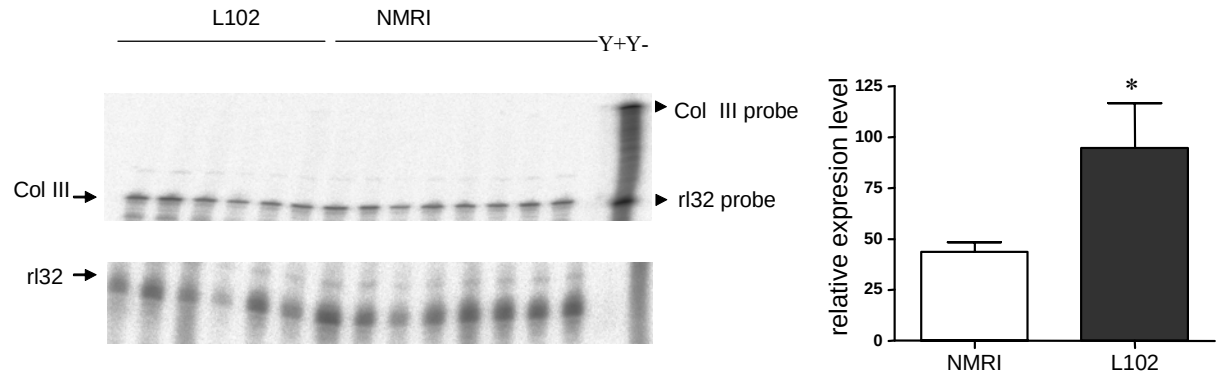

Fig. 4.17. RPA for cardiac collagen III gene expression
Left panel : Expression of collagen III (Col III) by RPA right panel : quantification of RPA. Y+, yeast RNA with RNase digestion, Y-, yeast RNA without RNase digestion. rl 32 probe was used as housekeeping gene expression control. L102 (n=6), NMRI (n=8) ∗ $p<0.05$

4.2.6. BNP in the heart of TGM L102 mice

Since brain natriuretic peptide (BNP) is synthesized in the ventricular myocardium and is reported to be a biochemical marker for hypertrophy, we measured ventricular BNP concentration by radioimmunoassay (RIA). Homogenates of L102 mice ventricles contained significantly more BNP than WT mice (Fig. 4.19, $p<0.001$).

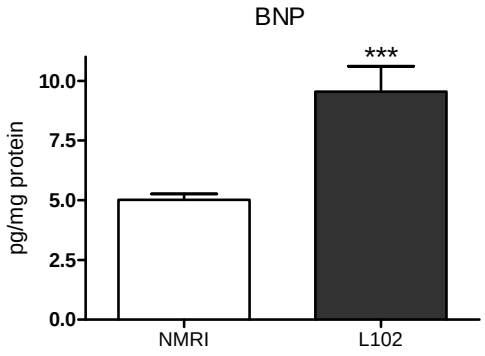

Fig. 4.19 BNP measurement in the heart
BNP was measured in ventricle extracts by RIA. Values were normalized with protein concentration. L102: n=7, NMRI: n=7, *** $p<0.001$

4.2.7. Apoptosis in the heart of TGM L102

Apoptosis is often associated with cardiac hypertrophy (Adams et al. 1998). Evidence for apoptosis in the heart can be detected by histological markers of cell morphology and biochemical markers such as DNA fragmentation, caspase activation and mitochondrial cytochrome C (Cyt C) release. The DNA fragmentation of apoptotic cells was often identified by the terminal deoxynucleotidyl transferase dUTP nick end labelling (TUNEL) method, which permits the specific labeling of the 3'-OH end of DNA breaks. Applying this method to the paraffin section of heart from 3 month old mice, some positive nuclear staining was found in both hearts of L102 and WT, but there was no difference between the two lines (Fig. 4.18A).
Caspase 3 is the final target responding to apoptotic stimuli. The levels of total caspase 3 and the cleaved activated fragment represent evidence for apoptosis. However, caspase 3 protein levels in the cytosolic heart homogenates were not different between L102 and WT either (Fig. 4.18B).
Moreover, upon intracellular apoptotic stimulation, Cytochrome C (Cyt C) shuttles from mitochondria into the cytoplasm. Therefore different subcellular distributions of Cyt C also reflect apoptosis. Cyt C levels in cardiac cytoplasm detected by the western blot and compared to mitochondrial level did not reveal any increase in the heart of L102 mice (Fig. 4.18C). Thus, by no method could we detect increased apoptosis in the heart of TGM L102 mice.

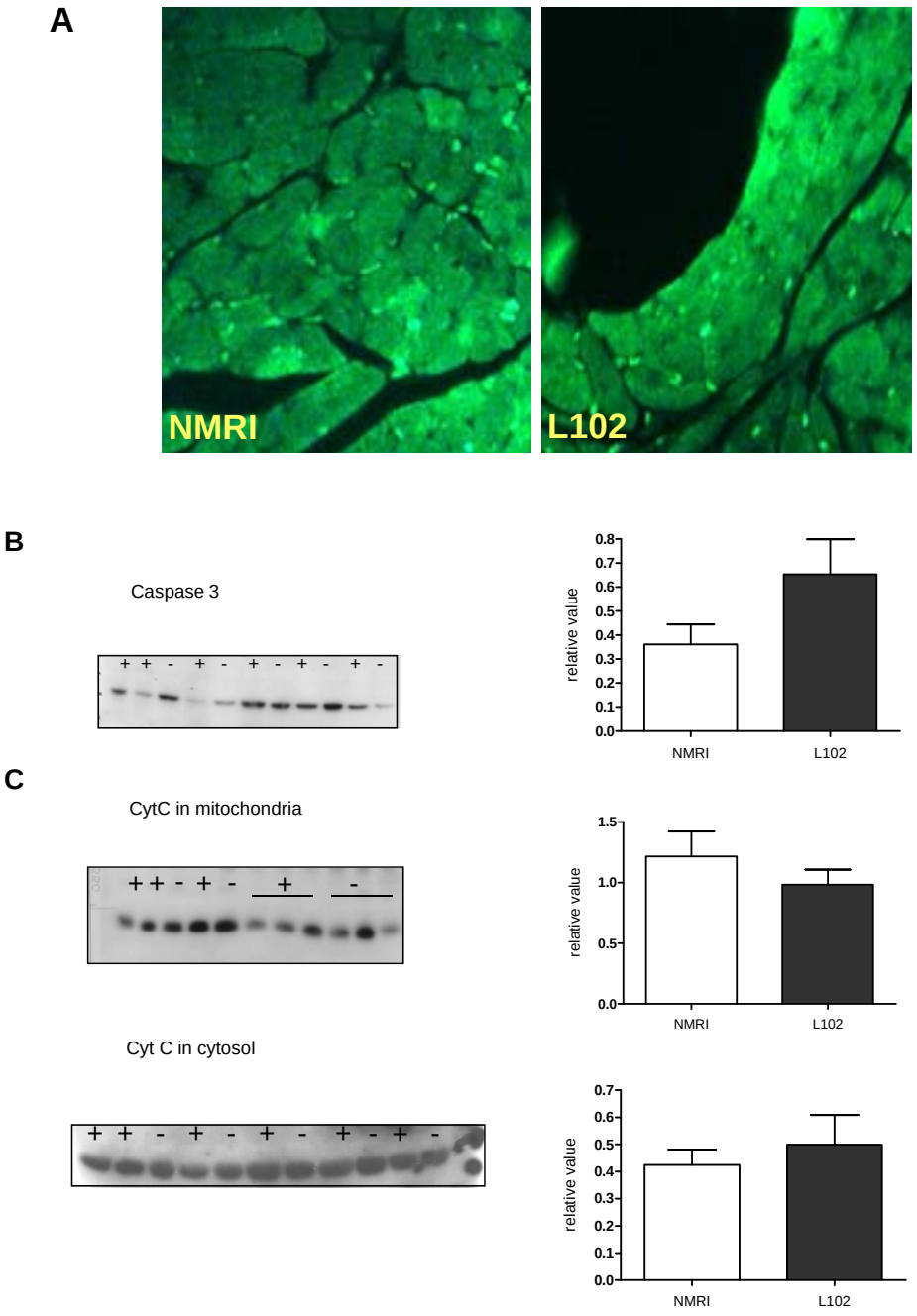

Fig. 4.18. **Apoptosis in the heart of TGM L102 mice**(A) TUNEL staining (B) Western blot for caspase 3 (C) Western blot for cytochrome C (Cyt C), upper panel: mitochondrial protein (15µg); lower panel cytosolic protein (40µg) +: L102 mice; -: NMRI mice.

4.3. AVP-Ang II transgenic rats (AVP-Ang II rats)

4.3.1. Generation of AVP-Ang II rats

The main aim of this part of the thesis was the generation of a transgenic rat, overexpressing Ang II exclusively in the hypothalamus using the "biological pump" system developed by T. Reudelhuber (Methot et al. 2001). The DNA construct contains the promoter and all exons of the AVP gene, the expression caste including the coding sequence for the Ang II inserted in exon 3. Specially, all ATGs in the exons were deleted to avoid endogenous AVP gene translation so that the target gene would be translated. This construct was verified by sequencing and used for microinjection into rat zygotes to generate transgenic rats.

Transgenic offsprings were analyzed by PCR, and one positive founder was found (Fig. 4.20).

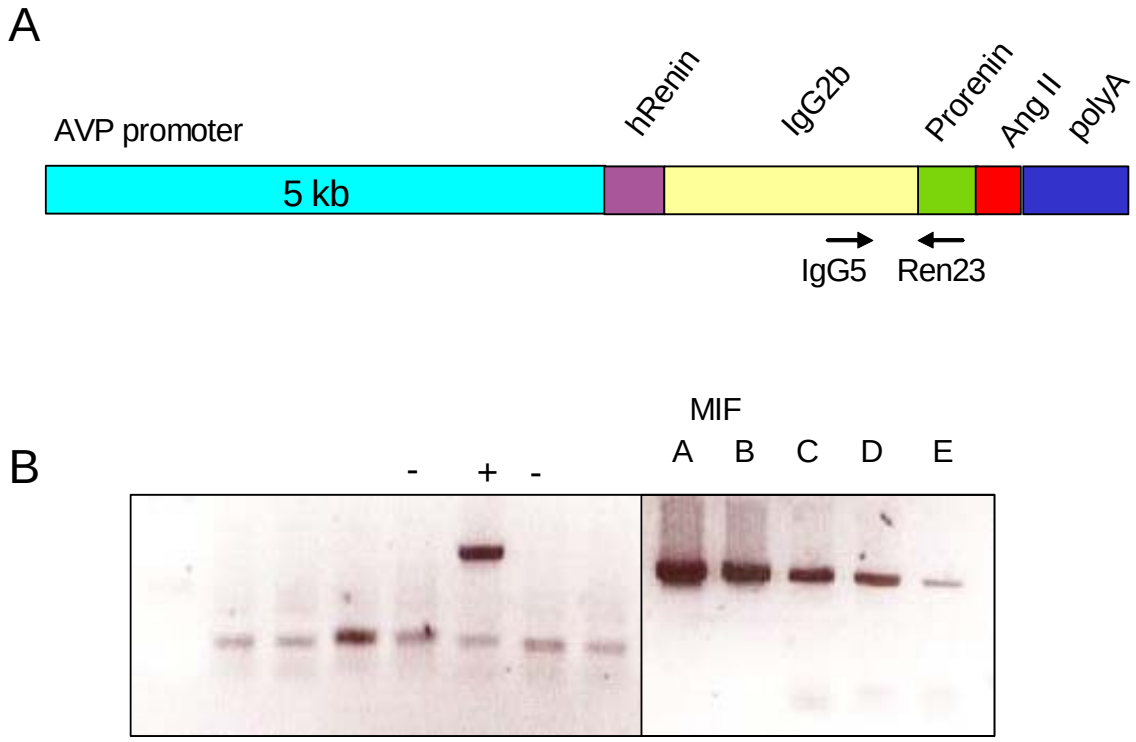

Fig. 4.20. Generation of transgenic AVP-AngII rats
(A) Scheme of the construct for the generation of transgenic rats. (B) Genotyping of founders PCR results with primers Ren 23 and Ig 5. +: positive rat; - : SD control; MIF: microinjection fragment A: 600 pg, B:6 pg, C: 60 fg, D: 6 fg, E: 0.6 fg

4.3.2. Gene expression analysis of AVP-Ang II rats

One 2.5 months old female F1 positive rat and one SD control were used to analyze the transgene expression by RPA. Probe A including mouse IgG2b and human prorenin sequence was hybridized with the total brain and thymus RNA. After 5 days exposure, we could see a weak protected band in the whole brain of transgenic rat, but not in the thymus and in control rats (Fig. 4.21).

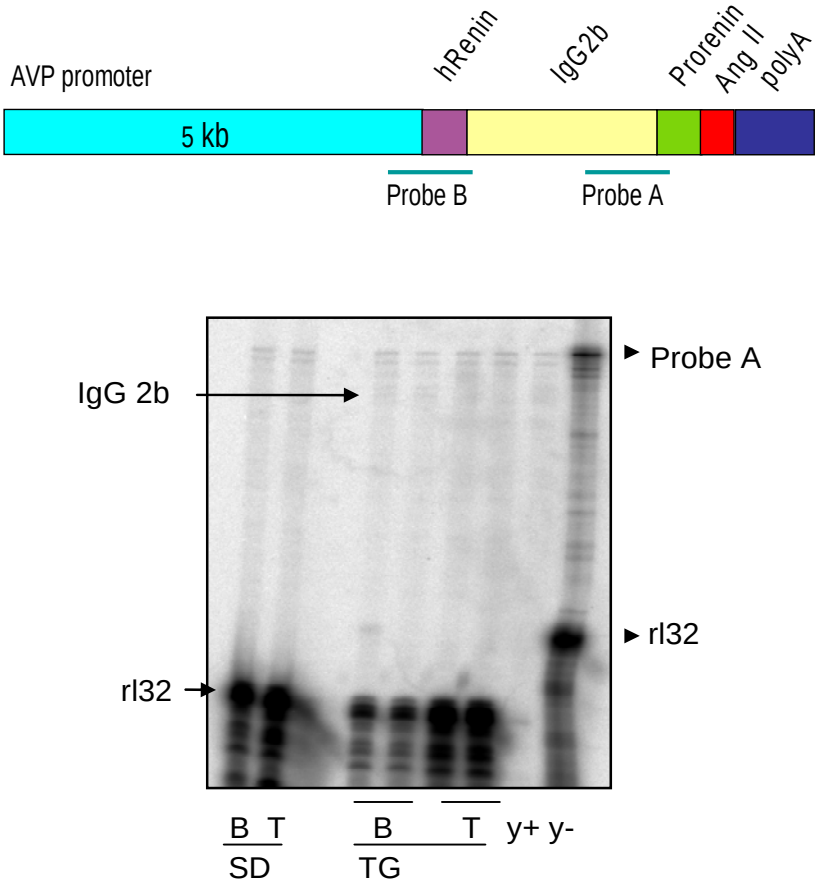

Fig. 4.21. Gene expression by RPA
Upper panel: Scheme of the construct of AVP-Ang II, probe A was located on IgG 2b and prorenin sequence. Lower panel: Expression of transgene by RPA with probe A, B: brain; T: thymus, 40 ug RNA from SD control; 20 ug thymus RNA from TG: AVP-Ang II rats. IgG2b, protected RNA band hybridized with probe, y+, yeast RNA with RNase digestion, y-, yeast RNA without RNase digestion. rl 32 probe was used as housekeeping gene expression control.

Next, we generated a new probe B including IgG2b and a short fragment of AVP exon 2-3. Endogenous AVP exon 2-3 bands in hypothalamus of both transgenic and control rats were discerned, but no full length protected band appeared in transgenic rats in brain stem, hypothalamus, and pituitary (Fig. 4.22).

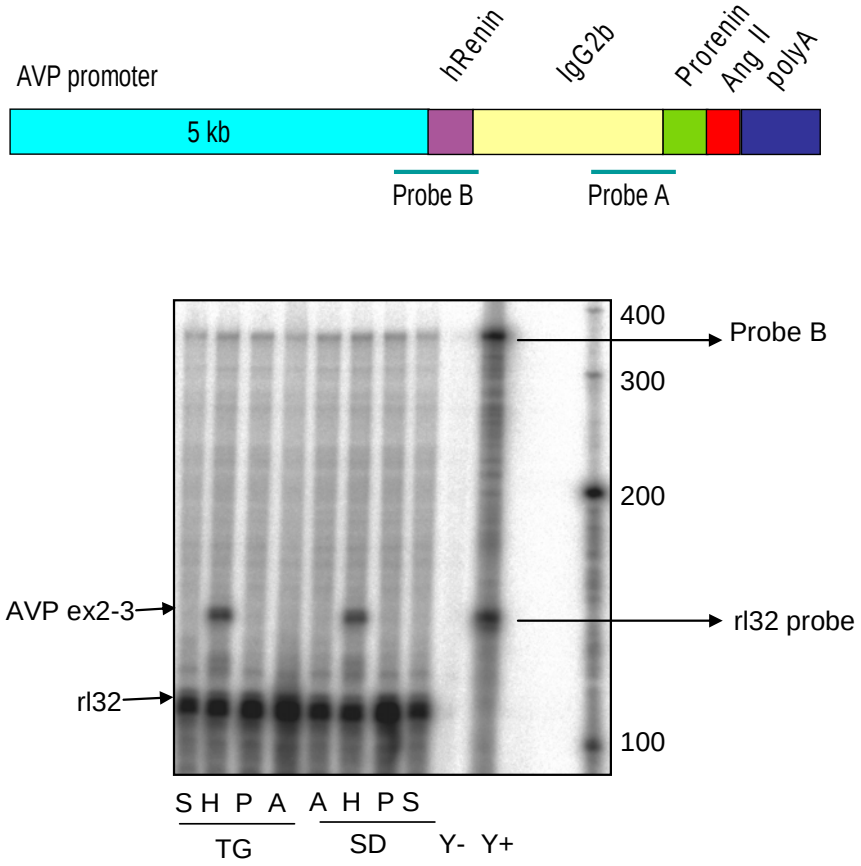

Fig. 4.22. Gene expression by RPA
Upper panel: Scheme of the construct of AVP-Ang II, probe B was located on AVP gene 3´ EST and IgG 2b sequence. Lower panel: Expression of transgene with probe B by RPA, S: brain stem; H: hypothalamus; P: pituitary; A: amygdala; AVP ex2-3, AVP gene exon 2 and 3 fragment hybridized with probe; Y+, yeast RNA with RNase digestion, Y-, yeast RNA without RNase digestion; rl 32 probe was used as housekeeping gene expression control.

AVP promoter activity can be induced by water deprivation. We supposed that after 48 hours stimulation, transgene expression may become detectable by RPA. Protected bands of endogenous AVP exon 2-3 gene expression in hypothalamus and pituitary were visible in both transgenic and control rats. However no matter before or after water deprivation, no transgene specific bands could be recognized in the tissues like hypothalamus and pituitary from transgenic rats, AVP expression level was not augmented after water deprivation in any of the TG rats (Fig. 4.23).

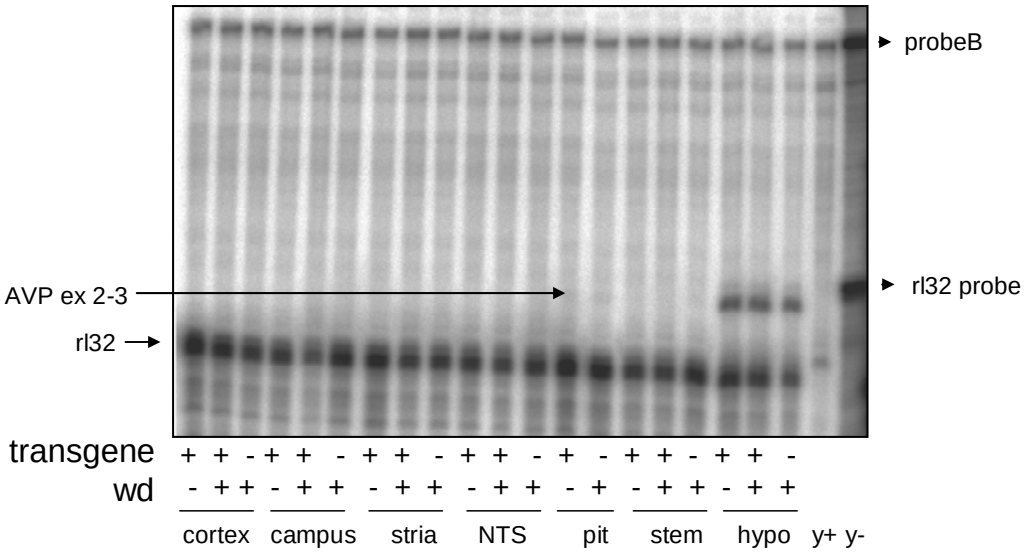

Fig. 4.23. Gene expression after water deprivation
Expression of transgene by RPA with probe B, campus: hippocampus; stri: stria terminalis; NTS: nucleus tractus solitarius; pit : pituitary; stem : brain stem; hypo: hypothalamus. wd-: without water deprivation, wd+: with water deprivation. Transgene +: AVP-Ang II rat, transgene-: SD control rat. AVP ex2-3: AVP gene exon 2 and 3 fragment hybridized with probe B, y+, yeast RNA with RNase digestion, y-, yeast RNA without RNase digestion. rl 32 probe was used as housekeeping gene expression control.

Since RPA did not easily detect transgene expression we decided to use a more sensitive method to detect transgenic mRNA. Nested PCR is supposed to be the most sensitive PCR. Products from first round RT-PCR (primer 4 and primer 3) were diluted, and amplified for an additional 35 cycles using the primers 5 and 3nest. As expected, lower bands around 270 bp were present indicating the transgenic expression in the cortex, brain stem, hypothalamus and pituitary of the transgenic rat and not in the control rat. The upper 530 bp bands were amplified on genomic DNA, since the construct used for the generation of the rats gave the same band (Fig. 4.24).

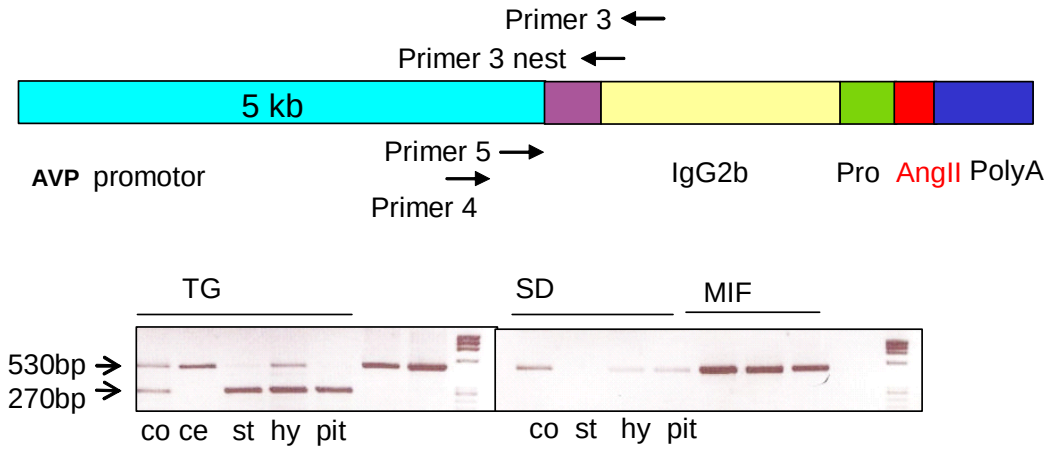

Fig. 4.24 Gene expression by nested RT-PCR
Upper panel: Scheme of the construct of AVP-Ang II, primer 4 and 5 are the 5´primers; primer 3 and 3 nest are the 3´ primers. Lower panel: Results of nested RT-PCR using primer 4 and 3 then 5 and 3 nest. MIF, microinjection fragment, st: stem; co: cortex; ce: cerebellum; hy: hypothalamus, pit, pituitary

4.3.3. Blood pressure in AVP-Ang II rats after water deprivation

To measure blood pressure, the tail cuff method was applied on 5-month old male TG and SD control rats (MAP was 118.5±1.5 mmHg in SD control rats *vs* 138±20 mmHg in TG rats, $p>0.05$). After water deprivation, MAP did not change in control rats (125±7.0 mmHg) and in TG rats (112±22 mmHg) (Fig. 4.25).

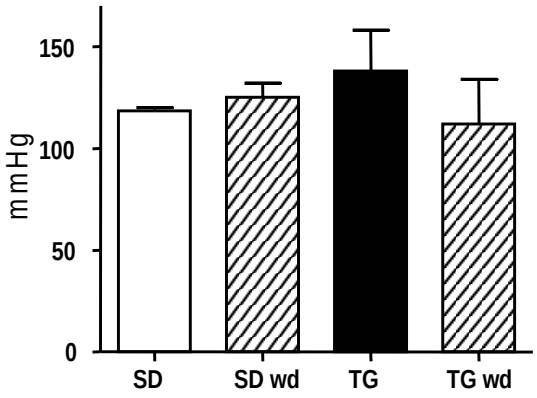

Fig. 4.25. Blood pressure after water deprivation
SD: 5 month old male SD control rats, n=2. SDwd: control rats after water deprivation, n=2. TG: AVP-Ang II rats, TG wd: AVP-Ang II rats after water deprivation.

4.3.4. Blood pressure in AVP-Ang II rats after high salt diet

Since tail cuff is a very inaccurate method, blood pressure and heart rate were recorded in 3 conscious female transgenic and 3 control rats by invasive catheter. Neither at base line nor after 2 weeks of high salt diet, blood pressure was altered in any of groups (Fig. 4.26).

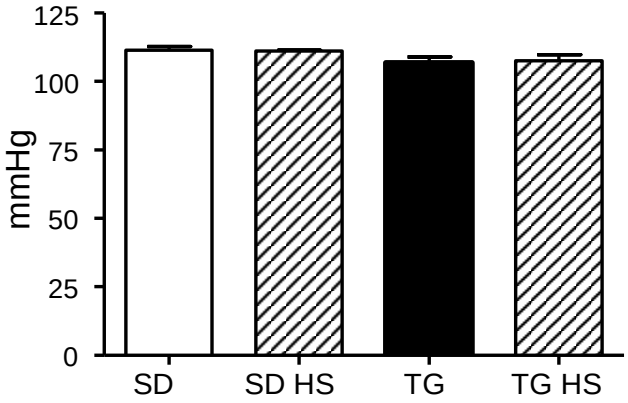

Fig. 4.26. Mean blood pressure measurement in conscious rats at base line and after high salt diet
All groups are 3 month old female rats (n=3), SD HS: SD control rats fed with 8% salt diet for 2 weeks; TG: AVP-Ang II rats; TG HS: AVP-Ang II rats fed with 8% salt diet for 2 weeks.

5. Discussion

5.1 *Mas* Knockout mice

The results presented in this thesis are the first to show that *Mas*-deficiency on the FVB/N genetic background leads to elevated blood pressure in mice accompanied by a decreased heart rate probably caused by a normal baroreflex. This is in contrast to the normal blood pressure and heart rate observed on a mixed 129/C57Bl/6 genetic background and on a pure C57Bl/6 background (Walther et al. 2000). Concerning the molecular mechanism, there was an imbalance between NO and ROS in both inbred lines of *Mas*-deficient mice.

5.1.1 Hypertension and strain differences

Why are *Mas*-deficient mice on a mixed or C57Bl/6 background normotensive? The primary reason is the animals´ genetic background, which is known to be an important factor influencing cardiovascular parameters.

Gene targeting allows to create null mutations in mice and to analyze how the mutant organism responds to the lack of a single gene product. However, the inherent problem of background genes linked to the mutation of interest might severely hamper the scientific interpretation of the results of transgenic and knockout studies (Rodgers et al. 2002). Knockout mice are typically generated on the mixed 129xC57Bl/6 genetic background, where the alleles of genes that surround the targeted locus are of 129-type in the null mutant mice and C57Bl/6 in the wild type mice. It was already reported that at baseline conditions, 129/Sv mice have higher blood pressure compared to C57Bl/6 mice (Deschepper et al. 2004). Consequently, any phenotypical differences observed between mutant and control littermates of the hybrid genetic origin may be due to either the introduced null mutation or the background genes linked to the targeted locus (Gerlai 2001). A classical solution to decrease the probability of contribution of background genes is the backcross of the mutant hybrid animals, for at least seven times, to the strain of choice and creation of a congenic strain that carries the mutation on the desired genetic background. FVB/N and C57Bl/6 mouse strain were chosen for the backcross of *Mas*-knockout mice.

One further example is the ACE2 knockout mouse in which background, the effect of the knockout on blood pressure was inconsistent. Blood pressure in 129/Sv ACE2-deficient mice was identical to the 129/Sv controls. In contrast, deletion of ACE2 was associated with a significant increase in blood pressure on the C57Bl/6 background (Gurley et al. 2006).

Specially, the C57Bl/6 genetic background is resistant to hypertension in several animal models, including those with a genetically modified RAS (Wu et al. 2002; Hartner et al. 2003). Genetic differences underlying this phenomenon are poorly understood. Muller *et al*. recently reported on reduced activities of cytochrome P450 4a isoforms in C57Bl/6 mice in relationship to 20-hydroxyeicosatetraenoic in acid (20-HETE) production, suggesting another reason for strain differences in the susceptibility to hypertension and target-organ damage in mice (Muller et al. 2007).

One other reason could be changes in the balance between NO and superoxide generation in C57Bl/6 mice compared to other strains (Bendall et al. 2002) or differences in plasma renin activity, caused by different number of renin genes: C57Bl/6 mice have only one renin gene, while FVB/N mice harbor two renin genes (Lum et al. 2004). Our data confirmed that higher plasma renin activity was present in FVB/N mice than in Bl/6 mice. Additionally Bl/6 mice possess higher NOx levels than FVB/N mice in plasma, implicating a stronger systemic NO buffering capability in C57Bl/6 mice. On the other hand, Bl/6 mice produce more isoprostane than FVB/N mice. Together with higher plasma TBARS levels, this argues for a higher endogenous oxidative state in Bl/6 compared to FVB/N mice. It would be interesting to identify the differences in the sources of ROS production in these two mouse lines. Moreover the activities of the antioxidative enzymes, SOD and catalase, were reduced in Bl/6 mice compared to FVB/N mice. Thus, we can conclude that FVB/N mice have stronger antioxidative activity than Bl/6 mice. It will be interesting to test if there is a difference in endothelial function in FVB/N and Bl/6 mice.

Furthermore, anesthesia may have influenced the assessment of the cardiovascular parameters. General anesthesia has well-recognized depressor effects (Janssen et al. 2004), which might have masked the differences in blood pressure and heart rate in previous studies (Walther et al. 2000).

5.1.2 Endothelial dysfunction in *Mas*-deficient mice

Taking into consideration the fact that short-term infusions of Ang (1-7) improved endothelial function *in vivo* (Loot et al. 2002; Lemos et al. 2005) and that *Mas*-deficient mice presented a blunted vasorelaxation of aortic rings in response to Ang (1-7) (Santos et al. 2003), we hypothetised that Ang (1-7) could modulate endothelial function via its receptor Mas. To define endothelial function in our mice, we investigated the vascular reactivity *in vivo* in *Mas*-deficient mice and control mice by administration of ACh and SNP. The sensitivity of vascular smooth muscle to relaxation by NO could be evaluated by its sensitivity to relaxation by exogenous NO

donors such as SNP. SNP slightly altered the magnitude of vasorelaxation in FVB/N *Mas* mice, thereby indicating increased sensitivity of vascular smooth muscle cells in these animals. The molecular mechanisms underlying this effect should be further investigated. In Bl/6 *Mas* mice, SNP caused an identical reaction like Bl/6 mice. However *Mas*-ablation in FVB/N and Bl/6 led to a drastic decrease in the vasodilatory response to ACh. This effect was even more pronounced after normalization of the response to the endothelium-independent relaxant SNP, indicating that deletion of *Mas* impairs endothelial function in mice unrelated to the genetic background.

The vascular endothelium is known to release relaxing factors such as NO (Ignarro et al. 1987; Furchgott and Vanhoutte 1989). The reduced ACh induced relaxation in *Mas*-deficient mice could be due to the decrease in the synthesis/release of NO from endothelial cells or decreased bioavailability of NO or may reflect a change in the sensitivity of vascular smooth muscle to relaxation by NO. The provided evidence that the sensitivity of vascular smooth muscle to relaxation by NO is not impaired in *Mas*-deficient mice suggest that the attenuated ACh-induced relaxation in *Mas*-deficient mice is due to a decrease in the synthesis or release (or both) of NO from endothelial cells. Accordingly, when eNOS activity was inhibited, vascular relaxation was identical between *Mas*-deficient mice and controls.

5.1.3 Decreased NO in *Mas*-deficient mice

Our studies of the molecular mechanism causing the observed phenotypes in *Mas*-deficient mice suggest that an imbalance between NO and ROS in *Mas*-deficient mice could possibly be responsible for both elevated blood pressure and/or endothelial dysfunction. First, we found significantly decreased plasma NO_2 levels in FVB/N *Mas* mice, compared to controls; the same trend was observed for the Bl/6 *Mas* mice. The plasma level of nitrite correlates with the level of NO biosynthesis (Kleinbongard et al. 2003; Kleinbongard et al. 2006).

Urinary NOx excretion reflects NO synthesis, too (Radovic et al. 2006). We have also observed that the 24-hour urinary excretion of NO metabolites, nitrate and nitrite, is significantly reduced in both strains of *Mas*-deficient mice compared to WT mice, indicating that NO bioavailability is low in *Mas*-deficient mice. 24-h urine samples are preferable, because they better represent the steady state levels. It is likely that daily urine values reflect the nitrate produced over the previous 24 h, since the majority of nitrate entering the circulation is eliminated in the urine (Boockvar et al. 1994). Many studies relied on the measurement of NOx in the plasma. Plasma NOx reflects the level of renal function and plasma volume as well as gives an indirect index of systemic NO production. NO generated in the proximal tubule also contributes to plasma NOx

levels, because there is tubular reabsorption of NOx (Suto et al. 1995). But the plasma level will also be influenced by the clearance. Plasma and urine levels together allow some estimation of approximate total NO generation. Nevertheless, measurement of NOx should only be used as part of a panel of functional (e.g. vascular reactivity) and biochemical (e.g. cGMP) assays (Baylis and Vallance 1998). Hence, the expression of eNOS, which is the major source for vascular NO generation, was found to be decreased in aortas of *Mas*-deficient mice. The eNOS expression level reflects the chronic regulation by many factors. Our findings are in agreement with recent research in human aortic endothelial cells, showing that stimulation of Mas by Ang (1-7) improves endothelial function through facilitation of NO release via eNOS activation *in vitro* (Sampaio et al. 2007).

5.1.4 Possibilities of NO abnormalities in hypertension

NO is known to promote vascular relaxation by producing cGMP in vascular smooth muscle. Decreased cGMP in Bl/6 *Mas* mice implicated direct effect of reduced NO bioavailability.

What are the reasons that eNOS mRNA and urinary NO level were reduced in *Mas* knockout mice? There are a number of ways in which NO levels or activity could be downregulated in hypertension (Fig. 5.1). Possibilities include excessive degradation of NO by ROS and reduced levels or activity of eNOS, all observed in *Mas* knockout mice. Additionally, reduced availability of the major eNOS substrate, arginine is involved in hypertension, too. The recently described substance, asymmetric dimethylarginine (ADMA), which seems to be present in increased levels in hypertension, can interact with and inhibit eNOS (Surdacki et al. 1999).

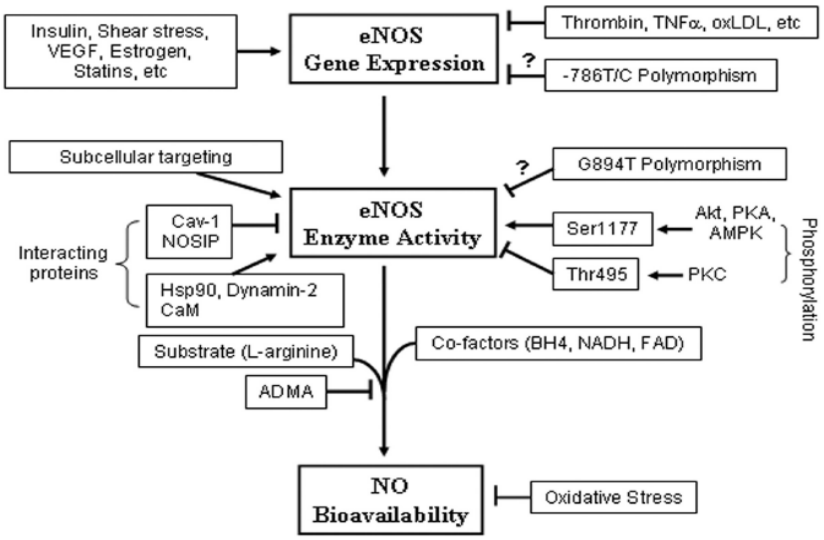

Fig. 5.1 eNOS regulation (Yang and Ming).
The activity of eNOS is influenced in different levels in a chronic way by its expression, e.g. Shear stress stimulates expression and genetic polymorphisms influence eNOS expression. eNOS activity is regulated in a fast way, by the phosphorylation status of the enzyme, posttranslational modifications and interacting proteins. As a product of eNOS activity, NO bioavailability depends on the intrinsic half life and the reaction with ROS.

Acutely, eNOS activity is regulated by different mechanisms involving eNOS interacting proteins such as caveolin-1, Akt and Hsp 90. Our preliminary data showed that caveolin-1 level was unaffected in both *Mas* knockout mice by western blot. This was confirmed by immunofluorescence staining in FVB/N and FV *Mas* mice.

In a complex attached to caveolae in the membrane, eNOS interacts with the molecular chaperone Hsp 90 which regulates eNOS activity. Hsp 90 forms a complex with NOS and facilitates its phosphorylation; thus, the Hsp90-eNOS complex augments the activation of eNOS (Wu 2002). Furthermore, eNOS activity can be regulated via the phosphatidylinositol 3-kinase/protein kinase Akt (PI3K/Akt) pathway. Akt stimulates eNOS activity through phosphorylating eNOS at serine 1179. A few studies reported that Hsp 90 and Akt synergistically activate eNOS in endothelial cells. Hsp90 association is a prerequisite for subsequent Akt-mediated stimulation of eNOS (Brouet et al. 2001). Since urinary NOx and eNOS mRNA levels were decreased in *Mas* knockout mice, as a compensatory mechanism eNOS protein level could be upregulated by Akt and Hsp 90 stimulation, in a posttranslational regulation mechanism. Further studies need to clarify this by measuring the eNOS protein level and the phosphorylation state of eNOS in the aorta.

5.1.5 Increase of ROS production in *Mas*-deficient mice

A host of abnormalities in superoxide formation and degradation are described in hypertension. Some of these are endothelial related, others are not. Increased degradation of NO does appear to play a major role in hypertension. The reduced NO levels observed in *Mas*-deficient mice could result not only from depressed endothelial NO synthesis, but also from increased NO sequestration by ROS.

In order to find out if ROS was produced from NAD(P)H oxidases, the expression levels of the main catalytic subunit, the major membrane component of the functional enzyme gp91phox (Nox 2) were checked. Our results showed a significant upregulation of gp91phox in vascular homogenates from *Mas*-deficient mice in FVB/N and Bl/6 background compared to controls, and Nox 2 mRNA level was higher in Bl/6 *Mas* than in Bl/6 mice. Increased expression of this subunit may account for at least part of the increase in oxidase activity. Membrane-bound NADH and NAD(P)H oxidases are the predominant source of $O_2^{\cdot -}$ in vasculature and gp91phox is a critical component for $O_2^{\cdot -}$generating NAD(P)H oxidase in endothelial cells (Gorlach et al. 2000). Gp91phox gene-deficient mice not only showed decreased blood pressure (Wang et al. 2001), but also exhibited enhanced endothelium-dependent relaxation in aorta, indicating that impaired $O_2^{\cdot -}$ generation caused by a lack of this subunit may enhance the NO activity in vascular tissue (Gorlach et al. 2000). It has been reported that incubation with Ang II increases gp91phox expression and $O_2^{\cdot -}$ production in the mouse aorta (Cifuentes et al. 2000). Thus, these findings together with ours indicate an essential functional role of gp91phox in the regulation of normal vascular tone as well as in various vascular disorders.

However, an increase in Nox 2 level is not invariably due to transcriptional activation (Touyz et al. 2002). In the case of FVB/N *Mas* mice, Nox 2 mRNA level were reduced, gp91phox protein elevation may also be due to increased de novo protein synthesis, regulated at a posttranscriptional level.

5.1.6 ROS effects in *Mas*-deficient mice

ROS such as $O_2^{\cdot -}$, H_2O_2, and the extremely toxic ·OH are difficult to detect *in vivo* because of their short half-life. Therefore, byproducts of lipid peroxidation have often been used as indirect markers for free radical generation. MDA is a 3-carbon compound, which reflects autooxidation and oxygen radical–mediated peroxidation of polyunsaturated fatty acids, in particular, arachidonic acid. TBARS were increased in both aorta (Fig. 4.7A) and plasma (Fig. 4.7B) in

FVB/N *Mas* mice. Lipid peroxidation is an autocatalytic free-radical-mediated destructive process whereby polyunsaturated fatty acids in cell membranes undergo degradation to form lipid hydroperoxides. Thus, lipid peroxidation leads to an accumulation of oxidative damage in diverse cellular locations, to the deregulation of redox-sensitive metabolic and signaling pathways, and finally to cellular injury (Irani 2000).

Isoprostanes, which are a bioactive prostaglandin-like compounds formed by free radical-catalyzed peroxidation of arachidonic acid, are potent vasoconstrictors (Morrow et al. 1990). Urinary isoprostane measurement mainly reflects the systemic rather than renal formation of the compound, which is suggested by the correlation of isoprostane and its metabolite concentrations in human urine (Chiabrando et al. 1992). Specially, 8-isoprostane is an indirect marker for oxidative stress (Haas et al. 1999). Interestingly, we found that Bl/6 *Mas* mice exhibit higher isoprostane levels compared to WT mice. However, we did not observe a significant difference in the urinary isoprostane excretion in FV *Mas* and FVB/N mice. This may be due to the fact that unidentified sources of ROS such as cyclooxygenase and lipoxygenase changed differently in FVB/N and Bl/6 *Mas* mice.

5.1.7 Decreased antioxidant systems in FVB/N *Mas*-deficient mice

The oxidative process is counterbalanced leading to a final activity, which is the consequence of both producing and degrading mechanisms. NAD(P)H oxidase is the major source of $O_2^{\cdot -}$ in the vasculature, SOD and catalase are of critical importance for ROS metabolism. Three SOD isoenzymes (CuZnSOD, MnSOD, and ecSOD) are known as ROS scavengers. H_2O_2 released by the $O_2^{\cdot -}$ dismutation is mainly removed by catalase that converts H_2O_2 into water. Thus, catalase has an important protective function against the toxic effects of peroxides and removes them with high efficiency (Siraki et al. 2002). Both, SOD and catalase activity, were reduced in FV *Mas* mice compared to controls, indicating impaired antioxidant capacity in these animals.

Together with the increased Gp91phox protein and TBARS levels, the inefficiency of SOD and catalase to provide clearance of ROS might be responsible for the increased ROS content in FV *Mas* aortic tissue.

Bl/6 *Mas* mice did not show any reduction in SOD and catalase activity compared to WT. Since we did not measure other antioxidant enzymes, such as glutathione reductase, we can not exclude that other antioxidant systems are active in Bl/6 *Mas* mice.

Although we did not directly measure H_2O_2 and $O_2^{\cdot -}$ concentration, from the increased ROS production and decreased antioxidant enzyme activity, we can deduce that H_2O_2 and $O_2^{\cdot -}$ should

be increased in FVB/N *Mas* mice. H_2O_2 is known to be more stable than its precursor $O_2^{\cdot -}$ and can readily cross plasma membranes due to its uncharged nature. H_2O_2 can elicit irreversible endothelial damage. $O_2^{\cdot -}$ and H_2O_2 contribute to hypertension by different mechanisms: $O_2^{\cdot -}$ by inactivating NO and H_2O_2 by altering vascular remodeling. H_2O_2 has been shown to cause constriction in a variety of vascular beds (Suvorava et al. 2005). Vascular overexpression of human catalase decreases systolic blood pressure and vascular constriction *per se*, suggesting a relevance of endogenous H_2O_2 as a vasoconstrictor and regulator of blood pressure. One possibility is that sustained increases in H_2O_2 enhance the pathways involved in smooth muscle contraction (Ca^{2+}-dependent or sensitization pathways), leading to vascular dysfunction. A few studies show that H_2O_2 can reduce vascular NO production. Wedgwood and Black suggest that endothelin 1–induced stimulation of H_2O_2 release in pulmonary VSMCs decreases eNOS expression and activity in pulmonary endothelial cells (Wedgwood and Black 2005). H_2O_2 can decrease NO production by inactivation of eNOS cofactors without affecting eNOS activity (Jaimes et al. 2001). Taken together, H_2O_2 plays an important role in the regulation of NOS activity and bioavailability of NO, leading to an overall reduced NO bioactivity.

We used tempol (a stable, low molecular-weight superoxide dismutase mimetic) to determine whether or not increased ROS could account for the observed higher blood pressure in FV *Mas* mice. Similar to other results found in various models of experimental hypertension (Schnackenberg et al. 1998; Xu et al. 2004; Kopkan and Majid 2005), tempol reduced blood pressure in FV *Mas* mice to levels comparable to WT mice, supporting the notion that ROS are involved in the increased blood pressure we observed in FVB/N *Mas* mice. Tempol may lower blood pressure by reducing $O_2^{\cdot -}$ levels in the vasculature and in the sympathetic nervous system, or perhaps in both tissues. Additionally, tempol may affect blood pressure through $O_2^{\cdot -}$/NO independent mechanisms (Xu et al. 2004). Even we have not yet direct evidence, most likely the reduction in blood pressure after tempol treatment in FV *Mas* mice, is related to the reduction in $O_2^{\cdot -}$ and H_2O_2 levels in the vasculature.

Generally increased ROS levels in aortas of *Mas*-deficient mice support the notion that Mas may influence ROS generation and/or degradation in this tissue. On the other side, the deletion of *Mas* blocks the Ang (1-7)-mediated generation of NO and could thereby change the balance between NO and ROS with considerable impact on blood pressure regulation.

5.1.8 Role of endothelial dysfunction in increased blood pressure of Mas-deficient mice, primary or secondary?

Hypertension and endothelial dysfunction are commonly associated and the question arises, which is primary and which is secondary. Certainly abnormalities in endothelial function can lead to hypertension as demonstrated experimentally, but it has also been shown that hypertension itself can alter endothelial function. For example, experimentally induced acute elevations in blood pressure in humans caused impaired endothelial mediated vasodilation (Millgard and Lind 1998). Similar abnormalities in endothelial function are evident in secondary causes of hypertension and can be reversed by eliminating the secondary cause (Taddei et al. 1993). An analysis of the time course of the changes in vascular reactivity and the increase in blood pressure should help to determine whether the relationship between these two parameters is causal or associative in nature and should, therefore, represent an important area for future investigations.

Although the present results suggest that the decrease in endothelial function and the increase in vascular reactivity observed in the FV *Mas* mice could contribute to the observed increase in blood pressure, these results should be interpreted with caution because the changes in endothelial function and vascular reactivity may also be secondary to blood pressure elevation. Tempol reverses the blood pressure by lowering ROS, and increasing NO bioavailability. However, it needs to be clarified if endothelial function is indeed improved after tempol treatment. This would support a primary role of endothelial dysfunction in the increased blood pressure of FV *Mas* mice.

Although compelling evidence points towards the interaction between Mas and Ang (1-7) (Santos et al. 2003), Mas can also interact with Ang II receptors (Castro et al. 2005; Kostenis et al. 2005). Many of the pathophysiological effects of Ang II are mediated by ROS through stimulation of NAD(P)H oxidase. Therefore, one could speculate that the increase in NAD(P)H oxidase protein levels associated with the reduction of SOD and catalase activity in FVB/N *Mas*-ablated mice is a result of the absence of both, the moderating effect on the AT_1 receptor and the signalling of Ang (1-7).

Based on our data and since Ang (1-7) seems to counteract many cardiovascular effects of Ang II (Reudelhuber 2006), this peptide and its receptor Mas are potential targets for the development of novel cardioprotective or anti-hypertensive agents.

5.2 Gene expression profile in the heart of *Mas*-deficient mice

Based on the cardiac failure described for Bl/6 *Mas* mice (Santos et al. 2006), cardiac gene expression profiles were analyzed using the Affymetrix platform. Among 82 increased and 87 decreased transcripts, the following genes were subjected to further analysis: Rgs 2, ADMA 19, and collagen VI.

Rgs 2 was verified to be down regulated in Bl/6 *Mas* mice by RPA. The Rgs 2 gene is expressed in tissues and cell types involved in blood pressure regulation, including the nervous system, kidney (Chen et al. 1997), and VSMC, and its expression is induced by Ang II as a potential inhibitory feedback mechanism (Grant et al. 2000). Rgs 2 plays key role in accelerating the deactivation of G proteins to reduce Gqα signalling, and serves as the most potent negative regulator of Gqα, which mediates the action of most physiological vasoconstrictors, including norepinephrine, Ang II, endothelin-1, and thrombin. Downregulated Rgs 2 expression levels in Bl/6 *Mas* mice could accordingly result in elevated Gqα activity and lead to vasoconstriction. This needs to be tested in the future.

Disintegrin and metalloproteinases (ADAM) is a family of ectoproteases expressed in cardiac tissue that disrupts connections between integrins and extracellular matrix components. Although ADAMs are known to regulate cell-cell and cell-matrix interactions in a variety of contexts, their pathophysiological role in cardiac diseases has not been well characterized. ADAM19, was found activated in both ischemic and dilated cardiomyopathic specimens. Most Adam19 knock out animals die perinatally (Kurohara et al. 2004; Zhou et al. 2004), due to abnormal formation of the aortic and pulmonary valves, leading to valvular stenosis, and abnormalities of the cardiac vasculature. We confirmed by RPA that ADAM 19 mRNA level was increased in Bl/6 *Mas* mice, but its involvement in the heart failure of Bl/6 *Mas* mice remains hypothetical.

Changes in the accumulation, composition, or organization of the extracellular matrix are known to deleteriously affect heart function. Collagen VI is a ubiquitous extracellular matrix protein which forms a microfibrillar network in close association with the basement membrane around muscle cells and which interacts with several other matrix constituents. Collagen VI is composed of three different peptide chains a1 (VI) and a2 (VI)—both 140 kDa in size—and a3 (VI), which is much larger (260–300 kDa). COL6A3, the gene coded for the a3 (VI) chain, collagen VI forms a highly branched filamentous network in the extracellular matrix which encircles interstitial collagen fibers and is particularly abundant close to the cells and in intimate contact with basement membranes surrounding muscle fibers. COL6A3 mRNA level was shown to be increased in *Mas* knockout mice by Affymetrix, but we could not verify this by RPA. In the

contrary, expression of type VI collagen was shown to be decreased in the left ventricles of Bl/6 *Mas* mice by immunohistology (Santos et al. 2006). Our results were limited to the RNA level, but the collagen protein level could be regulated posttranscriptionally. Furthermore, COL6A1 and COL6A2 were not investigated, which may be changed in Bl/6 *Mas* mice.
Collectively, Mas plays a complex role in cardiac function by gene expression regulation.

5.3 Gene expression profile in the testis of *Mas*-deficient mice

In order to know if Mas is involved in testis function, we performed gene expression profile analysis in the testis of Bl/6 *Mas* and WT mice. Among others the following genes were found to be altered: StAR, 3ß-HSD and Gfer.
Steroidogenic acute regulatory protein (StAR) is a transport protein involved in the transfer of cholesterol from the outer membrane to the inner membrane of mitochondria, the first and rate-limiting step in steroid hormone biosynthesis. StAR was one of the proteins, of which the expression was found attenuated concordantly by Affymetrix chip analysis and real-time PCR in *Mas*-deficient mice.
3ß-Hydroxysteroid-dehydrogenases (3ß-HSD) are key enzymes necessary for the biosynthesis of testosterone in Leydig cells (Baker et al. 1999). Several isoenzymes catalyze different reactions in steroidogenic pathways. To date, six isoforms have been identified in mouse with a tissue- and temporal-specific expression pattern. In the mouse, the two major isoforms involved in steroid hormone biosynthesis are 3ß-HSD1 and 3ß-HSD6. Both isoenzymes were found to be expressed in adult Leydig cells of mouse testis (Simard et al. 2005). Clearly, regulation of 3ß-HSD expression is central for the modulation of testicular androgen production. Affymetrix analysis and real-time PCR showed an upregulation of 3ß-HSD1 and downregulation of 3ß-HSD6 in *Mas*-deficient mice, indicating that *Mas* may specifically alter steroidogenic pathways.
Growth factor erv1 (Saccharomyces cerevisiae)-like (Gfer), is a component of the mitochondrial intermembrane space and the highest amounts of this protein are detected in spermatogonia and early spermatocytes (Lange et al. 2001). As a sulphydryl oxidase, Gfer could be responsible for the introduction of specific disulphide bridges into integral mitochondrial membrane proteins, and changes in the level and activity of Gfer would result in morphological changes in mitochondria. This would make sense because mitochondria, in particular, undergo a highly complicated change in their structure during spermatogenesis (Meinhardt et al. 1999). Unexpectedly, the expression of Gfer was found by real-time PCR to be significantly decreased,

in contrast to the Affymetrix data, which showed a near 4 fold increase (Affymetrix Gfer: KO/WT=3.98, P=0.0427), indicating that the Affymetrix data were false positive.

Taken together, the depletion of *Mas* affects the expression of important determinants of steroidogenesis in the testis, such as StAR and 3ß-HSDs, and therefore Mas may also be involved in the regulation of androgen production.

5.4 TGM (rAOGEN) L102

5.4.1 Hypertension

The expression of the rat AOGEN transgene in the TGM L102 mouse line was characterized. The foreign gene was highly expressed in the liver and brain. Extremely high blood pressure was observed in TGM L102 mice by invasive catheter measurement, comparable to the results obtained from the other line TGM L123 (Kang et al. 2002) with the same transgene. These results indicated that the presence of the rat AOGEN transgene is responsible for the increment of blood pressure in the transgenic mice and not the destruction of an endogenous gene by the integration of the transgene.

5.4.2 Heart hypertrophy and fibrosis

High blood pressure is an important factor determining end organ damage and organ damage is a common sequel of hypertension. Higher heart weight ratios and increased cardiac BNP protein levels revealed the left ventricular hypertrophy (LVH) in the TGM L102 mice. Increased hemodynamic overload is fundamental to the development of LVH, and LVH could contribute to the maintenance of hypertension.

Initially, LVH is an adaptive response of the heart and involves cardiomyocyte growth and accumulation of extracellular matrix, which was shown by increased collagen III mRNA levels (our data) and collagen I in TGM L123 (Kang et al. 2002) and more pronounced von Gieson staining in heart and kidney, corresponding to TGM L123. However, lung was shown fibrosis for the first time in TGM L102. In the myocardium, collagen fibres are enzymatically cross-linked to form the collagen matrix, which in turn support the normal function of myocytes (Jugdutt 2003). The unique organization of collagen and elastic fibres in the extracellular matrix provides the cardiovascular structural integrity and optimal function. Therefore, alterations in collagen may contribute significantly to the impairment of cardiovascular function (Covell 1990) and changes in the collagen amount or collagen types have been associated with altered function of

the myocardium (Zile et al. 2004). Nevertheless, TGM L102 is a good model to assess the mechanisms of systemic fibrosis. Ang II has been identified as important regulator of fibrosis and is a potential target of antifibrotic drugs.

5.4.3 Apoptosis

The cellular derangement observed in LVH is the consequence of remodeling processes involving the two major cell types of ventricular tissue: cardiomyocytes and fibroblasts (Cooper 1997). Apoptosis would happen as consequences of hypertrophy in cardiomyocytes and it is now recognized as a fundamental process in cell biology that is critical for organ development, physiologic adaptation and disease (Feuerstein 2001). Diverse stimuli have been shown to produce apoptosis in cardiac myocytes, one of these is Ang II (Fortuno et al. 1998), thus we expected to find an increased amount of apoptotic cells in the heart of TGM L102 mice. However, 3 different methods did not show any sign of apoptosis in the heart of these animals. One reason for this result could be that the time point (3 month old mice) chosen for detection was not suitable. Apoptosis may initiate at an older age of mice. If apoptosis occurs during compensatory hypertrophy or the process of remodeling is still not a resolved question (Elsasser et al. 2000). Alternatively pressure overload induces also a survival pathway. There might be balance between hypertrophic and protective signals in TGM L102 mice.

5.5 Transgenic rats with Ang II expression in the brain

5.5.1 Possible reasons for low transgene expression

To learn more about brain RAS function in homeostasis, we generated Ang II transgenic rats under AVP promoter control. The foreign gene was transmitted to the offspring. By mating we got homozygous rats, but we could only detect the transgene mRNA expression by nested RT-PCR. The transgene was very lowly expressed and remained nearly undetectable by RPA, even after water deprivation and high salt diet stimulation, which should increase AVP promoter driven transcription.

Endogenous promoter fragments are commonly used to express transgenes in a tissue-specific and developmentally regulated fashion. However, the use of endogenous promoter fragments is often limited by low to intermediate transgene expression (Lewandoski 2001).

Moreover, appropriate expression of any transgene is dependent on the presence and correct integration of regulatory sequences required for the cell-specific expression of the gene products

(Grosveld et al. 1987; Bonifer et al. 1990). From previous studies of the AVP locus in heterologous cell lines and in transgenic animals, it has been shown that constructs containing 5 kb upstream and 3 kb downstream of the AVP gene (Waller et al.) will direct cell-specific expression and regulation in magnocellular AVP neurones. However, expression has not been seen in parvocellular AVP systems and it seems that the AVP genes are regulated by complex interactions between regulatory proteins which bind directly or indirectly to flanking sequences in both loci (Burbach et al. 2001). Until now, the sequences have not yet been defined which are necessary to obtain reliable expression of transgene at levels comparable to endogenous AVP gene expression in a copy-number, position-independent fashion (Waller et al. 1998; Murphy & Wells, 2003).

Another reason for low transgene expression could be that gene dosage profoundly influences the phenotype. We did not check the copy number of the transgene, which probably was very low.

5.5.2 Physiological reasons of low transgenic expression

Although previous transgenic studies have shown osmotic regulation of transgenes in the vasopressinergic system, the transgenes have generally shown exaggerated (up to 50-fold) responses above relatively low basal expression (Murphy et al. 2000). However, our transgenic model did not show upregulation of AVP and foreign gene expression in response to salt loading or dehydration.

AVP gene expression in the SON responds both transcriptionally and post-transcriptionally to osmotic challenges, such as the physiological challenge of dehydration. Osmotic challenge stimulates AVP release, which engenders an increase in plasma AVP levels and a depletion of pituitary stores. Functional demand leads to an increase in AVP gene transcription (Murphy and Carter 1990), but AVP-Ang II and WT rats did not respond to water deprivation. Possibly 48 hours of dehydration is not sufficient, Sanvitto reported after 5 days dehydration that the expression of the AT1 receptor in the subfornical organ was regulated (Sanvitto et al. 1997).

Increasing sodium ingestion resulting in fluid retention and an increased cardiac output, but no rise in blood pressure in AVP-AngII and WT rats was seen. The possible reason may be that 2 weeks ingestion of salt was not enough. Rats can easily adapt to the stimuli, which may cause the failure in cardiovascular response to the volume expansion.

Since neither WT nor TG rats reacted to the high salt diet, it seemed that they are salt resistant.

In conclusion, this line of transgenic rats was not suitable for the intended project. New lines should be generated for functional research on brain Ang II.

6. Summary

The main interest of this thesis is the renin-angiotensin system, which is composed of 2 major arms: a vasoconstrictor/proliferative mediator Ang II, and a vasodilator/anti-proliferative effector Ang (1-7) receptor GPCR Mas.

A heterogeneous genetic background limited earlier studies of *Mas*-deficient mice, which resulted in no clear-cut cardiovascular phenotype. We backcrossed *Mas*-gene deleted mice onto an FVB/N and Bl/6 background over 7 generations and found that only FVB/N *Mas*-deficient mice exhibit higher blood pressures, compared to controls. Both lines of *Mas*-deficient mice also had impaired endothelial function, decreased nitric oxide production, and lower endothelial nitric oxide synthase expression. NAD(P)H oxidase catalytic subunit gp91phox protein content was higher in *Mas*-deficient mice than in controls, moreover superoxide dismutase and catalase activities were reduced in FVB/N *Mas*-deficient mice. The superoxide dismutase mimetic, tempol, decreased blood pressure in FVB/N *Mas*-deficient mice.

Taken together, our results show a major cardiovascular phenotype in *Mas*-deficient mice on a homogeneous FVB/N background. We conclude that enhanced $O_2^{\cdot-}$ generation and decreased antioxidant activities and NO levels in the vasculature lead to endothelial dysfunction and increased blood pressure in these animals. Since Mas seems to counteract many cardiovascular effects of Ang II, this receptor is a potential target for the development of novel cardioprotective or anti-hypertensive agents.

Additionally we found many differential phenotypes between FVB/N and Bl/6 mice. Bl/6 mice exhibited higher endogenous NO levels and oxidant state and less antioxidant activity than FVB/N mice. As a consequence, FVB/N mice inclined to have higher blood pressure accompanied by higher renin activity and lower NO levels. Therefore, the genetic background influences the phenotype of genetically modified animals.

Genetic deletion of *Mas* impaired heart function of *Mas*-knockout mice. To analyze the involved genes, we performed Affymetrix gene expression profiling. Among 12488 transcripts, 87 genes were significantly downregulated and 182 genes were upregulated in *Mas*-deficient mice including Rgs2 and ADAM19, both involved in the regulation of vascular tone.

Since *Mas* is highly expressed in testis, Affymetrix gene expression profiling was also performed

with testes of *Mas*-deficient mice. In the testes of Bl6 *Mas*-knockout mice 65 genes were upregulated and 67 genes were downregulated including StAR and 3ß-HSDs involved in the regulation of steroidogenesis.

Ang II plays a key role in the etiology of cardiovascular diseases. Thus transgenic mice with the rat angiotensinogen gene were investigated for the impact of Ang II on end organ damage. The aim of our study was to characterize the already generated transgenic line TGM L102. The transgenic mice had a significantly elevated blood pressure compared with control mice. The rise in blood pressure was paralleled by cardiac hypertrophy and raised concentrations of BNP. Concomitantly, fibrosis in the heart, lung, and kidney of the transgenic mice was more pronounced than in the wild type, and collagen III mRNA expression was increased. However, apoptosis was not detected in the heart.

The last part of the work was intended to better understand the function of Ang II in the brain. The AVP promoter drove Ang II peptide secretion in newly generated transgenic rats, but the foreign gene was very lowly expressed. Even after stimulation by dehydration or high salt diet, there was neither an increased expression of the transgene, nor an increase in blood pressure. The main reason could be a low copy number of transgene integration.

6. Summary

Zusammenfassung

Das Hauptinteresse der vorliegenden Arbeit gilt dem Renin-Angiotensin System und seinen zwei Hauptkomponenten, dem vasokonstriktorisch-/proliferatorativen Mediator Ang II und dem vasodilatorisch/anti-proliferativen Effektor Ang (1-7) mit seinem Rezeptor *Mas.*

Bedingt durch einen heterogenen genetischen Hintergrund, konnte in bisherigen Studien *Mas*-defizienten Mäusen kein eindeutiger kardiovaskulärer Phenotyp zugeordnet werden. Durch Rückkreuzungen dieser Mäuse über 7 Generationen, auf einen FVB/N und B1/6 Hintergrund, fanden wir heraus, dass ausschließlich die FVB/N *Mas*-defizienten Mäuse höhere Blutdruckwerte als die Wildtypen aufwiesen. Darüber hinaus zeigten beide *Mas*-defizienten Mauslinien eine beeinträchtigte Endothelfunktion, eine verminderte NO-Produktion sowie eine geringere endotheliale NO-Synthase Expression.

Der Gehalt der katalytischen Untereinheit der NAD(P)H Oxidase gp91phox war in den *Mas*-defizienten Mäusen höher als in den Kontrolltieren. Außerdem waren in FVB/N *Mas*-defizienten Mäusen die Aktivitäten der Superoxiddismutase und der Katalase reduziert. Das SOD-Mimetikum Tempol zeigte eine stärkere Blutdruck-senkende Wirkung in den FVB/N *Mas*-defizienten Tieren als in Kontrolltieren.

Unsere Ergebnisse zeigen also einen deutlichen kardiovaskulären Phenotypen in *Mas*-defizienten Mäusen auf einem homogenen FVB/N Hintergrund. Wir nehmen an, dass die erhöhte $O_2^{\cdot -}$ Bildung, die verringerte antioxidative Aktivität, sowie geringere NO-Konzentrationen im Gefäßsystem endotheliale Dysfunktion und damit erhöhten Blutdruck in diesen Tieren hervorrufen. Da Mas vielen kardiovaskulären Effekten von Ang II entgegenzuwirken scheint, ist dieser Rezeptor ein potentielles Target für die Entwicklung neuer kardioprotektiver und anti-hypertensiver Wirkstoffe.

Außerdem fanden wir zwischen FVB/N und B1/6 Mäusen viele Unterschiede. B1/6 Mäuse wiesen höhere NO-Werte und mehr oxidativen Stress sowie geringere antioxidative Aktivität auf als FVB/N Mäuse. Dementsprechend tendierten FVB/N Mäuse zu höheren Blutdruckwerten, begleitet von höherer Renin-Aktivität und geringeren NO-Werten. Folglich beeinflußt der genetische Hintergrund den Phänotypen von genetisch modifizierten Tieren.

Das genetische Ausschalten von *Mas* beeinträchtigte die Herzfunktion von Mäusen. Zur Analyse

der entsprechenden genetischen Prozesse haben wir ein Affymetrix Genexpressions-Profil erstellt. Unter 12488 Transkripten, waren 87 Gene in *Mas*-defizienten Mäuse signifikant herunterreguliert, z.B. Rgs2 und ADAM19, welche beide an der Regulierung des Gefäßtonus beteiligt sind. 182 Gene waren dagegen hochreguliert. Da Mas stark im Hoden exprimiert wird, wurden Affymetrix Genexpressions-Profile auch für Hoden von *Mas*-defizienten Mäusen erstellt. In den Hoden der B1/6 *Mas*-knockout Mäuse waren 65 Gene hochreguliert und 67 Gene herunterreguliert, einschließlich der in die Steroidogenese involvierten Faktoren StAR und 3β-HSDs.

Ang II spielt eine Schlüsselrolle in der Ätiologie von kardiovaskulären Erkrankungen. Deshalb wurden transgene Mäuse, die das Ratten-Angiotensinogen überexprimieren, auf den Einfluss von Ang II auf Endorganschäden untersucht. Das Ziel unserer Studie war die Charakterisierung der bereits generierten transgenen Linie TGM L102. Die transgenen Mäuse hatten, verglichen mit den Kontrollmäusen, einen signifikant höheren Blutdruck. Der Anstieg des Blutdrucks korrelierte mit Herz-Hypertrophie und erhöhten Konzentrationen von BNP. Begleitend dazu waren Fibrose in Herz, Lunge und Nieren der transgenen Mäuse mehr ausgeprägt als im Wildtyp. Außerdem war die Kollagen III mRNA-Expression erhöht. Allerdings konnte im Herz keine Apoptose detektiert werden.

Der letzte Abschnitt der Arbeit zielte auf ein besseres Verständnis der Funktion von Ang II im Gehirn ab. Für die Kontrolle der transgenen Ang II Freisetzung wurde der Promotor für AVP in transgenen Ratten verwendet. Allerdings zeigte dieser nur eine sehr geringe Expressionsrate. Selbst nach einer Stimulation durch Dehydrierung oder einer Hochsalz-Diät war weder eine erhöhte Expression des Transgens noch eine Blutdrucksteigerung festzustellen. Hauptursache für dieses Problem könnte die geringe Anzahl ins Genom integrierter Transgen-Kopien sein.

7. Literature

Abbas, A., G. Gorelik, L. A. Carbini, et al. Angiotensin-(1-7) induces bradykinin-mediated hypotensive responses in anesthetized rats. Hypertension 1997; 30**:** 217-21.

AbdAlla, S., H. Lother, A. M. Abdel-tawab, et al. The angiotensin II AT2 receptor is an AT1 receptor antagonist. J Biol Chem 2001; 276**:** 39721-6.

Abel, T., K. C. Martin, D. Bartsch, et al. Memory suppressor genes: inhibitory constraints on the storage of long-term memory. Science 1998; 279**:** 338-41.

Adams, J. W., Y. Sakata, M. G. Davis, et al. Enhanced Galphaq signaling: a common pathway mediates cardiac hypertrophy and apoptotic heart failure. Proc Natl Acad Sci U S A 1998; 95**:** 10140-5.

Aguilera, G. and A. Kiss. Regulation of the hypothalmic-pituitary-adrenal axis and vasopressin secretion. Role of angiotensin II. Adv Exp Med Biol 1996; 396**:** 105-12.

Alenina, N., T. Baranova, E. Smirnow, et al. Cell type-specific expression of the Mas proto-oncogene in testis. J Histochem Cytochem 2002; 50**:** 691-6.

Alzamora, A. C., R. A. Santos and M. J. Campagnole-Santos. Baroreflex modulation by angiotensins at the rat rostral and caudal ventrolateral medulla. Am J Physiol Regul Integr Comp Physiol 2006; 290**:** R1027-34.

Ambroz, C., A. J. Clark and K. J. Catt. The mas oncogene enhances angiotensin-induced [Ca2+]i responses in cells with pre-existing angiotensin II receptors. Biochim Biophys Acta 1991; 1133**:** 107-11.

Ananthakrishnan, R., G. W. Moe, M. J. Goldenthal, et al. Akt signaling pathway in pacing-induced heart failure. Mol. Cell. Biol 2005; 268**:** 103-10.

Andrawis, N. S. and D. R. Abernethy. Verapamil blocks basal and angiotensin II-induced RNA synthesis of rat aortic vascular smooth muscle cells. Biochem Biophys Res Commun 1992; 183**:** 767-73.

Ang, H. L., D. A. Carter and D. Murphy. Neuron-specific expression and physiological regulation of bovine vasopressin transgenes in mice. Embo J 1993; 12**:** 2397-409.

Archer, S. L., J. M. Huang, V. Hampl, et al. Nitric oxide and cGMP cause vasorelaxation by activation of a charybdotoxin-sensitive K channel by cGMP-dependent protein kinase. Proc Natl Acad Sci U S A 1994; 91**:** 7583-7.

Aruoma OI, H. B. Molecular Biology of Free Radicals in Human Diseases. 1998.

Averill, D. B. and D. I. Diz. Angiotensin peptides and baroreflex control of sympathetic outflow: pathways and mechanisms of the medulla oblongata. Brain Res Bull 2000; 51**:** 119-28.

Babior, B. M. NADPH oxidase: an update. Blood 1999; 93**:** 1464-76.

Bader, M., J. Peters, O. Baltatu, et al. Tissue renin-angiotensin systems: new insights from experimental animal models in hypertension research. J Mol Med 2001; 79**:** 76-102.

Bains, J. S., A. Potyok and A. V. Ferguson. Angiotensin II actions in paraventricular nucleus: functional evidence for neurotransmitter role in efferents originating in subfornical organ. Brain Res 1992; 599**:** 223-9.

Baker, P. J., J. A. Sha, M. W. McBride, et al. Expression of 3beta-hydroxysteroid dehydrogenase type I and type VI isoforms in the mouse testis during development. Eur J Biochem 1999; 260**:** 911-7.

Baltatu, O. and M. Bader. Brain renin-angiotensin system. Lessons from functional genomics. Neuroendocrinology 2003; 78**:** 253-9.

Baltatu, O., J. A. Silva, Jr., D. Ganten, et al. The brain renin-angiotensin system modulates angiotensin II-induced hypertension and cardiac hypertrophy. Hypertension 2000; 35**:** 409-12.

7. Literature

Basu, S. Isoprostanes: novel bioactive products of lipid peroxidation. Free Radic Res 2004; 38**:** 105-22.

Bauer, P. M., D. Fulton, Y. C. Boo, et al. Compensatory phosphorylation and protein-protein interactions revealed by loss of function and gain of function mutants of multiple serine phosphorylation sites in endothelial nitric-oxide synthase. J Biol Chem 2003; 278**:** 14841-9.

Baylis, C. and P. Vallance. Measurement of nitrite and nitrate levels in plasma and urine--what does this measure tell us about the activity of the endogenous nitric oxide system? Curr Opin Nephrol Hypertens 1998; 7**:** 59-62.

Becker, L. K., G. M. Etelvino, T. Walther, et al. Immunofluorescence localization of the receptor Mas in cardiovascular-related areas of the rat brain. Am J Physiol Heart Circ Physiol 2007; 293**:** H1416-24.

Bendall, J. K., C. Heymes, T. J. Wright, et al. Strain-dependent variation in vascular responses to nitric oxide in the isolated murine heart. J Mol Cell Cardiol 2002; 34**:** 1325-33.

Beswick, R. A., A. M. Dorrance, R. Leite, et al. NADH/NADPH oxidase and enhanced superoxide production in the mineralocorticoid hypertensive rat. Hypertension 2001; 38**:** 1107-11.

Bohlender, J., J. Menard, O. Edling, et al. Mouse and rat plasma renin concentration and gene expression in (mRen2)27 transgenic rats. Am J Physiol 1998; 274**:** H1450-6.

Bohlender, J., J. Menard, J. Wagner, et al. Human renin-dependent hypertension in rats transgenic for human angiotensinogen. Hypertension 1996; 27**:** 535-40.

Boockvar, K. S., D. L. Granger, R. M. Poston, et al. Nitric oxide produced during murine listeriosis is protective. Infect Immun 1994; 62**:** 1089-100.

Brechler, V., W. N. Chu, J. D. Baxter, et al. A protease processing site is essential for prorenin sorting to the regulated secretory pathway. J Biol Chem 1996; 271**:** 20636-40.

Brouet, A., P. Sonveaux, C. Dessy, et al. Hsp90 ensures the transition from the early Ca2+-dependent to the late phosphorylation-dependent activation of the endothelial nitric-oxide synthase in vascular endothelial growth factor-exposed endothelial cells. J Biol Chem 2001; 276**:** 32663-9.

Brown, G. C. Nitric oxide and mitochondrial respiration. Biochim Biophys Acta 1999; 1411**:** 351-69.

Bunnemann, B., K. Fuxe, R. Metzger, et al. Autoradiographic localization of mas proto-oncogene mRNA in adult rat brain using in situ hybridization. Neurosci Lett 1990; 114**:** 147-53.

Burbach, J. P., M. J. De Hoop, H. Schmale, et al. Differential responses to osmotic stress of vasopressin-neurophysin mRNA in hypothalamic nuclei. Neuroendocrinology 1984; 39**:** 582-4.

Burstein, E. S., T. R. Ott, M. Feddock, et al. Characterization of the Mas-related gene family: structural and functional conservation of human and rhesus MrgX receptors. Br J Pharmacol 2006; 147**:** 73-82.

Cai, H. and D. G. Harrison. Endothelial dysfunction in cardiovascular diseases: the role of oxidant stress. Circ Res 2000; 87**:** 840-4.

Campagnole-Santos, M. J., S. B. Heringer, E. N. Batista, et al. Differential baroreceptor reflex modulation by centrally infused angiotensin peptides. Am J Physiol 1992; 263**:** R89-94.

Canals, M., L. Jenkins, E. Kellett, et al. Up-regulation of the angiotensin II type 1 receptor by the MAS proto-oncogene is due to constitutive activation of Gq/G11 by MAS. J Biol Chem 2006; 281**:** 16757-67.

Castro, C. H., R. A. Santos, A. J. Ferreira, et al. Evidence for a functional interaction of the angiotensin-(1-7) receptor Mas with AT1 and AT2 receptors in the mouse heart. Hypertension 2005; 46**:** 937-42.

7. Literature

Castro, C. H., R. A. Santos, A. J. Ferreira, et al. Effects of genetic deletion of angiotensin-(1-7) receptor Mas on cardiac function during ischemia/reperfusion in the isolated perfused mouse heart. Life Sci 2006; 80**:** 264-8.

Chen, C., B. Zheng, J. Han, et al. Characterization of a novel mammalian RGS protein that binds to Galpha proteins and inhibits pheromone signaling in yeast. J Biol Chem 1997; 272**:** 8679-85.

Chiabrando, C., L. Rivoltella, L. Martelli, et al. Urinary excretion of thromboxane and prostacyclin metabolites during chronic low-dose aspirin: evidence for an extrarenal origin of urinary thromboxane B2 and 6-keto-prostaglandin F1 alpha in healthy subjects. Biochim Biophys Acta 1992; 1133**:** 247-54.

Cifuentes, M. E., F. E. Rey, O. A. Carretero, et al. Upregulation of p67(phox) and gp91(phox) in aortas from angiotensin II-infused mice. Am J Physiol Heart Circ Physiol 2000; 279**:** H2234-40.

Condorelli, G., A. Drusco, G. Stassi, et al. Akt induces enhanced myocardial contractility and cell size in vivo in transgenic mice. Proc Natl Acad Sci U S A 2002; 99**:** 12333-8.

Cooper, G. t. Basic determinants of myocardial hypertrophy: a review of molecular mechanisms. Annu Rev Med 1997; 48**:** 13-23.

Covell, J. W. Factors influencing diastolic function. Possible role of the extracellular matrix. Circulation 1990; 81**:** III155-8.

Crackower, M. A., R. Sarao, G. Y. Oudit, et al. Angiotensin-converting enzyme 2 is an essential regulator of heart function. Nature 2002; 417**:** 822-8.

da Costa Goncalves, A. C., R. Leite, R. A. Fraga-Silva, et al. Evidence that the vasodilator angiotensin-(1-7)-Mas axis plays an important role in erectile function. Am J Physiol Heart Circ Physiol 2007; 293**:** H2588-96.

Dahl, L. K. Possible role of salt intake in the development of essential hypertension. 1960. Int J Epidemiol 2005; 34**:** 967-72; discussion 72-4, 75-8.

Datta, S. R., A. Brunet and M. E. Greenberg. Cellular survival: a play in three Akts. Genes Dev 1999; 13**:** 2905-27.

Davies, J., S. Waller, Q. Zeng, et al. Further delineation of the sequences required for the expression and physiological regulation of the vasopressin gene in transgenic rat hypothalamic magnocellular neurones. J Neuroendocrinol 2003; 15**:** 42-50.

Davis, L. G., R. Arentzen, J. M. Reid, et al. Glucocorticoid sensitivity of vasopressin mRNA levels in the paraventricular nucleus of the rat. Proc Natl Acad Sci U S A 1986; 83**:** 1145-9.

DeBosch, B., I. Treskov, T. S. Lupu, et al. Akt1 is required for physiological cardiac growth. Circulation 2006; 113**:** 2097-104.

Denton, D. A., M. J. McKinley and R. S. Weisinger. Hypothalamic integration of body fluid regulation. Proc Natl Acad Sci U S A 1996; 93**:** 7397-404.

Deschepper, C. F., J. L. Olson, M. Otis, et al. Characterization of blood pressure and morphological traits in cardiovascular-related organs in 13 different inbred mouse strains. J Appl Physiol 2004; 97**:** 369-76.

DiBona, G. F. and L. L. Sawin. Effect of metoprolol administration on renal sodium handling in experimental congestive heart failure. Circulation 1999; 100**:** 82-6.

Dimmeler, S., I. Fleming, B. Fisslthaler, et al. Activation of nitric oxide synthase in endothelial cells by Akt-dependent phosphorylation. Nature 1999; 399**:** 601-5.

Dobrian, A. D., S. D. Schriver and R. L. Prewitt. Role of angiotensin II and free radicals in blood pressure regulation in a rat model of renal hypertension. Hypertension 2001; 38**:** 361-6.

Dong, X., S. Han, M. J. Zylka, et al. A diverse family of GPCRs expressed in specific subsets of nociceptive sensory neurons. Cell 2001; 106**:** 619-32.

7. Literature

Donoghue, M., F. Hsieh, E. Baronas, et al. A novel angiotensin-converting enzyme-related carboxypeptidase (ACE2) converts angiotensin I to angiotensin 1-9. Circ Res 2000; 87**:** E1-9.

Dunn, A. R. and J. Sambrook. Mapping viral mRNAs by sandwich hybridization. Methods Enzymol 1980; 65**:** 468-78.

Ellgaard, L., M. Molinari and A. Helenius. Setting the standards: quality control in the secretory pathway. Science 1999; 286**:** 1882-8.

Elsasser, A., K. Suzuki and J. Schaper. Unresolved issues regarding the role of apoptosis in the pathogenesis of ischemic injury and heart failure. J Mol Cell Cardiol 2000; 32**:** 711-24.

Feinberg, A. P. and B. Vogelstein. "A technique for radiolabeling DNA restriction endonuclease fragments to high specific activity". Addendum. Anal Biochem 1984; 137**:** 266-7.

Ferguson, A. V., D. L. Washburn and K. J. Latchford. Hormonal and neurotransmitter roles for angiotensin in the regulation of central autonomic function. Exp Biol Med (Maywood) 2001; 226**:** 85-96.

Ferrario, C. M., J. Jessup, P. E. Gallagher, et al. Effects of renin-angiotensin system blockade on renal angiotensin-(1-7) forming enzymes and receptors. Kidney Int 2005; 68**:** 2189-96.

Ferreira, A. J., R. A. Santos and A. P. Almeida. Angiotensin-(1-7) improves the post-ischemic function in isolated perfused rat hearts. Braz J Med Biol Res 2002; 35**:** 1083-90.

Feuerstein, G. Z. Apoptosis--new opportunities for novel therapeutics for heart diseases. Cardiovasc Drugs Ther 2001; 15**:** 547-51.

Fink, G. D. Long-term sympatho-excitatory effect of angiotensin II: a mechanism of spontaneous and renovascular hypertension. Clin Exp Pharmacol Physiol 1997; 24**:** 91-5.

Fitzsimons, J. T. Angiotensin, thirst, and sodium appetite. Physiol Rev 1998; 78**:** 583-686.

Fortuno, M. A., S. Ravassa, J. C. Etayo, et al. Overexpression of Bax protein and enhanced apoptosis in the left ventricle of spontaneously hypertensive rats: effects of AT1 blockade with losartan. Hypertension 1998; 32**:** 280-6.

Franke, T. F., D. R. Kaplan and L. C. Cantley. PI3K: downstream AKTion blocks apoptosis. Cell 1997; 88**:** 435-7.

Freeman, E. J., G. M. Chisolm, C. M. Ferrario, et al. Angiotensin-(1-7) inhibits vascular smooth muscle cell growth. Hypertension 1996; 28**:** 104-8.

Fulton, D., J. P. Gratton, T. J. McCabe, et al. Regulation of endothelium-derived nitric oxide production by the protein kinase Akt. Nature 1999; 399**:** 597-601.

Furchgott, R. F. and P. M. Vanhoutte. Endothelium-derived relaxing and contracting factors. Faseb J 1989; 3**:** 2007-18.

Ganten, D., J. L. Minnich, P. Granger, et al. Angiotensin-forming enzyme in brain tissue. Science 1971; 173**:** 64-5.

Garcia-Cardena, G., R. Fan, V. Shah, et al. Dynamic activation of endothelial nitric oxide synthase by Hsp90. Nature 1998; 392**:** 821-4.

Gentles, A. J. and S. Karlin. Why are human G-protein-coupled receptors predominantly intronless? Trends Genet 1999; 15**:** 47-9.

Gerlai, R. Gene targeting: technical confounds and potential solutions in behavioral brain research. Behav Brain Res 2001; 125**:** 13-21.

Gerzer, R., E. Bohme, F. Hofmann, et al. Soluble guanylate cyclase purified from bovine lung contains heme and copper. FEBS Lett 1981; 132**:** 71-4.

Giani, J. F., M. M. Gironacci, M. C. Munoz, et al. Angiotensin-(1 7) stimulates the phosphorylation of JAK2, IRS-1 and Akt in rat heart in vivo: role of the AT1 and Mas receptors. Am J Physiol Heart Circ Physiol 2007; 293**:** H1154-63.

Gorlach, A., R. P. Brandes, K. Nguyen, et al. A gp91phox containing NADPH oxidase selectively expressed in endothelial cells is a major source of oxygen radical generation in the arterial wall. Circ Res 2000; 87**:** 26-32.

7. Literature

Grant, F. D., J. Reventos, J. W. Gordon, et al. Expression of the rat arginine vasopressin gene in transgenic mice. Mol Endocrinol 1993; 7**:** 659-67.

Grant, S. L., B. Lassegue, K. K. Griendling, et al. Specific regulation of RGS2 messenger RNA by angiotensin II in cultured vascular smooth muscle cells. Mol Pharmacol 2000; 57**:** 460-7.

Griendling, K. K. and D. G. Harrison. Out, damned dot: studies of the NADPH oxidase in atherosclerosis. J Clin Invest 2001; 108**:** 1423-4.

Gulati, K. and S. B. Lall. Angiotensin II--receptor subtypes characterization and pathophysiological implications. Indian J Exp Biol 1996; 34**:** 91-7.

Gurley, S. B., A. Allred, T. H. Le, et al. Altered blood pressure responses and normal cardiac phenotype in ACE2-null mice. J Clin Invest 2006; 116**:** 2218-25.

Haas, J. A., J. D. Krier, R. J. Bolterman, et al. Low-dose angiotensin II increases free isoprostane levels in plasma. Hypertension 1999; 34**:** 983-6.

Hartner, A., N. Cordasic, B. Klanke, et al. Strain differences in the development of hypertension and glomerular lesions induced by deoxycorticosterone acetate salt in mice. Nephrol Dial Transplant 2003; 18**:** 1999-2004.

Heinrikson, R. L., J. Hui, H. Zurcher-Neely, et al. A structural model to explain the partial catalytic activity of human prorenin. Am J Hypertens 1989; 2**:** 367-80.

Heitsch, H., S. Brovkovych, T. Malinski, et al. Angiotensin-(1-7)-Stimulated Nitric Oxide and Superoxide Release From Endothelial Cells. Hypertension 2001; 37**:** 72-6.

Hellner, K., T. Walther, M. Schubert, et al. Angiotensin-(1-7) enhances LTP in the hippocampus through the G-protein-coupled receptor Mas. Mol Cell Neurosci 2005; 29**:** 427-35.

Holtz, J. Pathophysiology of heart failure and the renin-angiotensin-system. Basic Res Cardiol 1993; 88 Suppl 1**:** 183-201.

Igase, M., W. B. Strawn, P. E. Gallagher, et al. Angiotensin II AT1 receptors regulate ACE2 and angiotensin-(1-7) expression in the aorta of spontaneously hypertensive rats. Am J Physiol Heart Circ Physiol 2005; 289**:** H1013-9.

Ignarro, L. J., G. M. Buga, K. S. Wood, et al. Endothelium-derived relaxing factor produced and released from artery and vein is nitric oxide. Proc Natl Acad Sci U S A 1987; 84**:** 9265-9.

Irani, K. Oxidant signaling in vascular cell growth, death, and survival : a review of the roles of reactive oxygen species in smooth muscle and endothelial cell mitogenic and apoptotic signaling. Circ Res 2000; 87**:** 179-83.

Iwata, M., R. T. Cowling, D. Gurantz, et al. Angiotensin-(1-7) binds to specific receptors on cardiac fibroblasts to initiate antifibrotic and antitrophic effects. Am J Physiol Heart Circ Physiol 2005; 289**:** H2356-63.

Jackson, T. R., L. A. Blair, J. Marshall, et al. The mas oncogene encodes an angiotensin receptor. Nature 1988; 335**:** 437-40.

Jackson, T. R. and M. R. Hanley. Tumor promoter 12-O-tetradecanoylphorbol 13-acetate inhibits mas/angiotensin receptor-stimulated inositol phosphate production and intracellular Ca2+ elevation in the 401L-C3 neuronal cell line. FEBS Lett 1989; 251**:** 27-30.

Jaimes, E. A., C. Sweeney and L. Raij. Effects of the reactive oxygen species hydrogen peroxide and hypochlorite on endothelial nitric oxide production. Hypertension 2001; 38**:** 877-83.

Jaiswal, N., D. I. Diz, M. C. Chappell, et al. Stimulation of endothelial cell prostaglandin production by angiotensin peptides. Characterization of receptors. Hypertension 1992; 19**:** II49-55.

Janssen, B. J., T. De Celle, J. J. Debets, et al. Effects of anesthetics on systemic hemodynamics in mice. Am J Physiol Heart Circ Physiol 2004; 287**:** H1618-24.

Janssen, J. W., A. C. Steenvoorden, M. Schmidtberger, et al. Activation of the mas oncogene during transfection of monoblastic cell line DNA. Leukemia 1988; 2**:** 318-20.

7. Literature

Jeong, S. W., M. Castel, B. J. Zhang, et al. Cell-specific expression and subcellular localization of neurophysin-CAT-fusion proteins expressed from oxytocin and vasopressin gene promoter-driven constructs in transgenic mice. Exp Neurol 2001; 171**:** 255-71.

Jugdutt, B. I. Remodeling of the myocardium and potential targets in the collagen degradation and synthesis pathways. Curr Drug Targets Cardiovasc Haematol Disord 2003; 3**:** 1-30.

Jutras, I., N. G. Seidah and T. L. Reudelhuber. A predicted alpha -helix mediates targeting of the proprotein convertase PC1 to the regulated secretory pathway. J Biol Chem 2000; 275**:** 40337-43.

Kang, N., T. Walther, X. L. Tian, et al. Reduced hypertension-induced end-organ damage in mice lacking cardiac and renal angiotensinogen synthesis. J Mol Med 2002; 80**:** 359-66.

Kim, J. K., S. N. Summer, W. M. Wood, et al. Osmotic and non-osmotic regulation of arginine vasopressin (AVP) release, mRNA, and promoter activity in small cell lung carcinoma (SCLC) cells. Mol Cell Endocrinol 1996; 123**:** 179-86.

Kimura, S., J. J. Mullins, B. Bunnemann, et al. High blood pressure in transgenic mice carrying the rat angiotensinogen gene. Embo J 1992; 11**:** 821-7.

Kitaoka, T., M. Sharif, M. R. Hanley, et al. Expression of the MAS proto-oncogene in the retinal pigment epithelium of the rhesus macaque. Curr Eye Res 1994; 13**:** 345-51.

Kleinbongard, P., A. Dejam, T. Lauer, et al. Plasma nitrite concentrations reflect the degree of endothelial dysfunction in humans. Free Radic Biol Med 2006; 40**:** 295-302.

Kleinbongard, P., A. Dejam, T. Lauer, et al. Plasma nitrite reflects constitutive nitric oxide synthase activity in mammals. Free Radic Biol Med 2003; 35**:** 790-6.

Kopkan, L. and D. S. Majid. Superoxide contributes to development of salt sensitivity and hypertension induced by nitric oxide deficiency. Hypertension 2005; 46**:** 1026-31.

Kostenis, E., G. Milligan, A. Christopoulos, et al. G-protein-coupled receptor Mas is a physiological antagonist of the angiotensin II type 1 receptor. Circulation 2005; 111**:** 1806-13.

Kucharewicz, I., E. Chabielska, D. Pawlak, et al. The antithrombotic effect of angiotensin-(1-7) closely resembles that of losartan. J Renin Angiotensin Aldosterone Syst 2000; 1**:** 268-72.

Kulik, G., A. Klippel and M. J. Weber. Antiapoptotic signalling by the insulin-like growth factor I receptor, phosphatidylinositol 3-kinase, and Akt. Mol Cell Biol 1997; 17**:** 1595-606.

Kumar, M., P. Grammas, F. Giacomelli, et al. Selective expression of c-mas proto-oncogene in rat cerebral endothelial cells. Neuroreport 1996; 8**:** 93-6.

Kurohara, K., K. Komatsu, T. Kurisaki, et al. Essential roles of Meltrin beta (ADAM19) in heart development. Dev Biol 2004; 267**:** 14-28.

Landmesser, U., H. Cai, S. Dikalov, et al. Role of p47(phox) in vascular oxidative stress and hypertension caused by angiotensin II. Hypertension 2002; 40**:** 511-5.

Lange, H., T. Lisowsky, J. Gerber, et al. An essential function of the mitochondrial sulfhydryl oxidase Erv1p/ALR in the maturation of cytosolic Fe/S proteins. EMBO Rep 2001; 2**:** 715-20.

Langenickel, T. H., I. Pagel, J. Buttgereit, et al. Rat corin gene: molecular cloning and reduced expression in experimental heart failure. Am J Physiol Heart Circ Physiol 2004; 287**:** H1516-21.

Lassegue, B. and R. E. Clempus. Vascular NAD(P)H oxidases: specific features, expression, and regulation. Am J Physiol Regul Integr Comp Physiol 2003; 285**:** R277-97.

Lemos, V. S., D. M. Silva, T. Walther, et al. The endothelium-dependent vasodilator effect of the nonpeptide Ang(1-7) mimic AVE 0991 is abolished in the aorta of mas-knockout mice. J Cardiovasc Pharmacol 2005; 46**:** 274-9.

Lewandoski, M. Conditional control of gene expression in the mouse. Nat Rev Genet 2001; 2**:** 743-55.

7. Literature

Lochard, N., D. W. Silversides, J. P. van Kats, et al. Brain-specific restoration of angiotensin II corrects renal defects seen in angiotensinogen-deficient mice. J Biol Chem 2003; 278**:** 2184-9.

Lolait, S. J., A. M. O'Carroll, O. W. McBride, et al. Cloning and characterization of a vasopressin V2 receptor and possible link to nephrogenic diabetes insipidus. Nature 1992; 357**:** 336-9.

Loot, A. E., A. J. Roks, R. H. Henning, et al. Angiotensin-(1-7) attenuates the development of heart failure after myocardial infarction in rats. Circulation 2002; 105**:** 1548-50.

Lum, C., E. G. Shesely, D. L. Potter, et al. Cardiovascular and renal phenotype in mice with one or two renin genes. Hypertension 2004; 43**:** 79-86.

Lykkesfeldt, J. Malondialdehyde as biomarker of oxidative damage to lipids caused by smoking. Clin Chim Acta 2007; 380**:** 50-8.

Marnett, L. J. Oxyradicals and DNA damage. Carcinogenesis 2000; 21**:** 361-70.

Martin, K. A., S. G. Grant and S. Hockfield. The mas proto-oncogene is developmentally regulated in the rat central nervous system. Brain Res Dev Brain Res 1992; 68**:** 75-82.

Martin, K. A. and S. Hockfield. Expression of the mas proto-oncogene in the rat hippocampal formation is regulated by neuronal activity. Brain Res Mol Brain Res 1993; 19**:** 303-9.

Maul, B., W. E. Siems, M. R. Hoehe, et al. Alcohol consumption is controlled by angiotensin II. Faseb J 2001; 15**:** 1640-2.

McKinley, M. J., A. L. Albiston, A. M. Allen, et al. The brain renin-angiotensin system: location and physiological roles. Int J Biochem Cell Biol 2003; 35**:** 901-18.

Meinhardt, A., B. Wilhelm and J. Seitz. Expression of mitochondrial marker proteins during spermatogenesis. Hum Reprod Update 1999; 5**:** 108-19.

Meneely, G. R., R. G. Tucker, W. J. Darby, et al. Chronic sodium chloride toxicity in the albino rat. II. Occurrence of hypertension and of a syndrome of edema and renal failure. J Exp Med 1953; 98**:** 71-80.

Methot, D., J. P. vanKats, N. Lochard, et al. Development and application of a biological peptide pump for the study of the in vivo actions of angiotensin peptides. Am J Hypertens 2001; 14**:** 38S-43S.

Metzger, R., M. Bader, T. Ludwig, et al. Expression of the mouse and rat mas proto-oncogene in the brain and peripheral tissues. FEBS Lett 1995; 357**:** 27-32.

Millgard, J. and L. Lind. Acute hypertension impairs endothelium-dependent vasodilation. Clin Sci (Lond) 1998; 94**:** 601-7.

Molloy, S. S., E. D. Anderson, F. Jean, et al. Bi-cycling the furin pathway: from TGN localization to pathogen activation and embryogenesis. Trends Cell Biol 1999; 9**:** 28-35.

Monnot, C., V. Weber, J. Stinnakre, et al. Cloning and functional characterization of a novel mas-related gene, modulating intracellular angiotensin II actions. Mol Endocrinol 1991; 5**:** 1477-87.

Morrow, J. D., K. E. Hill, R. F. Burk, et al. A series of prostaglandin F2-like compounds are produced in vivo in humans by a non-cyclooxygenase, free radical-catalyzed mechanism. Proc Natl Acad Sci U S A 1990; 87**:** 9383-7.

Mukoyama, M., M. Nakajima, M. Horiuchi, et al. Expression cloning of type 2 angiotensin II receptor reveals a unique class of seven-transmembrane receptors. J Biol Chem 1993; 268**:** 24539-42.

Muller, D. N., C. Schmidt, E. Barbosa-Sicard, et al. Mouse Cyp4a isoforms: enzymatic properties, gender- and strain-specific expression, and role in renal 20-hydroxyeicosatetraenoic acid formation. Biochem J 2007; 403**:** 109-18.

Murad, F. Nitric oxide signaling: would you believe that a simple free radical could be a second messenger, autacoid, paracrine substance, neurotransmitter, and hormone? Recent Prog Horm Res 1998; 53**:** 43-59; discussion -60.

7. Literature

Murphy, D. and D. Carter. Vasopressin gene expression in the rodent hypothalamus: transcriptional and posttranscriptional responses to physiological stimulation. Mol Endocrinol 1990; 4**:** 1051-9.

Murphy, D., A. Levy, S. Lightman, et al. Vasopressin RNA in the neural lobe of the pituitary: dramatic accumulation in response to salt loading. Proc Natl Acad Sci U S A 1989; 86**:** 9002-5.

Murphy, D., J. Xu and S. Waller. Transgenic studies in rats and mice on the osmotic regulation of vasopressin gene expression. Exp Physiol 2000; 85 Spec No**:** 211S-22S.

Nair, V. and G. A. Turner. The Thiobarbituric Acid Test for Lipid-Peroxidation - Structure of the Adduct with Malondialdehyde. Lipids 1984; 19**:** 804-5.

Needleman, P., J. Turk, B. A. Jakschik, et al. Arachidonic acid metabolism. Annu Rev Biochem 1986; 55**:** 69-102.

Obst, M., V. Gross and F. C. Luft. Systemic hemodynamics in non-anesthetized L-NAME- and DOCA-salt-treated mice. J Hypertens 2004; 22**:** 1889-94.

Oliver, W. J. and F. Gross. Unique specificity of mouse angiotensinogen to homologous renin. Proc Soc Exp Biol Med 1966; 122**:** 923-6.

Ortiz, M. C., M. C. Manriquez, J. C. Romero, et al. Antioxidants block angiotensin II-induced increases in blood pressure and endothelin. Hypertension 2001; 38**:** 655-9.

Pagliaro, P. and C. Penna. Rethinking the renin-angiotensin system and its role in cardiovascular regulation. Cardiovasc Drugs Ther 2005; 19**:** 77-87.

Panza, J. A., P. R. Casino, C. M. Kilcoyne, et al. Role of endothelium-derived nitric oxide in the abnormal endothelium-dependent vascular relaxation of patients with essential hypertension. Circulation 1993; 87**:** 1468-74.

Peiro, C., S. Vallejo, F. Gembardt, et al. Endothelial dysfunction through genetic deletion or inhibition of the G protein-coupled receptor Mas: a new target to improve endothelial function. J Hypertens 2007; 25**:** 2421-5.

Pinheiro, S. V., A. C. Simoes e Silva, W. O. Sampaio, et al. Nonpeptide AVE 0991 is an angiotensin-(1-7) receptor Mas agonist in the mouse kidney. Hypertension 2004; 44**:** 490-6.

Plotsky, P. M., E. T. Cunningham, Jr. and E. P. Widmaier. Catecholaminergic modulation of corticotropin-releasing factor and adrenocorticotropin secretion. Endocr Rev 1989; 10**:** 437-58.

Porsti, I., A. T. Bara, R. Busse, et al. Release of nitric oxide by angiotensin-(1-7) from porcine coronary endothelium: implications for a novel angiotensin receptor. Br J Pharmacol 1994; 111**:** 652-4.

Probst, W. C., L. A. Snyder, D. I. Schuster, et al. Sequence alignment of the G-protein coupled receptor superfamily. DNA Cell Biol 1992; 11**:** 1-20.

Qin, L. X., R. P. Beyer, F. N. Hudson, et al. Evaluation of methods for oligonucleotide array data via quantitative real-time PCR. BMC Bioinformatics 2006; 7**:** 23.

Rabin, M., D. Birnbaum, D. Young, et al. Human ros1 and mas1 oncogenes located in regions of chromosome 6 associated with tumor-specific rearrangements. Oncogene Res 1987; 1**:** 169-78.

Radovic, M., Z. Miloradovic, T. Popovic, et al. Allopurinol and enalapril failed to conserve urinary NOx and sodium in ischemic acute renal failure in spontaneously hypertensive rats. Am J Nephrol 2006; 26**:** 388-99.

Rajagopalan, S., S. Kurz, T. Munzel, et al. Angiotensin II-mediated hypertension in the rat increases vascular superoxide production via membrane NADH/NADPH oxidase activation. Contribution to alterations of vasomotor tone. J Clin Invest 1996; 97**:** 1916-23.

Reudelhuber, T. L. A place in our hearts for the lowly angiotensin 1-7 peptide? Hypertension 2006; 47**:** 811-5.

7. Literature

Robertson, G. L. The regulation of vasopressin function in health and disease. Recent Prog Horm Res 1976; 33**:** 333-85.

Robinson, B. G., D. M. Frim, W. J. Schwartz, et al. Vasopressin mRNA in the suprachiasmatic nuclei: daily regulation of polyadenylate tail length. Science 1988; 241**:** 342-4.

Rodgers, R. J., E. Boullier, P. Chatzimichalaki, et al. Contrasting phenotypes of C57BL/6JOlaHsd, 129S2/SvHsd and 129/SvEv mice in two exploration-based tests of anxiety-related behaviour. Physiol Behav 2002; 77**:** 301-10.

Ross, P. C., R. A. Figler, M. H. Corjay, et al. RTA, a candidate G protein-coupled receptor: cloning, sequencing, and tissue distribution. Proc Natl Acad Sci U S A 1990; 87**:** 3052-6.

Sampaio, W. O., R. A. Souza dos Santos, R. Faria-Silva, et al. Angiotensin-(1-7) through receptor Mas mediates endothelial nitric oxide synthase activation via Akt-dependent pathways. Hypertension 2007; 49**:** 185-92.

Santilli, F., F. Cipollone, A. Mezzetti, et al. The role of nitric oxide in the development of diabetic angiopathy. Horm Metab Res 2004; 36**:** 319-35.

Santos, E. L., R. I. Reis, R. G. Silva, et al. Functional rescue of a defective angiotensin II AT1 receptor mutant by the Mas protooncogene. Regul Pept 2007; 141**:** 159-67.

Santos, R. A. and M. J. Campagnole-Santos. Central and peripheral actions of angiotensin-(1-7). Braz J Med Biol Res 1994; 27**:** 1033-47.

Santos, R. A., C. H. Castro, E. Gava, et al. Impairment of in vitro and in vivo heart function in angiotensin-(1-7) receptor MAS knockout mice. Hypertension 2006; 47**:** 996-1002.

Santos, R. A., A. J. Ferreira, A. P. Nadu, et al. Expression of an angiotensin-(1-7)-producing fusion protein produces cardioprotective effects in rats. Physiol Genomics 2004; 17**:** 292-9.

Santos, R. A., A. C. Simoes e Silva, C. Maric, et al. Angiotensin-(1-7) is an endogenous ligand for the G protein-coupled receptor Mas. Proc Natl Acad Sci U S A 2003; 100**:** 8258-63.

Sanvitto, G. L., O. Johren, W. Hauser, et al. Water deprivation upregulates ANG II AT1 binding and mRNA in rat subfornical organ and anterior pituitary. Am J Physiol 1997; 273**:** E156-63.

Sasaki, K., Y. Yamano, S. Bardhan, et al. Cloning and expression of a complementary DNA encoding a bovine adrenal angiotensin II type-1 receptor. Nature 1991; 351**:** 230-3.

Sato, S., N. Fujita and T. Tsuruo. Modulation of Akt kinase activity by binding to Hsp90. Proc Natl Acad Sci U S A 2000; 97**:** 10832-7.

Sausville, E., D. Carney and J. Battey. The human vasopressin gene is linked to the oxytocin gene and is selectively expressed in a cultured lung cancer cell line. J Biol Chem 1985; 260**:** 10236-41.

Sawchenko, P. E. Adrenalectomy-induced enhancement of CRF and vasopressin immunoreactivity in parvocellular neurosecretory neurons: anatomic, peptide, and steroid specificity. J Neurosci 1987; 7**:** 1093-106.

Schelling, P., J. S. Hutchinson, U. Ganten, et al. Impermeability of the blood-cerebrospinal fluid barrier for angiotensin II in rats. Clin Sci Mol Med Suppl 1976; 3**:** 399s-402s.

Schiavone, M. T., R. A. Santos, K. B. Brosnihan, et al. Release of vasopressin from the rat hypothalamo-neurohypophysial system by angiotensin-(1-7) heptapeptide. Proc Natl Acad Sci U S A 1988; 85**:** 4095-8.

Schinke, M., O. Baltatu, M. Bohm, et al. Blood pressure reduction and diabetes insipidus in transgenic rats deficient in brain angiotensinogen. Proc Natl Acad Sci U S A 1999; 96**:** 3975-80.

Schmale, H., S. Heinsohn and D. Richter. Structural organization of the rat gene for the arginine vasopressin-neurophysin precursor. Embo J 1983; 2**:** 763-7.

Schnackenberg, C. G., W. J. Welch and C. S. Wilcox. Normalization of blood pressure and renal vascular resistance in SHR with a membrane-permeable superoxide dismutase mimetic: role of nitric oxide. Hypertension 1998; 32**:** 59-64.

7. Literature

Schrader, M. and H. D. Fahimi. Peroxisomes and oxidative stress. Biochim Biophys Acta 2006; 1763**:** 1755-66.

Schrier, R. W. and D. G. Bichet. Osmotic and nonosmotic control of vasopressin release and the pathogenesis of impaired water excretion in adrenal, thyroid, and edematous disorders. J Lab Clin Med 1981; 98**:** 1-15.

Schweifer, N., P. J. Valk, R. Delwel, et al. Characterization of the C3 YAC contig from proximal mouse chromosome 17 and analysis of allelic expression of genes flanking the imprinted Igf2r gene. Genomics 1997; 43**:** 285-97.

Shan, Z. Z., S. M. Dai and D. F. Su. Relationship between baroreceptor reflex function and end-organ damage in spontaneously hypertensive rats. Am J Physiol 1999; 277**:** H1200-6.

Shaul, P. W., E. J. Smart, L. J. Robinson, et al. Acylation targets emdothelial nitric-oxide synthase to plasmalemmal caveolae. J Biol Chem 1996; 271**:** 6518-22.

Shiojima, I. and K. Walsh. Role of Akt signaling in vascular homeostasis and angiogenesis. Circ Res 2002; 90**:** 1243-50.

Shiojima, I., M. Yefremashvili, Z. Luo, et al. Akt signaling mediates postnatal heart growth in response to insulin and nutritional status. J Biol Chem 2002; 277**:** 37670-7.

Silva-Barcellos, N. M., S. Caligiorne, R. A. dos Santos, et al. Site-specific microinjection of liposomes into the brain for local infusion of a short-lived peptide. J Control Release 2004; 95**:** 301-7.

Silva-Barcellos, N. M., F. Frezard, S. Caligiorne, et al. Long-lasting cardiovascular effects of liposome-entrapped angiotensin-(1-7) at the rostral ventrolateral medulla. Hypertension 2001; 38**:** 1266-71.

Simard, J., M. L. Ricketts, S. Gingras, et al. Molecular biology of the 3beta-hydroxysteroid dehydrogenase/delta5-delta4 isomerase gene family. Endocr Rev 2005; 26**:** 525-82.

Sinnhuber, R. O., T. C. Yu and T. C. Yu. Citation Classic - Characterization of the Red Pigment Formed in the 2-Thiobarbituric Acid Determination of Oxidative Rancidity. Current Contents/Agriculture Biology & Environmental Sciences 1983; 16-.

Siraki, A. G., J. Pourahmad, T. S. Chan, et al. Endogenous and endobiotic induced reactive oxygen species formation by isolated hepatocytes. Free Radic Biol Med 2002; 32**:** 2-10.

Somers, M. J., K. Mavromatis, Z. S. Galis, et al. Vascular superoxide production and vasomotor function in hypertension induced by deoxycorticosterone acetate-salt. Circulation 2000; 101**:** 1722-8.

Sorescu, D., D. Weiss, B. Lassegue, et al. Superoxide production and expression of nox family proteins in human atherosclerosis. Circulation 2002; 105**:** 1429-35.

Soubrier, F., L. Wei, C. Hubert, et al. Molecular biology of the angiotensin I converting enzyme: II. Structure-function. Gene polymorphism and clinical implications. J Hypertens 1993; 11**:** 599-604.

Su, Z., J. Zimpelmann and K. D. Burns. Angiotensin-(1-7) inhibits angiotensin II-stimulated phosphorylation of MAP kinases in proximal tubular cells. Kidney Int 2006; 69**:** 2212-8.

Surdacki, A., M. Nowicki, J. Sandmann, et al. Reduced urinary excretion of nitric oxide metabolites and increased plasma levels of asymmetric dimethylarginine in men with essential hypertension. J Cardiovasc Pharmacol 1999; 33**:** 652-8.

Suto, T., G. Losonczy, C. Qiu, et al. Acute changes in urinary excretion of nitrite + nitrate do not necessarily predict renal vascular NO production. Kidney Int 1995; 48**:** 1272-7.

Suttorp, N., W. Toepfer and L. Roka. Antioxidant defense mechanisms of endothelial cells: glutathione redox cycle versus catalase. Am J Physiol 1986; 251**:** C671-80.

Suvorava, T., N. Lauer, S. Kumpf, et al. Endogenous vascular hydrogen peroxide regulates arteriolar tension in vivo. Circulation 2005; 112**:** 2487-95.

Taddei, S., A. Virdis, P. Mattei, et al. Vasodilation to acetylcholine in primary and secondary forms of human hypertension. Hypertension 1993; 21**:** 929-33.

7. Literature

Tallant, E. A., C. M. Ferrario and P. E. Gallagher. Angiotensin-(1-7) inhibits growth of cardiac myocytes through activation of the mas receptor. Am J Physiol Heart Circ Physiol 2005; 289**:** H1560-6.

Taniyama, Y. and K. K. Griendling. Reactive oxygen species in the vasculature: molecular and cellular mechanisms. Hypertension 2003; 42**:** 1075-81.

Tom, B., A. Dendorfer and A. H. Danser. Bradykinin, angiotensin-(1-7), and ACE inhibitors: how do they interact? Int J Biochem Cell Biol 2003; 35**:** 792-801.

Touyz, R. M., X. Chen, F. Tabet, et al. Expression of a functionally active gp91phox-containing neutrophil-type NAD(P)H oxidase in smooth muscle cells from human resistance arteries: regulation by angiotensin II. Circ Res 2002; 90**:** 1205-13.

Touyz, R. M., F. Tabet and E. L. Schiffrin. Redox-dependent signalling by angiotensin II and vascular remodelling in hypertension. Clin Exp Pharmacol Physiol 2003; 30**:** 860-6.

Tsutsumi, K. and J. M. Saavedra. Characterization and development of angiotensin II receptor subtypes (AT1 and AT2) in rat brain. Am J Physiol 1991; 261**:** R209-16.

Turner, A. J., S. R. Tipnis, J. L. Guy, et al. ACEH/ACE2 is a novel mammalian metallocarboxypeptidase and a homologue of angiotensin-converting enzyme insensitive to ACE inhibitors. Can J Physiol Pharmacol 2002; 80**:** 346-53.

Uddin, M., H. Yang, M. Shi, et al. Elevation of oxidative stress in the aorta of genetically hypertensive mice. Mech Ageing Dev 2003; 124**:** 811-7.

van 't Veer, L. J., L. A. van den Berg-Bakker, R. P. Hermens, et al. High frequency of mas oncogene activation detected in the NIH3T3 tumorigenicity assay. Oncogene Res 1988; 3**:** 247-54.

van Kats, J. P., D. Methot, P. Paradis, et al. Use of a biological peptide pump to study chronic peptide hormone action in transgenic mice. Direct and indirect effects of angiotensin II on the heart. J Biol Chem 2001; 276**:** 44012-7.

Vandesande, F., K. Dierickx and J. DeMey. Identification of the vasopressin-neurophysin II and the oxytocin-neurophysin I producing neurons in the bovine hypothalamus. Cell Tissue Res 1975; 156**:** 189-200.

Vauquelin, G., Y. Michotte, I. Smolders, et al. Cellular targets for angiotensin II fragments: pharmacological and molecular evidence. J Renin Angiotensin Aldosterone Syst 2002; 3**:** 195-204.

Venema, V. J., R. Zou, H. Ju, et al. Caveolin-1 detergent solubility and association with endothelial nitric oxide synthase is modulated by tyrosine phosphorylation. Biochem Biophys Res Commun 1997; 236**:** 155-61.

Vickers, C., P. Hales, V. Kaushik, et al. Hydrolysis of biological peptides by human angiotensin-converting enzyme-related carboxypeptidase. J Biol Chem 2002; 277**:** 14838-43.

Viinikka, L. Nitric oxide as a challenge for the clinical chemistry laboratory. Scand J Clin Lab Invest 1996; 56**:** 577-81.

Villar, A. J. and R. A. Pedersen. Parental imprinting of the Mas protooncogene in mouse. Nat Genet 1994; 8**:** 373-9.

Von Bohlen und Halbach, O., T. Walther, M. Bader, et al. Interaction between Mas and the angiotensin AT1 receptor in the amygdala. J Neurophysiol 2000; 83**:** 2012-21.

Waller, S., K. M. Fairhall, J. Xu, et al. Neurohypophyseal and fluid homeostasis in transgenic rats expressing a tagged rat vasopressin prepropeptide in hypothalamic neurons. Endocrinology 1996; 137**:** 5068-77.

Walther, T., D. Balschun, J. P. Voigt, et al. Sustained long term potentiation and anxiety in mice lacking the Mas protooncogene. J Biol Chem 1998; 273**:** 11867-73.

Walther, T., N. Wessel, N. Kang, et al. Altered heart rate and blood pressure variability in mice lacking the Mas protooncogene. Braz J Med Biol Res 2000; 33**:** 1-9.

7. Literature

Wang, H., B. S. Huang, D. Ganten, et al. Prevention of sympathetic and cardiac dysfunction after myocardial infarction in transgenic rats deficient in brain angiotensinogen. Circ Res 2004; 94**:** 843.

Wang, H. D., S. Xu, D. G. Johns, et al. Role of NADPH oxidase in the vascular hypertrophic and oxidative stress response to angiotensin II in mice. Circ Res 2001; 88**:** 947-53.

Wedgwood, S. and S. M. Black. Endothelin-1 decreases endothelial NOS expression and activity through ETA receptor-mediated generation of hydrogen peroxide. Am J Physiol Lung Cell Mol Physiol 2005; 288**:** L480-7.

WHO, World Health Organization--International Society of Hypertension Guidelines for the Management of Hypertension. Guidelines Sub-Committee. Blood Press Suppl 1999; 1**:** 9-43.

Wodicka, L., H. Dong, M. Mittmann, et al. Genome-wide expression monitoring in Saccharomyces cerevisiae. Nat Biotechnol 1997; 15**:** 1359-67.

Wolf, G., U. Haberstroh and E. G. Neilson. Angiotensin II stimulates the proliferation and biosynthesis of type I collagen in cultured murine mesangial cells. Am J Pathol 1992; 140**:** 95-107.

Wolin, M. S. Interactions of oxidants with vascular signaling systems. Arterioscler Thromb Vasc Biol 2000; 20**:** 1430-42.

Wright, J. W. and J. W. Harding. Important role for angiotensin III and IV in the brain renin-angiotensin system. Brain Res Brain Res Rev 1997; 25**:** 96-124.

Wu, K. K. Regulation of endothelial nitric oxide synthase activity and gene expression. Ann N Y Acad Sci 2002; 962**:** 122-30.

Wu, L., M. Iwai, H. Nakagami, et al. Effect of angiotensin II type 1 receptor blockade on cardiac remodeling in angiotensin II type 2 receptor null mice. Arterioscler Thromb Vasc Biol 2002; 22**:** 49-54.

Xu, H., G. D. Fink and J. J. Galligan. Tempol lowers blood pressure and sympathetic nerve activity but not vascular O2- in DOCA-salt rats. Hypertension 2004; 43**:** 329-34.

Xu, X., A. B. Quiambao, L. Roveri, et al. Degeneration of cone photoreceptors induced by expression of the Mas1 protooncogene. Exp Neurol 2000; 163**:** 207-19.

Yagil, Y. and C. Yagil. Hypothesis: ACE2 modulates blood pressure in the mammalian organism. Hypertension 2003; 41**:** 871-3.

Yang, Z. and X. F. Ming. Recent advances in understanding endothelial dysfunction in atherosclerosis. Clin Med Res 2006; 4**:** 53-65.

Young, D., K. O'Neill, T. Jessell, et al. Characterization of the rat mas oncogene and its high-level expression in the hippocampus and cerebral cortex of rat brain. Proc Natl Acad Sci U S A 1988; 85**:** 5339-42.

Young, D., G. Waitches, C. Birchmeier, et al. Isolation and characterization of a new cellular oncogene encoding a protein with multiple potential transmembrane domains. Cell 1986; 45**:** 711-9.

Zeng, Q., D. A. Carter and D. Murphy. Cell specific expression of a vasopressin transgene in rats. J Neuroendocrinol 1994; 6**:** 469-77.

Zeng, Q., N. C. Foo, J. M. Funkhouser, et al. Expression of a rat vasopressin transgene in rat testes. J Reprod Fertil 1994; 102**:** 471-81.

Zhou, H. M., G. Weskamp, V. Chesneau, et al. Essential role for ADAM19 in cardiovascular morphogenesis. Mol Cell Biol 2004; 24**:** 96-104.

Zile, M. R., C. F. Baicu and W. H. Gaasch. Diastolic heart failure--abnormalities in active relaxation and passive stiffness of the left ventricle. N Engl J Med 2004; 350**:** 1953-9.

Zingg, H. H., D. Lefebvre and G. Almazan. Regulation of vasopressin gene expression in rat hypothalamic neurons. Response to osmotic stimulation. J Biol Chem 1986; 261**:** 12956-9.

Zohn, I. E., M. Symons, M. Chrzanowska-Wodnicka, et al. Mas oncogene signaling and transformation require the small GTP-binding protein Rac. Mol Cell Biol 1998; 18**:** 1225-35.

8. Curriculum Vitae

8. Curriculum Vitae

9. Acknowledgments

In the years I have studied at the MDC, I have not only learned a lot of things, but I also received a lot of help from people. I spent an excellent time here, wherever and whenever I will remember everything and everyone forever!

Firstly and foremost I am rather grateful to my advisor, Dr. Michael Bader, who has given me the opportunity and provided me the financial support to perform my Ph.D. study in his lab. His wise supervision helped greatly to keep me in high motivation and to guarantee the best outcome from me and my projects. His knowledge, kindness, patience, open-mindedness, and vision pictured the best boss I have met. For his guidance, encouragement, inspiration as well as fair criticisms throughout my graduate study and his critical reading of my thesis and thoughtful comments provided me with lifetime benefits.

I would like to express my sincere gratitude to Dr. Thomas Walther for his acceptance me coming to Berlin in 2003. His positive attitude, hard working and enthusiasm for science influenced me a lot. During the first year in Berlin, I got great help from professor Sterner-Kock and her technicians from the animal clinic.

I would also like to gratefully acknowledge the support of Dr. Natalia Alenina who is the person that I could always count on to discuss the details of the projects, get the technical advice and methodological help from her anytime, that was very essential during my first year at the MDC. Especially, she corrected my thesis with great patience. From her thoughtfulness and consistency I could learn the qualities of a good scientist.

I would like to thank Prof. Mihail Todiras for his perfect skilled hands as well as excellent experience in physiology calculating and interpreting of the blood pressure data in conscious mice and rats. I highly appreciated his diligent work attitude and trustable data.

I would like to thank Prof. Robson Santos, who provided me with the valuable chance to go to Brazil. He and his team supported me with fruitful collaboration, direction and pleasant atmosphere, no matter work or life. I will never forget, Walkyria O. Sampaio, Beth, Sérgio Santos, Bealtrix Fauler, especially Luiza A. Rabelo, for their considerable support and sincere friendship.

9. Acknowledgments

I acknowledge Dr. Elena Popova´s help during my first step in the generation of transgenic mice. My special thanks to Dr. Fatimunnisa Qadri, an expert for immunohistological work. She has wealthy experience on that and I gained a lot of help for my doctoral studies. I am very grateful to all other colleagues of Dr. Michael Bader's lab for their kindness, and friendly assistance. Special thanks also go to Dr. Katja Tenner, Dr. Gabin Sihn, Dr. Jens Buttgereit, who were always available when I needed their help and advice. I spent a nice time with all other colleagues, Ines Schadock, Katarina Kotnik, Brit Rentzsch, Santosh Ghadge, Alexander Krivokharchenko, Larisa Vilianovich, Tanja Shmidt, Irina Lapidus, Aline Hilzendeger, Markus May, Michael Ridders, I cherish the time we had worked together.

I will never forget Lieselotte Winkler´s help, no matter lab work or life problems, her concern of my study and work through all these years and constant encouragement was highly regarded. I greatly appreciate Ms. Monika Nitz and Adelheid Böttger, Petra Rohrmoser, Andrea Mueller, Susanne Wollenzin, Tanja Schalow, and Vera Saul for their excellent technical support in molecular biology experiments performed in this work, as well as Sabine Grueger, in assisting in the animals´ management, surgical help, and motivating me to learn German. Her lively enthusiasm and helpful advices concerning mouse nature were very helpful for my work. I also extend my thanks to Mrs Dahlke, Mrs, Bergemann, Mrs Strauss, Reika Langanhi, Cathrin Rudolph, for maintaining the rat lines and their kindness with me all the time.

Dr. Wallukat and his group, thank you for sharing the same lab always having access to your equipment, and Ms. Karczewski for all the time kind greetings and helping me with all my demand.

Thanks to Dr. Seyfried and his group, I freely used his modern microscope. Whenever I met problems, I always got the help from his group members Stefan, David, Elena, Nicole, Jana.

I would like to express my sincere gratitude to Dana Lafuente, the administrative assistant of Prof. Bader's group for her great help to resolve many of my problems in the lab and life. After her, Iris Apostel-Krause continued her sincere concern about my work and life problems. Without them, I could not have solved the troubles easily and concentrated on the work.

I am deeply grateful to MDC computer service people, Ute Berndt, Dennis Siuchninski, Andreas Mathan. Without them I cannot have managed my laptop and saved my data correctly. Also the MDC user email system is very helpful for us to exchange information effectively.

9. Acknowledgments

There are numerous other people in MDC who assisted me in the course of this project.
I am also very grateful to Mrs Sylvia Sibilak and Mrs Sonja Laboda for their help in dealing with public affairs.

I am very grateful to all my Chinese friends, Wang yong, Wang jizheng, Cheng xiangdong, Liang zhong, Sun pengming, Zhang junjie, Xiang li xin, Huang wei, Xie cuimei, Hu xiaomin, Chen chen, Fu qin, Wang chengcheng, Sha xiaojin, Li li, Shi yu, Gong maolian, Sun xiaoou, Gan miao, Li langping, Zhang jingjing, who have been working in Berlin for their kind help and friendship. We shared our joy and sorrow. It is valuable to get their friendship.

I owe my sincerest gratitude to my parents and sisters for their care, love, and support. I am sorry for being far away from them.
Finally, it was a great opportunity to work in Germany. I have had a valuable time and experience that I will never forget.

10. Abbreviations

AA	**arachidonic acid**
ACE	**angiotensin converting enzyme**
ACEI	**angiotensin converting enzyme inhibitors**
ACh	**acetylcholine**
ADAM	**disintegrin and metalloproteinases**
ADMA	**asymmetric dimethylarginine**
AOGEN	**angiotensinogen**
Ang I	**angiotensin I**
Ang II	**angiotensin II**
APS	**ammonium persulfate**
ATP	**adenosine triphosphate**
BH4	**tetrahydrobiopterin**
BK	**bradykinin**
BNP	**brain natriuretic peptide**
Bp	**base pair**
BPV	**blood pressure variability**
BSA	**bovine serum albumine**
cDNA	**complementary DNA**
CNS	**central nervous system**
Col6a3	**procollagen, type VI, alpha 3**
COX	**cycloxygenase**
Cox-2	**cyclooxygenase-2**
Cpxm2	**carboxypeptidase X 2**
Cyt C	**cytochrome C**
DAN	**2,3-diaminonaphthalene**
DEPC	**diethylpyrocarbonate**
DNA	**deoxyribonucleic acid**
DTT	**dithiothreitol**
cGMP	**cyclic GMP**
EB	**ethidium bromid**
EDHF	**endothelium-derived hyperpolarizing factor**
EDTA	**ethylendiaminetetraacetic acid**

10. Abbreviations

ET-1	**endothelin-1**
GC	**guanylate cyclase**
Gfer	**growth factor erv1 (Saccharomyces cerevisiae)-like**
GPCR	**G protein–coupled receptor**
Gpx1	**glutathione peroxidase**
HEPES	**N-2-hydroxyethylpiperazine-N`-2-ethanesulfonic acid**
HETEs	**hydroxyeicosatetraenoic acids**
HPETEs	**hydroperoxyeicosatetranoicacids**
H_2O_2	**hydrogen peroxide**
HRV	**heart rate variability**
IPTG	**isopropyl-beta-D-thiogalactopyranoside**
L-NAME	**N(omega)-L-arginine methyl ester**
LO	**lipoxygenase**
LVH	**left ventricle hypertrophy**
LTP	**long term potentiation**
PI3-K	**phosphoinositide 3-kinase**
PGH_2	**prostaglandin H2**
PGI_2	**prostacyclin**
M	**mol/l**
MDA	**malondialdehyde**
mRNA	**messenger RNA**
NMMA	**NG-monomethyl-L-arginine**
NO	**nitric oxide**
NO_2	**nitrites**
NO_3	**nitrates**
NOS	**nitric oxide synthase**
NEP	**neutral endopeptidase**
$O^{2.-}$	**superoxide anions**
·OH	**hydroxyl radical**
PAGE	**polyacrylamide gel electrophoresis**
PBS	**phosphate buffered saline**
PCR	**polymerase chain reaction**
P-EP	**prolyl-endopeptidase**
PGs	**prostaglandins**

10. Abbreviations

PLA	**phospholipase A**
PLC	**phospholipase C**
PUFA	**polyunsaturated fatty acid**
PVN	**paraventricular nucleus**
RAS	**renin angiotensin system**
RE	**restriction endonucleases**
Rgs2	**regulator of G-protein signalling 2**
RIA	**radioimmunoassay**
RNA	**ribonucleic acid**
RNase	**ribonuclease**
ROS	**reactive oxygen species**
RPA	**ribonuclease protection assay**
RT-PCR	**reverse transcription-polymerase chain reaction**
RVLM	**rostral ventral lateral medulla**
SDS	**sodium dodecyl sulfate**
SFO	**subfornical organ**
SMC	**smooth muscle cell**
SNP	**sodium nitroprusside**
SOD	**superoxide dismutase**
StAR	**steroidogenic acute regulatory protein**
TAE	**Tris acetate**
TBA	**thiobarbituric acid**
TBARS	**thiobarbituric acid reactive substances**
TdT	**terminal deoxynucleotidyl transferase**
TEMED	**N,N,N',N'-tetramethylethylenediamine**
Tempol	**4-hydroxy 2,2,6,6,-tetramethyl piperidine 1-oxyl**
Tris	**2-amino-2-(hydroxymethyl)-1,3-propanediol**
TUNEL	**terminal deoxynucleotidyl transferase dUTP nick end labelling**
UV	**ultraviolet light**
VSMC	**vascular smooth muscle cell**
WT	**wild type**
X-Gal	**5-bromo-4-chloro-3-indolyl-ß-D-galactoside**
3ß-HSD	**3ß-Hydroxysteroid-dehydrogenases**
8-oxo-dG	**8-oxo-7,8-dihydro-2′-deoxyguanosine**

11. Appendix

Table 1. Genes of which the expresssion are upregulated in hearts of Bl/6 *Mas* mice, p<0.05

ID –Affymetrix identification number of the EST, KO/WT - fold change *Mas*-knockout mice compare to WT, t-test, statistic comparison between *Mas*-knockout mice and WT, Gene symbol - abbreviation of gene. The red colored rows were genes which were interesting and tested further.

ID	KO/WT	t-test	Gene Symbol
97484_at	**1,07**	**0,0419**	Zmynd11
99651_at	**1,09**	**0,0184**	2610209M04Rik
96268_at	**1,11**	**0,0106**	Suclg1
92629_f_at	**1,12**	**0,0322**	Hdgf
93752_at	**1,13**	**0,0429**	Iars
160558_at	**1,13**	**0,0488**	Akt2
100568_at	**1,14**	**0,0355**	Abce1
103371_at	**1,14**	**0,0109**	Slc39a7
102215_at	**1,14**	**0,0126**	Cdv1
98065_at	**1,15**	**0,0366**	Ormdl3
93982_at	**1,15**	**0,0047**	Derl1
99078_at	**1,16**	**0,0222**	1110033C18Rik
160198_at	**1,16**	**0,0145**	---
97559_at	**1,18**	**0,0360**	Eef2
97550_at	**1,18**	**0,0422**	Hdac7a
97880_at	**1,18**	**0,0376**	Dlst
97807_at	**1,19**	**0,0371**	1110021H02Rik
99666_at	**1,20**	**0,0383**	Cs
101837_g_at	**1,20**	**0,0411**	Ppm1b
97859_at	**1,21**	**0,0337**	Inpp5a
94453_at	**1,21**	**0,0361**	1810046J19Rik
98595_at	**1,22**	**0,0047**	Irak1
98610_at	**1,22**	**0,0170**	Mrps28
103435_at	**1,22**	**0,0121**	9430080K19Rik
95690_at	**1,22**	**0,0294**	1110030L07Rik
96754_s_at	**1,23**	**0,0107**	---
98490_at	**1,23**	**0,0146**	Arl10c
100977_at	**1,23**	**0,0405**	Pdk1
93826_at	**1,23**	**0,0492**	Ppp2r5a
93917_at	**1,24**	**0,0300**	Tnfsf12
92401_at	**1,25**	**0,0388**	Ltc4s
99544_at	**1,25**	**0,0221**	Dguok

97301_at	**1,26**	**0,0156**	Rab14
95666_at	**1,26**	**0,0312**	Cops8
162125_f_at	**1,26**	**0,0288**	Ubc
160162_at	**1,26**	**0,0128**	Tagln2
160965_at	**1,27**	**0,0359**	Rasa4
101542_f_at	**1,27**	**0,0397**	Fin14
97751_f_at	**1,27**	**0,0315**	---
96716_at	**1,27**	**0,0083**	1110003E01Rik
96789_i_at	**1,27**	**0,0358**	Galm
160920_at	**1,27**	**0,0123**	Bcl2l2
93083_at	**1,27**	**0,0062**	Anxa5
160493_at	**1,28**	**0,0381**	Cd63
98452_at	**1,28**	**0,0248**	Flt1
161859_f_at	**1,28**	**0,0507**	Sncg
98434_at	**1,28**	**0,0502**	Arhgef7
97279_at	**1,28**	**0,0188**	Hibadh
97985_f_at	**1,29**	**0,0319**	Kns2
94060_at	**1,29**	**0,0323**	Kctd10
160607_at	**1,29**	**0,0503**	Pard3
93667_at	**1,29**	**0,0232**	Fbxw7
95406_at	**1,30**	**0,0167**	1810037I17Rik
100633_at	**1,30**	**0,0498**	2810484M10Rik
101078_at	**1,30**	**0,0204**	Bsg
160385_at	**1,30**	**0,0096**	5730591C18Rik
160961_at	**1,31**	**0,0180**	Sipa1l2
160520_at	**1,31**	**0,0295**	Yap1
93349_at	**1,31**	**0,0135**	Pcolce
96061_at	**1,32**	**0,0022**	Usp14
98410_at	**1,32**	**0,0155**	AI481100
100927_at	**1,32**	**0,0355**	Pltp
96746_at	**1,32**	**0,0229**	Dlat
101843_at	**1,32**	**0,0341**	Sh2bpsm1
94899_at	**1,32**	**0,0401**	AA536749
99154_s_at	**1,33**	**0,0041**	1810020D17Rik
100514_at	**1,33**	**0,0246**	Gna13
95759_at	**1,34**	**0,0100**	2900092E17Rik
97984_i_at	**1,34**	**0,0282**	Kns2
97447_at	**1,35**	**0,0332**	Map1lc3a
103783_at	**1,35**	**0,0026**	Xpr1

99138_at	**1,35**	**0,0463**	Chc1
94079_at	**1,36**	**0,0452**	38231
94407_at	**1,37**	**0,0127**	B3gat3
160167_at	**1,37**	**0,0445**	Nup62
97383_at	**1,37**	**0,0379**	Slc6a6
92824_at	**1,37**	**0,0208**	Nme6
162501_at	**1,37**	**0,0503**	---
94072_g_at	**1,37**	**0,0374**	Gosr2
100928_at	**1,37**	**0,0249**	Fbln2
102322_at	**1,38**	**0,0070**	Ugdh
103994_at	**1,38**	**0,0292**	Eif2c2
103397_at	**1,38**	**0,0235**	Hrb
92828_at	**1,38**	**0,0497**	Dpm1
161025_f_at	**1,38**	**0,0065**	---
160835_i_at	**1,39**	**0,0363**	1110007C09Rik
161006_at	**1,40**	**0,0008**	---
94275_at	**1,40**	**0,0096**	Urod
160726_at	**1,41**	**0,0264**	Qk
93581_at	**1,41**	**0,0231**	Ndufb8
94817_at	**1,41**	**0,000009**	Serpinh1
160195_at	**1,41**	**0,0113**	1200013P24Rik
94981_i_at	**1,43**	**0,0199**	Nme3
160516_at	**1,43**	**0,0475**	Gaa
93215_at	**1,44**	**0,0159**	Tnfaip1
160188_at	**1,45**	**0,0306**	Nudt4
96180_at	**1,45**	**0,0469**	---
97888_at	**1,45**	**0,0434**	Frag1
97770_s_at	**1,45**	**0,0199**	D6Wsu176e
98787_at	**1,45**	**0,0117**	Kcnj11
96292_r_at	**1,45**	**0,0011**	BC059730
93120_f_at	**1,47**	**0,0200**	H2-D1
94057_g_at	**1,47**	**0,0078**	Scd1
99067_at	**1,48**	**0,0186**	Gas6
94912_at	**1,48**	**0,0299**	Mrps21
93866_s_at	**1,48**	**0,0282**	Mglap
99378_f_at	**1,49**	**0,0436**	---
94450_at	**1,49**	**0,0188**	Nsun2
100297_at	**1,49**	**0,0052**	Wdr26
100925_at	**1,50**	**0,0245**	2700089E24Rik

103015_at	**1,50**	**0,0386**	Bcl6
96708_at	**1,50**	**0,0068**	1200002G13Rik
92309_i_at	**1,51**	**0,0080**	Ptprm
160326_at	**1,51**	**0,0386**	Cdv3
93281_at	**1,53**	**0,0070**	Rcn2
97434_at	**1,54**	**0,0088**	2810405F18Rik
160189_at	**1,54**	**0,0213**	Nudt4
99322_at	**1,54**	**0,0328**	Kcnq1
161826_r_at	**1,55**	**0,0234**	Glul
98911_at	**1,55**	**0,0209**	Jak1
94004_at	**1,55**	**0,0463**	Cnn2
101918_at	**1,56**	**0,0152**	Tgfb1
97111_at	**1,56**	**0,0170**	Als2cr3
96764_at	**1,57**	**0,0426**	AW111922
101946_at	**1,57**	**0,0054**	Lypla1
104408_s_at	**1,57**	**0,0334**	Sox18
98004_at	**1,58**	**0,0156**	Pkia
94384_at	**1,59**	**0,0139**	Ier3
96056_at	**1,59**	**0,0157**	Rhoc
101876_s_at	**1,60**	**0,0052**	H2-T10 /// H2-T22 /// H2-T17 /// H2-T9
101681_f_at	**1,61**	**0,0018**	H2-Bl
104282_at	**1,61**	**0,0256**	AW112037
97426_at	**1,61**	**0,0301**	Emp1
160947_at	**1,62**	**0,0158**	E030006K04Rik
100064_f_at	**1,62**	**0,0311**	Gja1
101057_at	**1,62**	**0,0289**	A430005L14Rik
92310_at	**1,62**	**0,0212**	Plk2
95102_at	**1,63**	**0,0012**	Scotin
97490_at	**1,64**	**0,0080**	Bcl7b
100039_at	**1,66**	**0,0424**	Tmem4
98944_at	**1,67**	**0,0481**	Sec23b
100555_at	**1,68**	**0,0170**	Dscr1
97349_at	**1,68**	**0,0068**	4930488L10Rik
98931_at	**1,70**	**0,0231**	Gns
102221_at	**1,70**	**0,0057**	Syngr1
97448_at	**1,71**	**0,0457**	9030221M09Rik /// MGC65558
98319_at	**1,73**	**0,0065**	Dsg2
101430_at	**1,73**	**0,0393**	---
100597_at	**1,76**	**0,0077**	Gyg1

102791_at	**1,77**	**0,0302**	Psmb8
100970_at	**1,78**	**0,0353**	Akt1
93155_at	**1,82**	**0,0092**	A930004K21Rik
96679_at	**1,84**	**0,0223**	Dnajb9
101753_s_at	**1,85**	**0,0370**	Lzp-s /// Lyzs
97777_at	**1,86**	**0,0134**	Nkx2-5
96778_at	**1,91**	**0,0205**	Rrs1
100112_at	**1,91**	**0,0215**	Cxcl12
97253_at	**1,94**	**0,0193**	Tpd52l2
98045_s_at	**1,95**	**0,0016**	Dab2
104184_at	**1,97**	**0,0509**	Nppb
104265_at	**1,97**	**0,0437**	Kdr
103549_at	**1,98**	**0,0072**	Nes
104597_at	**2,03**	**0,0409**	Gbp2
94379_at	**2,03**	**0,0296**	Kif1b
99937_at	**2,04**	**0,0024**	Meox2
103006_at	**2,05**	**0,0362**	Atf5
102226_at	**2,07**	**0,0240**	Cpxm2
101020_at	**2,12**	**0,0116**	Ctsc
100998_at	**2,14**	**0,0412**	H2-Ab1 /// Rmcs1
100022_at	**2,16**	**0,0008**	Cish
97541_f_at	**2,22**	**0,0269**	H2-L /// LOC56628 /// H2-D1
93268_at	**2,35**	**0,0027**	Glo1
98506_r_at	**2,39**	**0,0045**	Cpox
97319_at	**2,49**	**0,0169**	Rrad
93269_at	**2,49**	**0,0005**	Glo1
100605_at	**2,52**	**0,0118**	Tpm2
92559_at	**2,67**	**0,0034**	---
102773_at	**2,70**	**0,0191**	Car8
97918_at	**2,71**	**0,0276**	AA536743
103554_at	**2,85**	**0,0244**	Adam19
102227_g_at	**2,93**	**0,0068**	Cpxm2
161858_f_at	**4,14**	**0,0094**	Rb1

Table 2. Genes of which the expresssion are down regulated in hearts of Bl/6 *Mas* mice, p<0.05

ID –Affymetrix identification number of the EST, KO/WT - fold change *Mas*-knockout mice compare to WT, t-test, statistic comparison between *Mas*-knockout mice and WT, Gene symbol - abbreviation of gene. The red colored rows were genes which were interesting and tested further.

11. Appendix

ID	KO/WT	t-test	Gene Symbol
94297_at	**0,32**	**0,0162**	Fkbp5
102049_at	**0,34**	**0,0073**	Pdk4
96513_at	**0,39**	**0,0252**	---
103460_at	**0,43**	**0,0114**	Ddit4
101561_at	**0,44**	**0,0300**	Mt2
161356_at	**0,48**	**0,0442**	---
160359_at	**0,49**	**0,0398**	1190002H23Rik
97844_at	**0,49**	**0,0020**	Rgs2
101554_at	**0,50**	**0,0211**	Nfkbia
95658_at	**0,52**	**0,0131**	Commd1
98322_at	**0,52**	**0,0485**	Slc22a5
96119_s_at	**0,53**	**0,0132**	Angptl4
94147_at	**0,53**	**0,0053**	Serpine1
104149_at	**0,54**	**0,0324**	---
103083_at	**0,54**	**0,0004**	---
102370_at	**0,54**	**0,0003**	Dhrs8
100042_at	**0,55**	**0,0001**	Hagh
104340_at	**0,55**	**0,0400**	Mbd1
93392_at	**0,55**	**0,0137**	Ucp3
95026_at	**0,56**	**0,0044**	0610039N19Rik
94906_at	**0,56**	**0,0117**	Adh1
102426_at	**0,57**	**0,0034**	---
103829_at	**0,57**	**0,0148**	Herc2
92925_at	**0,57**	**0,0012**	Cebpb
92195_at	**0,58**	**0,0444**	Cebpg
96646_at	**0,59**	**0,0001**	Usp39
92830_s_at	**0,59**	**0,0209**	Zfp36
93486_at	**0,59**	**0,0312**	Slc27a1
93006_at	**0,59**	**0,0073**	Nfic
95664_at	**0,60**	**0,0102**	Sec14l1
103891_i_at	**0,60**	**0,0369**	Ell2
92724_at	**0,61**	**0,0413**	---
101444_at	**0,61**	**0,0186**	Gt(ROSA #22)26asSor
97171_f_at	**0,66**	**0,0306**	---
103889_at	**0,66**	**0,0005**	Tbl1xr1
93573_at	**0,66**	**0,0134**	Mt1
92821_at	**0,67**	**0,0004**	Usp2

92652_at	**0,68**	**0,0092**	Notch4
92909_at	**0,68**	**0,0371**	Pgf
93975_at	**0,71**	**0,0214**	1300002F13Rik
92996_at	**0,72**	**0,0039**	Sox17
93266_at	**0,72**	**0,0285**	Tpm3
102248_f_at	**0,72**	**0,0131**	Cask
94396_at	**0,72**	**0,0363**	Ing1
AFFX-CreX-5_st	**0,72**	**0,0394**	---
101618_r_at	**0,72**	**0,0194**	---
162415_f_at	**0,73**	**0,0480**	Cant1
94502_at	**0,73**	**0,0076**	D13Wsu50e
97374_at	**0,73**	**0,0287**	2810025M15Rik
100570_at	**0,73**	**0,0368**	6330412F12Rik
99120_f_at	**0,73**	**0,0110**	Chd4
160492_at	**0,74**	**0,0258**	Ddx18
160981_at	**0,75**	**0,0089**	---
103620_s_at	**0,75**	**0,0109**	Smn1
98029_at	**0,75**	**0,0077**	3110056O03Rik
101529_g_at	**0,76**	**0,0428**	Tcea1
102327_at	**0,76**	**0,0027**	Aoc3
99027_at	**0,76**	**0,0309**	Bcl2l1
103420_at	**0,76**	**0,0161**	Emd
95393_at	**0,76**	**0,0472**	Btbd3
160341_at	**0,76**	**0,0480**	Jtv1
103636_at	**0,77**	**0,0355**	Brp17
99866_at	**0,77**	**0,0103**	---
104756_at	**0,78**	**0,0124**	2310047M15Rik
96300_f_at	**0,79**	**0,0231**	Rps27
93277_at	**0,79**	**0,0346**	Hspd1
101573_f_at	**0,79**	**0,0151**	Rpl27a
103913_at	**0,79**	**0,0436**	Sec61a2
100345_f_at	**0,80**	**0,0167**	Vamp8
93312_at	**0,80**	**0,0206**	Ube2g1
103843_at	**0,81**	**0,0470**	Gnao1
94312_at	**0,81**	**0,0403**	AA415817
100027_s_at	**0,81**	**0,0285**	Pex14
100515_at	**0,82**	**0,0436**	Furin
94258_at	**0,82**	**0,0445**	Arhgdib
95765_at	**0,83**	**0,0422**	Adh5

97885_at	**0,83**	**0,0171**	1810009M01Rik
93295_at	**0,84**	**0,0191**	Cct5
92829_at	**0,84**	**0,0096**	Hspe1
100543_s_at	**0,85**	**0,0207**	Brd7
104189_at	**0,85**	**0,0033**	Traf6
99127_at	**0,86**	**0,0215**	Sca10
93521_at	**0,87**	**0,0339**	Srrm1
93740_at	**0,87**	**0,0389**	Nsep1
160271_at	**0,89**	**0,0108**	0610007C21Rik
96615_at	**0,89**	**0,0295**	Ypel3
104514_at	**0,93**	**0,0042**	Epn1

Table 3. Genes of which the expresssion is upregulated in testes of Bl/6 *Mas* mice, p<0.05

ID –Affymetrix identification number of the EST, KO/WT - fold change *Mas*-knockout mice compare to WT, t-test, statistic comparison between *Mas*-knockout mice and WT, Gene symbol - abbreviation of gene. The red colored rows were genes which were interesting and tested further.

ID	KO/WT	t-test	Gene
161683_r_at	**1,14**	**0,0322**	---
98571_s_at	**1,14**	**0,0455**	Naca
94078_at	**1,16**	**0,0271**	1110020P15Rik
92610_at	**1,17**	**0,0589**	Rdbp
98912_at	**1,18**	**0,0531**	D13Wsu64e
96621_at	**1,18**	**0,0240**	1110061L23Rik
102949_g_at	**1,19**	**0,0553**	Hemt1
97329_at	**1,19**	**0,0346**	C77668
103893_at	**1,20**	**0,0411**	Fbxo38
93500_at	**1,20**	**0,0514**	Alas1
97273_at	**1,20**	**0,0103**	Ars2
160861_s_at	**1,21**	**0,0381**	Pde1a
160716_at	**1,21**	**0,0500**	2410018C17Rik
95091_at	**1,21**	**0,0486**	Sec13l1
93336_at	**1,21**	**0,0473**	1110014C03Rik
162428_i_at	**1,22**	**0,0267**	S100a14
101944_at	**1,22**	**0,0455**	Lypla1
96962_at	**1,22**	**0,0347**	Rpl6
160492_at	**1,22**	**0,0059**	Ddx18
103531_f_at	**1,23**	**0,0095**	1300013B24Rik
95551_at	**1,23**	**0,0487**	1700020M16Rik

104101_at	**1,23**	**0,0534**	Slc9a8
102400_at	**1,24**	**0,0140**	LOC433702
100066_at	**1,24**	**0,0450**	Gart
95473_s_at	**1,25**	**0,0237**	C77604
96707_at	**1,25**	**0,0577**	Zipro1
99166_at	**1,25**	**0,0130**	0610012G03Rik
98524_f_at	**1,25**	**0,0006**	---
104760_at	**1,26**	**0,0479**	Ifrd2
92845_at	**1,26**	**0,0425**	Oxct1
101573_f_at	**1,27**	**0,0276**	Rpl27a
102062_at	**1,28**	**0,0127**	Smarcc1
95602_at	**1,29**	**0,0533**	Trpc4ap
162153_i_at	**1,29**	**0,0079**	Exosc5
101929_at	**1,30**	**0,0139**	6720463E02Rik
160256_at	**1,30**	**0,0111**	Tomm7
98109_at	**1,31**	**0,0485**	Mrpl55
93835_at	**1,31**	**0,0267**	Fuca1
94971_at	**1,31**	**0,0236**	Cdkn3
104168_at	**1,31**	**0,0357**	Actr2
93897_at	**1,33**	**0,0138**	Theg
95715_at	**1,34**	**0,0503**	1200009C21Rik
103735_at	**1,34**	**0,0572**	Wnt6
102796_at	**1,34**	**0,0140**	Npm3
99581_at	**1,34**	**0,0554**	Hint1
96291_f_at	**1,35**	**0,0553**	BC059730
102988_at	**1,36**	**0,0451**	Inppl1
99024_at	**1,37**	**0,0078**	Mxd4
101096_s_at	**1,37**	**0,0294**	Hs1bp1
104576_at	**1,39**	**0,0261**	Ski
94218_at	**1,39**	**0,0528**	Tcp1
96174_at	**1,40**	**0,0360**	Pom121
100769_at	**1,40**	**0,0543**	---
101947_at	**1,40**	**0,0426**	Akap8l
103330_at	**1,41**	**0,0389**	Strbp
104439_at	**1,41**	**0,0460**	Nat6
103032_at	**1,42**	**0,0476**	Tpst1
97953_g_at	**1,43**	**0,0392**	Tsc2
103663_at	**1,44**	**0,0140**	4930467B06Rik
104100_at	**1,45**	**0,0320**	2310075E07Rik

103398_at	**1,45**	**0,0434**	---
160854_at	**1,46**	**0,0034**	Map3k7
101810_at	**1,47**	**0,0211**	Fshr
160521_at	**1,48**	**0,0579**	2610020N02Rik
98831_at	**1,50**	**0,0278**	Foxj1
97989_at	**1,50**	**0,0224**	Ppp3cb
100972_s_at	**1,51**	**0,0404**	Ccl27
103387_at	**1,52**	**0,0062**	Phf1
98149_s_at	**1,52**	**0,0580**	1110033J19Rik
93850_at	**1,53**	**0,0554**	Iqgap1
96789_i_at	**1,53**	**0,0296**	Galm
98356_at	**1,53**	**0,0555**	---
101446_at	**1,53**	**0,0262**	Tpd52l1
101017_at	**1,54**	**0,0518**	Cdk4
92481_at	**1,58**	**0,0586**	Chek2
161528_r_at	**1,64**	**0,0531**	Pold1
103072_at	**1,67**	**0,0057**	Hsd3b1
95694_at	**1,68**	**0,0344**	Top1
161238_f_at	**1,72**	**0,0583**	Cct3
161348_r_at	**1,74**	**0,0550**	Pdlim1
95590_at	**1,76**	**0,0145**	Alg5
161398_at	**1,83**	**0,0092**	Dnahc8
99384_at	**1,83**	**0,0029**	Pim1
103751_at	**1,94**	**0,0512**	AA409316
95247_at	**2,06**	**0,0294**	---
93268_at	**2,09**	**0,0176**	Glo1
161004_at	**2,34**	**0,0001**	1700097N02Rik
95299_at	**2,51**	**0,0147**	Dnahc8
160269_at	**3,98**	**0,0427**	Gfer

Table. 4. Genes of which the expresssion is downregulated in testes of Bl/6 *Mas* mice, p<0.05

ID –Affymetrix identification number of the EST, KO/WT - fold change *Mas*-knockout mice compare to WT, t-test, statistic comparison between *Mas*-knockout mice and WT, Gene symbol - abbreviation of gene. The red colored rows were genes which were interesting and tested further.

ID	KO/WT	t-test	Gene
102729_f_at	**0,35**	**0,0076**	Hsd3b6
99439_at	**0,41**	**0,0125**	Mas1

104738_at	**0,45**	**0,0022**	Zrf2
92953_at	**0,47**	**0,0270**	Fmn
95730_at	**0,49**	**0,0026**	Mrps34
103761_at	**0,54**	**0,0156**	Tcfcp2l1
101834_at	**0,56**	**0,0537**	Mapk3
102996_at	**0,57**	**0,0212**	Ell
160428_at	**0,58**	**0,0419**	Suclg2
160115_at	**0,58**	**0,0458**	Txnl1
98509_at	**0,59**	**0,0223**	BC002199
102026_s_at	**0,59**	**0,0385**	Chkb
92213_at	**0,59**	**0,0052**	Star
97836_at	**0,61**	**0,0419**	Rnf7
93939_at	**0,62**	**0,0223**	Lnk
103440_at	**0,62**	**0,0363**	Gabpa
101890_f_at	**0,62**	**0,0087**	Dnajc2 /// Zrf2
103814_at	**0,62**	**0,0361**	Pex11b
95718_f_at	**0,63**	**0,0253**	Usmg5
160970_at	**0,64**	**0,0463**	Odf2
93348_at	**0,64**	**0,0378**	Timm22
94233_at	**0,65**	**0,0545**	1110038F14Rik
92915_s_at	**0,65**	**0,0209**	Hoxb8 /// Hoxb7
160921_at	**0,66**	**0,0556**	Acas2l
97199_at	**0,66**	**0,0186**	Cpne1
94049_at	**0,66**	**0,0379**	Bhmt
102028_at	**0,67**	**0,0064**	Rassf5
98493_at	**0,67**	**0,0212**	3200002M19Rik
160547_s_at	**0,68**	**0,0467**	Txnip
97943_at	**0,69**	**0,0448**	Capn6
93029_at	**0,70**	**0,0324**	Idh3g
98001_at	**0,70**	**0,0476**	Arhgef1
97991_at	**0,70**	**0,0028**	Kras2
98439_at	**0,71**	**0,0398**	Rps6kb1
100042_at	**0,71**	**0,0209**	Hagh
98428_at	**0,71**	**0,0461**	Spg4
93562_at	**0,71**	**0,0524**	Ndufb3
104527_at	**0,71**	**0,0550**	Rad51
98092_at	**0,71**	**0,0396**	Plac8
97184_at	**0,71**	**0,0199**	D15Ertd781e
99140_at	**0,72**	**0,0591**	Mrpl16

99987_at	**0,72**	**0,0274**	Zfp574
92646_at	**0,72**	**0,0209**	Mrpl23
97745_at	**0,72**	**0,0304**	Hoxa4
100457_at	**0,73**	**0,0556**	Glg1
95695_at	**0,73**	**0,0293**	Slc25a20
94047_at	**0,74**	**0,0415**	0610031J06Rik
100293_at	**0,74**	**0,0458**	Cd59b
160333_at	**0,75**	**0,0346**	1110008F13Rik
104143_at	**0,75**	**0,0519**	Copz2
94778_at	**0,76**	**0,0190**	Aldh1a7
100466_f_at	**0,77**	**0,0266**	Iqcf4
160076_at	**0,77**	**0,0590**	Mtx2
96580_at	**0,77**	**0,0544**	Pbx3
93141_at	**0,78**	**0,0212**	Nr0b1
92228_at	**0,78**	**0,0140**	Catna2
95431_at	**0,79**	**0,0224**	Tomm70a
95910_f_at	**0,79**	**0,0128**	Rbed1
96493_at	**0,79**	**0,0417**	2810002I04Rik
160292_at	**0,80**	**0,0178**	Ecgf1
93191_at	**0,80**	**0,0582**	Vamp4
101362_at	**0,80**	**0,0108**	Mapk9
96186_at	**0,81**	**0,0334**	Lrp10
95742_at	**0,81**	**0,0107**	Psmd13
98124_at	**0,81**	**0,0110**	0610011F06Rik
160569_at	**0,81**	**0,0106**	2310008M10Rik
94457_at	**0,82**	**0,0424**	AL033326
97551_at	**0,83**	**0,0095**	Hip1r
160231_at	**0,83**	**0,0594**	Farsla
99591_i_at	**0,83**	**0,0337**	Rdh11
94521_at	**0,83**	**0,0522**	Cdkn2d
101357_at	**0,84**	**0,0187**	Ap2a1
96211_at	**0,84**	**0,0412**	2310004I03Rik
94022_at	**0,87**	**0,0197**	Gltscr2
93673_at	**0,87**	**0,0427**	Nrtn
97993_at	**0,87**	**0,0559**	Uros
160293_at	**0,88**	**0,0463**	2700038L12Rik
103628_at	**0,88**	**0,0335**	Lef1

DECLARATION

December 19, 2007

Herewith I declare that the experiments described in this thesis were carried out by myself.

Erklärung

Ich versichere hiermit, dass die von mir vorgelegte Dissertation selbständig angefertigt wurde und ich die Stellen der Arbeit, die anderen Werken in Wortlaut oder Sinn nach entnommen sind, in jedem Einzelfall als Entlehnung kenntlich gemacht habe. Diese Dissertation wurde noch keiner anderen Fakultät zur Prüfung vorgelegt.

10. Abbreviations

AA	**arachidonic acid**
ACE	**angiotensin converting enzyme**
ACEI	**angiotensin converting enzyme inhibitors**
ACh	**acetylcholine**
ADAM	**disintegrin and metalloproteinases**
ADMA	**asymmetric dimethylarginine**
AOGEN	**angiotensinogen**
Ang I	**angiotensin I**
Ang II	**angiotensin II**
APS	**ammonium persulfate**
ATP	**adenosine triphosphate**
BH4	**tetrahydrobiopterin**
BK	**bradykinin**
BNP	**brain natriuretic peptide**
Bp	**base pair**
BPV	**blood pressure variability**
BSA	**bovine serum albumine**
cDNA	**complementary DNA**
CNS	**central nervous system**
Col6a3	**procollagen, type VI, alpha 3**
COX	**cycloxygenase**
Cox-2	**cyclooxygenase-2**
Cpxm2	**carboxypeptidase X 2**
Cyt C	**cytochrome C**
DAN	**2,3-diaminonaphthalene**
DEPC	**diethylpyrocarbonate**
DNA	**deoxyribonucleic acid**
DTT	**dithiothreitol**
cGMP	**cyclic GMP**
EB	**ethidium bromid**
EDHF	**endothelium-derived hyperpolarizing factor**
EDTA	**ethylendiaminetetraacetic acid**

10. Abbreviations

ET-1	**endothelin-1**
GC	**guanylate cyclase**
Gfer	**growth factor erv1 (Saccharomyces cerevisiae)-like**
GPCR	**G protein–coupled receptor**
Gpx1	**glutathione peroxidase**
HEPES	**N-2-hydroxyethylpiperazine-N`-2-ethanesulfonic acid**
HETEs	**hydroxyeicosatetraenoic acids**
HPETEs	**hydroperoxyeicosatetranoicacids**
H_2O_2	**hydrogen peroxide**
HRV	**heart rate variability**
IPTG	**isopropyl-beta-D-thiogalactopyranoside**
L-NAME	**N(omega)-L-arginine methyl ester**
LO	**lipoxygenase**
LVH	**left ventricle hypertrophy**
LTP	**long term potentiation**
PI3-K	**phosphoinositide 3-kinase**
PGH_2	**prostaglandin H2**
PGI_2	**prostacyclin**
M	**mol/l**
MDA	**malondialdehyde**
mRNA	**messenger RNA**
NMMA	**NG-monomethyl-L-arginine**
NO	**nitric oxide**
NO_2	**nitrites**
NO_3	**nitrates**
NOS	**nitric oxide synthase**
NEP	**neutral endopeptidase**
$O^{2.-}$	**superoxide anions**
·OH	**hydroxyl radical**
PAGE	**polyacrylamide gel electrophoresis**
PBS	**phosphate buffered saline**
PCR	**polymerase chain reaction**
P-EP	**prolyl-endopeptidase**
PGs	**prostaglandins**

10. Abbreviations

PLA	**phospholipase A**
PLC	**phospholipase C**
PUFA	**polyunsaturated fatty acid**
PVN	**paraventricular nucleus**
RAS	**renin angiotensin system**
RE	**restriction endonucleases**
Rgs2	**regulator of G-protein signalling 2**
RIA	**radioimmunoassay**
RNA	**ribonucleic acid**
RNase	**ribonuclease**
ROS	**reactive oxygen species**
RPA	**ribonuclease protection assay**
RT-PCR	**reverse transcription-polymerase chain reaction**
RVLM	**rostral ventral lateral medulla**
SDS	**sodium dodecyl sulfate**
SFO	**subfornical organ**
SMC	**smooth muscle cell**
SNP	**sodium nitroprusside**
SOD	**superoxide dismutase**
StAR	**steroidogenic acute regulatory protein**
TAE	**Tris acetate**
TBA	**thiobarbituric acid**
TBARS	**thiobarbituric acid reactive substances**
TdT	**terminal deoxynucleotidyl transferase**
TEMED	**N,N,N',N'-tetramethylethylenediamine**
Tempol	**4-hydroxy 2,2,6,6,-tetramethyl piperidine 1-oxyl**
Tris	**2-amino-2-(hydroxymethyl)-1,3-propanediol**
TUNEL	**terminal deoxynucleotidyl transferase dUTP nick end labelling**
UV	**ultraviolet light**
VSMC	**vascular smooth muscle cell**
WT	**wild type**
X-Gal	**5-bromo-4-chloro-3-indolyl-ß-D-galactoside**
3ß-HSD	**3ß-Hydroxysteroid-dehydrogenases**
8-oxo-dG	**8-oxo-7,8-dihydro-2′-deoxyguanosine**

11. Appendix

Table 1. Genes of which the expresssion are upregulated in hearts of Bl/6 *Mas* mice, p<0.05

ID –Affymetrix identification number of the EST, KO/WT - fold change *Mas*-knockout mice compare to WT, t-test, statistic comparison between *Mas*-knockout mice and WT, Gene symbol - abbreviation of gene. The red colored rows were genes which were interesting and tested further.

ID	KO/WT	t-test	Gene Symbol
97484_at	1,07	0,0419	Zmynd11
99651_at	1,09	0,0184	2610209M04Rik
96268_at	1,11	0,0106	Suclg1
92629_f_at	1,12	0,0322	Hdgf
93752_at	1,13	0,0429	Iars
160558_at	**1,13**	**0,0488**	**Akt2**
100568_at	1,14	0,0355	Abce1
103371_at	1,14	0,0109	Slc39a7
102215_at	1,14	0,0126	Cdv1
98065_at	1,15	0,0366	Ormdl3
93982_at	1,15	0,0047	Derl1
99078_at	1,16	0,0222	1110033C18Rik
160198_at	1,16	0,0145	---
97559_at	1,18	0,0360	Eef2
97550_at	1,18	0,0422	Hdac7a
97880_at	1,18	0,0376	Dlst
97807_at	1,19	0,0371	1110021H02Rik
99666_at	1,20	0,0383	Cs
101837_g_at	1,20	0,0411	Ppm1b
97859_at	1,21	0,0337	Inpp5a
94453_at	1,21	0,0361	1810046J19Rik
98595_at	1,22	0,0047	Irak1
98610_at	1,22	0,0170	Mrps28
103435_at	1,22	0,0121	9430080K19Rik
95690_at	1,22	0,0294	1110030L07Rik
96754_s_at	1,23	0,0107	---
98490_at	1,23	0,0146	Arl10c
100977_at	**1,23**	**0,0405**	**Pdk1**
93826_at	1,23	0,0492	Ppp2r5a
93917_at	1,24	0,0300	Tnfsf12

92401_at	1,25	0,0388	Ltc4s
99544_at	1,25	0,0221	Dguok
97301_at	1,26	0,0156	Rab14
95666_at	1,26	0,0312	Cops8
162125_f_at	1,26	0,0288	Ubc
160162_at	1,26	0,0128	Tagln2
160965_at	1,27	0,0359	Rasa4
101542_f_at	1,27	0,0397	Fin14
97751_f_at	1,27	0,0315	---
96716_at	1,27	0,0083	1110003E01Rik
96789_i_at	1,27	0,0358	Galm
160920_at	1,27	0,0123	Bcl2l2
93083_at	1,27	0,0062	Anxa5
160493_at	1,28	0,0381	Cd63
98452_at	1,28	0,0248	Flt1
161859_f_at	1,28	0,0507	Sncg
98434_at	1,28	0,0502	Arhgef7
97279_at	1,28	0,0188	Hibadh
97985_f_at	1,29	0,0319	Kns2
94060_at	1,29	0,0323	Kctd10
160607_at	1,29	0,0503	Pard3
93667_at	1,29	0,0232	Fbxw7
95406_at	1,30	0,0167	1810037I17Rik
100633_at	1,30	0,0498	2810484M10Rik
101078_at	1,30	0,0204	Bsg
160385_at	1,30	0,0096	5730591C18Rik
160961_at	1,31	0,0180	Sipa1l2
160520_at	1,31	0,0295	Yap1
93349_at	1,31	0,0135	Pcolce
96061_at	1,32	0,0022	Usp14
98410_at	1,32	0,0155	AI481100
100927_at	1,32	0,0355	Pltp
96746_at	1,32	0,0229	Dlat
101843_at	1,32	0,0341	Sh2bpsm1
94899_at	1,32	0,0401	AA536749
99154_s_at	1,33	0,0041	1810020D17Rik
100514_at	1,33	0,0246	Gna13

95759_at	1,34	0,0100	2900092E17Rik
97984_i_at	1,34	0,0282	Kns2
97447_at	1,35	0,0332	Map1lc3a
103783_at	1,35	0,0026	Xpr1
99138_at	1,35	0,0463	Chc1
94079_at	1,36	0,0452	38231
94407_at	1,37	0,0127	B3gat3
160167_at	1,37	0,0445	Nup62
97383_at	1,37	0,0379	Slc6a6
92824_at	1,37	0,0208	Nme6
162501_at	1,37	0,0503	---
94072_g_at	1,37	0,0374	Gosr2
100928_at	1,37	0,0249	Fbln2
102322_at	1,38	0,0070	Ugdh
103994_at	1,38	0,0292	Eif2c2
103397_at	1,38	0,0235	Hrb
92828_at	1,38	0,0497	Dpm1
161025_f_at	1,38	0,0065	---
160835_i_at	1,39	0,0363	1110007C09Rik
161006_at	1,40	0,0008	---
94275_at	1,40	0,0096	Urod
160726_at	1,41	0,0264	Qk
93581_at	1,41	0,0231	Ndufb8
94817_at	1,41	0,000009	Serpinh1
160195_at	1,41	0,0113	1200013P24Rik
94981_i_at	1,43	0,0199	Nme3
160516_at	1,43	0,0475	Gaa
93215_at	1,44	0,0159	Tnfaip1
160188_at	1,45	0,0306	Nudt4
96180_at	1,45	0,0469	---
97888_at	1,45	0,0434	Frag1
97770_s_at	1,45	0,0199	D6Wsu176e
98787_at	1,45	0,0117	Kcnj11
96292_r_at	1,45	0,0011	BC059730
93120_f_at	1,47	0,0200	H2-D1
94057_g_at	1,47	0,0078	Scd1
99067_at	1,48	0,0186	Gas6

94912_at	1,48	0,0299	Mrps21
93866_s_at	1,48	0,0282	Mglap
99378_f_at	1,49	0,0436	---
94450_at	1,49	0,0188	Nsun2
100297_at	1,49	0,0052	Wdr26
100925_at	1,50	0,0245	2700089E24Rik
103015_at	1,50	0,0386	Bcl6
96708_at	1,50	0,0068	1200002G13Rik
92309_i_at	1,51	0,0080	Ptprm
160326_at	1,51	0,0386	Cdv3
93281_at	1,53	0,0070	Rcn2
97434_at	1,54	0,0088	2810405F18Rik
160189_at	1,54	0,0213	Nudt4
99322_at	1,54	0,0328	Kcnq1
161826_r_at	1,55	0,0234	Glul
98911_at	1,55	0,0209	Jak1
94004_at	1,55	0,0463	Cnn2
101918_at	**1,56**	**0,0152**	**Tgfb1**
97111_at	1,56	0,0170	Als2cr3
96764_at	1,57	0,0426	AW111922
101946_at	1,57	0,0054	Lypla1
104408_s_at	1,57	0,0334	Sox18
98004_at	1,58	0,0156	Pkia
94384_at	1,59	0,0139	Ier3
96056_at	1,59	0,0157	Rhoc
101876_s_at	1,60	0,0052	H2-T10 /// H2-T22 /// H2-T17 /// H2-T9
101681_f_at	1,61	0,0018	H2-Bl
104282_at	1,61	0,0256	AW112037
97426_at	1,61	0,0301	Emp1
160947_at	1,62	0,0158	E030006K04Rik
100064_f_at	1,62	0,0311	Gja1
101057_at	1,62	0,0289	A430005L14Rik
92310_at	1,62	0,0212	Plk2
95102_at	1,63	0,0012	Scotin
97490_at	1,64	0,0080	Bcl7b
100039_at	1,66	0,0424	Tmem4
98944_at	1,67	0,0481	Sec23b

100555_at	1,68	0,0170	Dscr1
97349_at	1,68	0,0068	4930488L10Rik
98931_at	1,70	0,0231	Gns
102221_at	1,70	0,0057	Syngr1
97448_at	1,71	0,0457	9030221M09Rik /// MGC65558
98319_at	1,73	0,0065	Dsg2
101430_at	1,73	0,0393	---
100597_at	1,76	0,0077	Gyg1
102791_at	1,77	0,0302	Psmb8
100970_at	**1,78**	**0,0353**	**Akt1**
93155_at	1,82	0,0092	A930004K21Rik
96679_at	1,84	0,0223	Dnajb9
101753_s_at	1,85	0,0370	Lzp-s /// Lyzs
97777_at	1,86	0,0134	Nkx2-5
96778_at	1,91	0,0205	Rrs1
100112_at	1,91	0,0215	Cxcl12
97253_at	1,94	0,0193	Tpd52l2
98045_s_at	1,95	0,0016	Dab2
104184_at	1,97	0,0509	Nppb
104265_at	1,97	0,0437	Kdr
103549_at	1,98	0,0072	Nes
104597_at	2,03	0,0409	Gbp2
94379_at	2,03	0,0296	Kif1b
99937_at	2,04	0,0024	Meox2
103006_at	2,05	0,0362	Atf5
102226_at	**2,07**	**0,0240**	**Cpxm2**
101020_at	2,12	0,0116	Ctsc
100998_at	2,14	0,0412	H2-Ab1 /// Rmcs1
100022_at	2,16	0,0008	Cish
97541_f_at	2,22	0,0269	H2-L /// LOC56628 /// H2-D1
93268_at	2,35	0,0027	Glo1
98506_r_at	2,39	0,0045	Cpox
97319_at	2,49	0,0169	Rrad
93269_at	2,49	0,0005	Glo1
100605_at	2,52	0,0118	Tpm2
92559_at	2,67	0,0034	---
102773_at	2,70	0,0191	Car8

97918_at	2,71	0,0276	AA536743
103554_at	**2,85**	**0,0244**	**Adam19**
102227_g_at	**2,93**	**0,0068**	**Cpxm2**
161858_f_at	4,14	0,0094	Rb1

Table 2. Genes of which the expresssion are down regulated in hearts of Bl/6 *Mas* mice, p<0.05

ID –Affymetrix identification number of the EST, KO/WT - fold change *Mas*-knockout mice compare to WT, t-test, statistic comparison between *Mas*-knockout mice and WT, Gene symbol - abbreviation of gene. The red colored rows were genes which were interesting and tested further.

ID	KO/WT	t-test	Gene Symbol
94297_at	0,32	0,0162	Fkbp5
102049_at	0,34	0,0073	Pdk4
96513_at	0,39	0,0252	---
103460_at	0,43	0,0114	Ddit4
101561_at	0,44	0,0300	Mt2
161356_at	0,48	0,0442	---
160359_at	0,49	0,0398	1190002H23Rik
97844_at	**0,49**	**0,0020**	**Rgs2**
101554_at	0,50	0,0211	Nfkbia
95658_at	0,52	0,0131	Commd1
98322_at	0,52	0,0485	Slc22a5
96119_s_at	0,53	0,0132	Angptl4
94147_at	0,53	0,0053	Serpine1
104149_at	0,54	0,0324	---
103083_at	0,54	0,0004	---
102370_at	0,54	0,0003	Dhrs8
100042_at	0,55	0,0001	Hagh
104340_at	0,55	0,0400	Mbd1
93392_at	0,55	0,0137	Ucp3
95026_at	0,56	0,0044	0610039N19Rik
94906_at	0,56	0,0117	Adh1
102426_at	0,57	0,0034	---
103829_at	0,57	0,0148	Herc2
92925_at	0,57	0,0012	Cebpb
92195_at	0,58	0,0444	Cebpg
96646_at	0,59	0,0001	Usp39
92830_s_at	0,59	0,0209	Zfp36

93486_at	0,59	0,0312	Slc27a1
93006_at	0,59	0,0073	Nfic
95664_at	0,60	0,0102	Sec14l1
103891_i_at	0,60	0,0369	Ell2
92724_at	0,61	0,0413	---
101444_at	0,61	0,0186	Gt(ROSA #22)26asSor
97171_f_at	0,66	0,0306	---
103889_at	0,66	0,0005	Tbl1xr1
93573_at	0,66	0,0134	Mt1
92821_at	0,67	0,0004	Usp2
92652_at	0,68	0,0092	Notch4
92909_at	0,68	0,0371	Pgf
93975_at	0,71	0,0214	1300002F13Rik
92996_at	0,72	0,0039	Sox17
93266_at	0,72	0,0285	Tpm3
102248_f_at	0,72	0,0131	Cask
94396_at	0,72	0,0363	Ing1
AFFX-CreX-5_st	0,72	0,0394	---
101618_r_at	0,72	0,0194	---
162415_f_at	0,73	0,0480	Cant1
94502_at	0,73	0,0076	D13Wsu50e
97374_at	0,73	0,0287	2810025M15Rik
100570_at	0,73	0,0368	6330412F12Rik
99120_f_at	0,73	0,0110	Chd4
160492_at	0,74	0,0258	Ddx18
160981_at	0,75	0,0089	---
103620_s_at	0,75	0,0109	Smn1
98029_at	0,75	0,0077	3110056O03Rik
101529_g_at	0,76	0,0428	Tcea1
102327_at	0,76	0,0027	Aoc3
99027_at	0,76	0,0309	Bcl2l1
103420_at	0,76	0,0161	Emd
95393_at	0,76	0,0472	Btbd3
160341_at	0,76	0,0480	Jtv1
103636_at	0,77	0,0355	Brp17
99866_at	0,77	0,0103	---

104756_at	0,78	0,0124	2310047M15Rik
96300_f_at	0,79	0,0231	Rps27
93277_at	0,79	0,0346	Hspd1
101573_f_at	0,79	0,0151	Rpl27a
103913_at	0,79	0,0436	Sec61a2
100345_f_at	0,80	0,0167	Vamp8
93312_at	0,80	0,0206	Ube2g1
103843_at	0,81	0,0470	Gnao1
94312_at	0,81	0,0403	AA415817
100027_s_at	0,81	0,0285	Pex14
100515_at	0,82	0,0436	Furin
94258_at	0,82	0,0445	Arhgdib
95765_at	0,83	0,0422	Adh5
97885_at	0,83	0,0171	1810009M01Rik
93295_at	0,84	0,0191	Cct5
92829_at	0,84	0,0096	Hspe1
100543_s_at	0,85	0,0207	Brd7
104189_at	0,85	0,0033	Traf6
99127_at	0,86	0,0215	Sca10
93521_at	0,87	0,0339	Srrm1
93740_at	0,87	0,0389	Nsep1
160271_at	0,89	0,0108	0610007C21Rik
96615_at	0,89	0,0295	Ypel3
104514_at	0,93	0,0042	Epn1

Table 3. Genes of which the expresssion is upregulated in testes of Bl/6 *Mas* mice, p<0.05

ID –Affymetrix identification number of the EST, KO/WT - fold change *Mas*-knockout mice compare to WT, t-test, statistic comparison between *Mas*-knockout mice and WT, Gene symbol - abbreviation of gene. The red colored rows were genes which were interesting and tested further.

ID	KO/WT	t-test	Gene
161683_r_at	1,14	0,0322	---
98571_s_at	1,14	0,0455	Naca
94078_at	1,16	0,0271	1110020P15Rik
92610_at	1,17	0,0589	Rdbp
98912_at	1,18	0,0531	D13Wsu64e
96621_at	1,18	0,0240	1110061L23Rik
102949_g_at	1,19	0,0553	Hemt1

97329_at	1,19	0,0346	C77668
103893_at	1,20	0,0411	Fbxo38
93500_at	1,20	0,0514	Alas1
97273_at	1,20	0,0103	Ars2
160861_s_at	1,21	0,0381	Pde1a
160716_at	1,21	0,0500	2410018C17Rik
95091_at	1,21	0,0486	Sec13l1
93336_at	1,21	0,0473	1110014C03Rik
162428_i_at	1,22	0,0267	S100a14
101944_at	1,22	0,0455	Lypla1
96962_at	1,22	0,0347	Rpl6
160492_at	1,22	0,0059	Ddx18
103531_f_at	1,23	0,0095	1300013B24Rik
95551_at	1,23	0,0487	1700020M16Rik
104101_at	1,23	0,0534	Slc9a8
102400_at	1,24	0,0140	LOC433702
100066_at	1,24	0,0450	Gart
95473_s_at	1,25	0,0237	C77604
96707_at	1,25	0,0577	Zipro1
99166_at	1,25	0,0130	0610012G03Rik
98524_f_at	1,25	0,0006	---
104760_at	1,26	0,0479	Ifrd2
92845_at	1,26	0,0425	Oxct1
101573_f_at	1,27	0,0276	Rpl27a
102062_at	1,28	0,0127	Smarcc1
95602_at	1,29	0,0533	Trpc4ap
162153_i_at	1,29	0,0079	Exosc5
101929_at	1,30	0,0139	6720463E02Rik
160256_at	1,30	0,0111	Tomm7
98109_at	1,31	0,0485	Mrpl55
93835_at	1,31	0,0267	Fuca1
94971_at	1,31	0,0236	Cdkn3
104168_at	1,31	0,0357	Actr2
93897_at	1,33	0,0138	Theg
95715_at	1,34	0,0503	1200009C21Rik
103735_at	1,34	0,0572	Wnt6
102796_at	1,34	0,0140	Npm3

99581_at	1,34	0,0554	Hint1
96291_f_at	1,35	0,0553	BC059730
102988_at	1,36	0,0451	Inppl1
99024_at	1,37	0,0078	Mxd4
101096_s_at	1,37	0,0294	Hs1bp1
104576_at	1,39	0,0261	Ski
94218_at	1,39	0,0528	Tcp1
96174_at	1,40	0,0360	Pom121
100769_at	1,40	0,0543	---
101947_at	1,40	0,0426	Akap8l
103330_at	1,41	0,0389	Strbp
104439_at	1,41	0,0460	Nat6
103032_at	1,42	0,0476	Tpst1
97953_g_at	1,43	0,0392	Tsc2
103663_at	1,44	0,0140	4930467B06Rik
104100_at	1,45	0,0320	2310075E07Rik
103398_at	1,45	0,0434	---
160854_at	1,46	0,0034	Map3k7
101810_at	1,47	0,0211	Fshr
160521_at	1,48	0,0579	2610020N02Rik
98831_at	1,50	0,0278	Foxj1
97989_at	1,50	0,0224	Ppp3cb
100972_s_at	1,51	0,0404	Ccl27
103387_at	1,52	0,0062	Phf1
98149_s_at	1,52	0,0580	1110033J19Rik
93850_at	1,53	0,0554	Iqgap1
96789_i_at	1,53	0,0296	Galm
98356_at	1,53	0,0555	---
101446_at	1,53	0,0262	Tpd52l1
101017_at	1,54	0,0518	Cdk4
92481_at	1,58	0,0586	Chek2
161528_r_at	1,64	0,0531	Pold1
103072_at	**1,67**	**0,0057**	**Hsd3b1**
95694_at	1,68	0,0344	Top1
161238_f_at	1,72	0,0583	Cct3
161348_r_at	1,74	0,0550	Pdlim1
95590_at	1,76	0,0145	Alg5

161398_at	1,83	0,0092	Dnahc8
99384_at	1,83	0,0029	Pim1
103751_at	1,94	0,0512	AA409316
95247_at	2,06	0,0294	---
93268_at	2,09	0,0176	Glo1
161004_at	2,34	0,0001	1700097N02Rik
95299_at	2,51	0,0147	Dnahc8
160269_at	**3,98**	**0,0427**	**Gfer**

Table. 4. Genes of which the expresssion is downregulated in testes of Bl/6 *Mas* mice, p<0.05

ID –Affymetrix identification number of the EST, KO/WT - fold change *Mas*-knockout mice compare to WT, t-test, statistic comparison between *Mas*-knockout mice and WT, Gene symbol - abbreviation of gene. The red colored rows were genes which were interesting and tested further.

ID	KO/WT	t-test	Gene
102729_f_at	**0,35**	**0,0076**	**Hsd3b6**
99439_at	**0,41**	**0,0125**	**Mas1**
104738_at	0,45	0,0022	Zrf2
92953_at	0,47	0,0270	Fmn
95730_at	0,49	0,0026	Mrps34
103761_at	0,54	0,0156	Tcfcp2l1
101834_at	0,56	0,0537	Mapk3
102996_at	0,57	0,0212	Ell
160428_at	0,58	0,0419	Suclg2
160115_at	0,58	0,0458	Txnl1
98509_at	0,59	0,0223	BC002199
102026_s_at	0,59	0,0385	Chkb
92213_at	0,59	0,0052	Star
97836_at	0,61	0,0419	Rnf7
93939_at	0,62	0,0223	Lnk
103440_at	0,62	0,0363	Gabpa
101890_f_at	0,62	0,0087	Dnajc2 /// Zrf2
103814_at	0,62	0,0361	Pex11b
95718_f_at	0,63	0,0253	Usmg5
160970_at	0,64	0,0463	Odf2
93348_at	0,64	0,0378	Timm22
94233_at	0,65	0,0545	1110038F14Rik

92915_s_at	0,65	0,0209	Hoxb8 /// Hoxb7
160921_at	0,66	0,0556	Acas2l
97199_at	0,66	0,0186	Cpne1
94049_at	0,66	0,0379	Bhmt
102028_at	0,67	0,0064	Rassf5
98493_at	0,67	0,0212	3200002M19Rik
160547_s_at	0,68	0,0467	Txnip
97943_at	0,69	0,0448	Capn6
93029_at	0,70	0,0324	Idh3g
98001_at	0,70	0,0476	Arhgef1
97991_at	0,70	0,0028	Kras2
98439_at	0,71	0,0398	Rps6kb1
100042_at	0,71	0,0209	Hagh
98428_at	0,71	0,0461	Spg4
93562_at	0,71	0,0524	Ndufb3
104527_at	0,71	0,0550	Rad51
98092_at	0,71	0,0396	Plac8
97184_at	0,71	0,0199	D15Ertd781e
99140_at	0,72	0,0591	Mrpl16
99987_at	0,72	0,0274	Zfp574
92646_at	0,72	0,0209	Mrpl23
97745_at	0,72	0,0304	Hoxa4
100457_at	0,73	0,0556	Glg1
95695_at	0,73	0,0293	Slc25a20
94047_at	0,74	0,0415	0610031J06Rik
100293_at	0,74	0,0458	Cd59b
160333_at	0,75	0,0346	1110008F13Rik
104143_at	0,75	0,0519	Copz2
94778_at	0,76	0,0190	Aldh1a7
100466_f_at	0,77	0,0266	Iqcf4
160076_at	0,77	0,0590	Mtx2
96580_at	0,77	0,0544	Pbx3
93141_at	0,78	0,0212	Nr0b1
92228_at	0,78	0,0140	Catna2
95431_at	0,79	0,0224	Tomm70a
95910_f_at	0,79	0,0128	Rbed1
96493_at	0,79	0,0417	2810002I04Rik

160292_at	0,80	0,0178	Ecgf1
93191_at	0,80	0,0582	Vamp4
101362_at	0,80	0,0108	Mapk9
96186_at	0,81	0,0334	Lrp10
95742_at	0,81	0,0107	Psmd13
98124_at	0,81	0,0110	0610011F06Rik
160569_at	0,81	0,0106	2310008M10Rik
94457_at	0,82	0,0424	AL033326
97551_at	0,83	0,0095	Hip1r
160231_at	0,83	0,0594	Farsla
99591_i_at	0,83	0,0337	Rdh11
94521_at	0,83	0,0522	Cdkn2d
101357_at	0,84	0,0187	Ap2a1
96211_at	0,84	0,0412	2310004I03Rik
94022_at	0,87	0,0197	Gltscr2
93673_at	0,87	0,0427	Nrtn
97993_at	0,87	0,0559	Uros
160293_at	0,88	0,0463	2700038L12Rik
103628_at	0,88	0,0335	Lef1

11. Appendix

DECLARATION

December 19, 2007

Herewith I declare that the experiments described in this thesis were carried out by myself.

Erklärung

Ich versichere hiermit, dass die von mir vorgelegte Dissertation selbständig angefertigt wurde und ich die Stellen der Arbeit, die anderen Werken in Wortlaut oder Sinn nach entnommen sind, in jedem Einzelfall als Entlehnung kenntlich gemacht habe. Diese Dissertation wurde noch keiner anderen Fakultät zur Prüfung vorgelegt.